EXPERIMENTAL ANALYSIS OF CROSS-FLOW GRAIN DRYING SYSTEMS IN DEEP CYLINDRICAL BINS

By

DONALD LEE DAY

Bachelor of Science in Agricultural Engineering
Oklahoma State University
1954

Master of Science in Agricultural Engineering
University of Missouri
1959

Submitted to the Faculty of the Graduate School of
the Oklahoma State University
in partial fulfillment of the requirements
for the degree of
DOCTOR OF PHILOSOPHY
August, 1962

OKLAHOMA
STATE UNIVERSITY
LIBRARY

NOV 7 1962

EXPERIMENTAL ANALYSIS OF CROSS-FLOW
GRAIN DRYING SYSTEMS IN DEEP
CYLINDRICAL BINS

Thesis Approved:

B. T. Nelson
Thesis Adviser

E. W. Schroeder

Robert D. Morrison

Dale E. Weibel

Robert Manuel
Dean of the Graduate School

504378

PREFACE

This investigation was a phase of the Oklahoma Agricultural Experiment Station Project 679 and was financed through project funds under the capable administration of Professor E. W. Schroeder, Head of the Agricultural Engineering Department.

I am very grateful for the privilege of studying under Professor Gordon L. Nelson who has served as major advisor. I extend sincere appreciation to Dr. Nelson for advice, consultation, and inspiration through all phases of the program.

I thank Professor Dale E. Weibel of the Agronomy Department and Professor Robert D. Morrison of the Statistics Department for serving on the advisory committe and for assistance and suggestions offered.

Appreciation is extended to all the staff of the Agricultural Engineering Department for their cooperation, encouragement, and suggestions. Jack Fryrear and Don McCrackin contributed considerably in preparing the illustrative material. Personnel of the research laboratory did excellent work in building special equipment.

Professor William Granet, Director of the Electronic Computing Center, is to be commended for support and guidance in programming. Appreciation is expressed to the Agronomy Department for furnishing grain for the experiments.

I am particularly grateful to Dorotha, my wife, and my children for the sacrifices they have made during this study.

TABLE OF CONTENTS

LIST OF TABLES

LIST OF FIGURES

CHAPTER I

INTRODUCTION

Background

Storage of cereal grains is an important phase of food supply. The stored grain may be in a dormant state, but it is usually alive and capable of responding to physiological and biological processes. The grain is subject to invasion by living fungi, yeast, and bacteria unless the storage environment is such that these enemies of stored grain are prevented from attacking the grain.

To prevent fungal invasion during conventional storage, excess moisture must be removed from the grain before mold or fungal damage can occur; and the grain must be maintained at a safe moisture content and temperature throughout the storage period. Grain stored in large quantities such as in terminal type elevators is not necessarily safe from mold damage even though the grain had an average moisture content considered safe when the grain was placed in storage. Moisture migration, temperature differences, mixed grain of unequal moisture contents, and pockets of high moisture grain can contribute to an intergranular environment favorable for mold growth. This can result in grain germ damage and even total loss of some or all of the grain in the zones which have accumulated excessive moisture. Once grain deterioration starts, it can spread rapidly into much larger zones. To keep stored grain in "condition," the zones which have a tendency

to increase in grain moisture content must be periodically dried to a safe storage moisture content. Drying of the grain in storage would be desirable to prevent removing the grain and drying it by conventional methods.

Because of the resistance encountered by air flowing through the full depth of a deep bin, excessive power would be required to force air uniformly from top to bottom or bottom to top in sufficient quantities to significantly dry grain after it is placed in storage. However, the power requirement could be significantly reduced if cross-flow circulation of air were used to dry the grain in place in deep cylindrical storages. The air would travel a shorter path through the grain and consequently, the resistance to air flow would be greatly reduced. Figure 1-1 illustrates a vertical, uniform flow system as contrasted to a cross-flow, nonuniform air circulation system.

The Problem

The effectiveness of forced air grain drying systems is determined by several parameters, such as: initial grain moisture content, temperature and humidity of drying air, air circulation rate, type of flow arrangement, and other factors. The effect of these parameters or factors on the amount of drying accomplished needs to be known to design or manage a grain drying installation. A method for determining the drying effect for a specified set of conditions would be useful in designing and in selecting operating conditions for cross-flow drying systems. Thus, it would seem that engineered systems are needed for cross-flow forced air drying of grain in deep

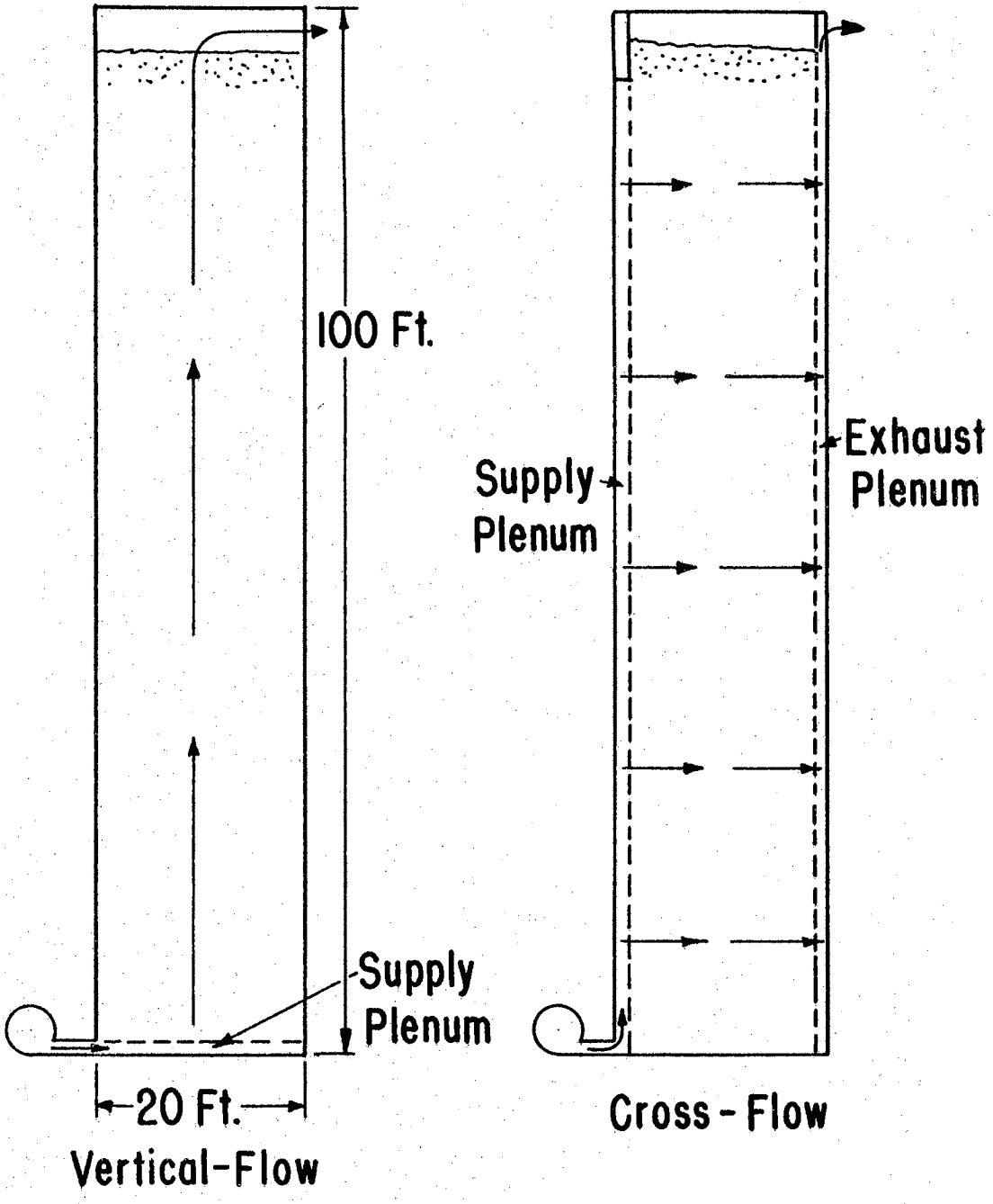

FIGURE 1-1. Schematic view of vertical-flow and cross-flow drying systems in deep cylindrical bins.

cylindrical storages.

Previous grain drying research studies have produced methods for analysing the drying effect in a uniform system in which the air travels through equal depths of grain. However, there seems to be very little information available on the nonuniform drying systems of cross-flow arrangements.

Objectives

The objectives of the study were:

1. To develop a general prediction equation that describes the drying process across cylindrical bins. The equation was to be a mathematical relationship relating drying accomplished or moisture removed to the many factors involved which influence the drying process.
2. To study the nature of the pressure, thermal, and moisture gradients which develop within the grain mass during drying.
3. To verify the prediction equation in different sizes of bins.

The experimental research was planned to incorporate the following situations:

Two agricultural grains, wheat and sorghum.

Three types of cross-flow bin configurations.

A range of air temperatures that included atmospheric air conditions and artificially heated air.

CHAPTER II

LITERATURE REVIEW

Mycology and Grain Storage

The intergranular atmosphere of stored grain can become a favorable environment for the growth of molds and fungi. Fungi seem to be universally present and the infestation appears to increase from harvesting through all of the stages of handling the grain.

Anderson and Alcock (2, p. 121) stated that molds, including several yeastlike fungi, which have been found growing in stored grain and grain products are chiefly members of the genera "Aspergillus" and "Penicillium," and are of the orders "Moniliales" and "Mucorales." They listed minimum, optimum, and maximum temperatures and minimum relative vapor pressures supporting growth of various species of microorganisms. (3, pp. 102-114).

One of the early results of microorganism infestation is grain germ damage manifested by a decrease in viability and a decrease in processing quality. This situation in wheat is known as "sick wheat" and is very difficult to recognize. Germs or embryos of "sick wheat" are off-color and either greatly weakened or dead. The damaged wheat has reduced germination and produces a poor grade of flour. Tuite and Christensen (34) found that germination itself is not known to be a quality factor in wheat to be used for milling, but it appears to be a sensitive indicator of beginning or impending deterioration as a

decrease in germination percentage always precedes the development of sick wheat. Other grains experience similar effects in the embryo damaging stage of fungal infection. Other stages of deterioration from fungi are grain unfit for seed and commercial use and finally grain unfit for livestock comsumption. These latter stages are manifest by sprouting, heating, mustiness, fermented odor, and putrefaction.

To prevent damage of the grain by microorganisms, an interseed environment must be maintained which is unsuited for growth of the microorganisms. Some of the major factors which determine whether grain will remain in sound condition are temperature and moisture content of the grain and length of time the grain is stored. A few methods of grain preservation are: low moisture content, low temperature, exclusion of oxygen, introduction of an inert gas, and use of a chemical toxic to microorganisms, a fungicide.

Hygroscopicity of Cereal Grains

Many organic substances possess the characteristic of taking on or giving up moisture so that the moisture content of the substance approaches an equilibrium condition determined by the thermodynamic properties of the surrounding atmosphere. Substances which exhibit this characteristic are termed hygroscopic materials and the moisture content of the material when in equilibrium with the surrounding atmosphere is known as the equilibrium moisture content.

The factors affecting the hygroscopic properties of cereal grains are not as well defined as would be desirable for processing and storage of the crops. Much of the equilibrium data found in technical literature does not specify whether the data were obtained under

absorptive or desorptive conditions. The temperature effect upon the equilibrium moisture relationships of several grains is not adequately described.

Most agricultural products exhibit hysteresis in the adsorption and desorption of water. Branauer (7) has described five isotherm types encountered in physical adsorption and gives a theoretical analysis of some of the types. The majority of the cereal grains are of "type two" in the desorptive phase and probably also in the adsorptive phase. The "type two" isotherms have a characteristic "S" or sigmoid shape of curve resulting from a plot of grain moisture versus ambient air humidity.

Babbit (4) reported sigmoid curves for desorption by wheat but reported an adsorptive curve distinctly convex to the relative humidity axis. In a more recent research study, Hubbard et al. (20) reported hysteresis loops for wheat and corn and both phases of the curves were found to be sigmoid as shown for wheat in Figure 2-1.

Some other distinctive phenomena noted in relation to wheat hygroscopicity have been reported. Babbit (5) found that in completing the desorption isotherm, it was never possible to remove all the moisture from wheat as evaluated by the equipment and methods which he employed. The residual moisture content was found to be a function of temperature. However, Becker and Sallans (6) suggest that the value for moisture content at zero relative humidity reflects a lack of complete equilibrium rather than any abnormal conditions of adsorption. Fairbrother (11) reported that dried wheat flour does not completely regain its moisture content when re-exposed to the original relative humidity. He also found that wheats of high and low moisture contents, when

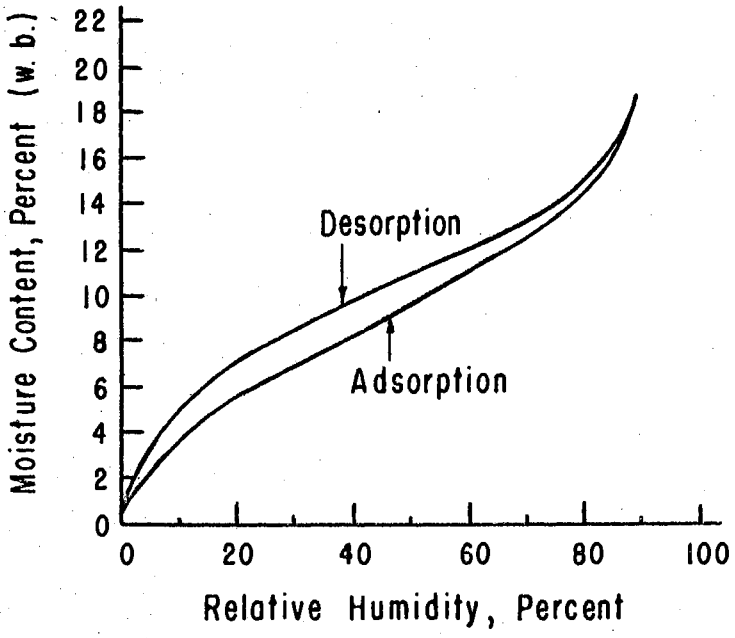

FIGURE 2-1. Hysteresis of moisture sorption in wheat, 35 C isotherms.

mixed, do not reach equal moisture contents. The low moisture wheat always remained at a moisture content about two per cent below that of the high moisture wheat.

The phenomenon of hygroscopicity has been studied by many researchers and as a result, several mathematical relationships have been formulated for defining the equilibrium moisture content and will be discussed as follows.

In an analysis by Henderson (18), the equilibrium moisture isotherms for a number of materials were found to follow a dimensionally restricted equation of the following form:

$$1-rh = e^{-k'M_e^{n}} \qquad 2-1$$

in which rh = equilibrium relative humidity, as a decimal

M_e = equilibrium moisture content, per cent dry basis

k' = factor varying with material

n = exponent varying with material.

The effect of temperature was introduced into the equation by a method based upon Gibbs' thermodynamic adsorption equation. By this approach, k' of equation 2-1 was found to be a function of temperature such that:

$$k' = kT$$

in which k = coefficient varying with material

T = temperature, F absolute.

Thus, the final equation was of the form:

$$1-rh = e^{-kTM_e^n}. \qquad 2-2$$

The factors k and n were evaluated by using equilibrium moisture data for a variety of products. For wheat $k = 5.59 \times 10^{-7}$ and $n = 3.03$.

Pichler (28) found that equation 2-2 does not permit the mathematical determination of the shift due to temperature of the equilibrium moisture curve because n and k are not constants independent of temperature. At a temperature change of 60 C the observed decrease in moisture content was four times the calculated value.

Hall (15, p. 20) comments that of data available at different temperatures for a variety of crops, only data for grain sorghum follows Henderson's equation. The temperature variation for the grain sorghum was 40, 70, and 90 F, but it was not specified whether the data was adsorptive or desorptive (12).

An analysis by Becker and Sallans (6) resulted in dividing the desorption isotherms into three portions: an initial curved section

concave downward, a linear region, and a curved section concave upward. An equation was developed for each of the three portions of the isotherm as in Figure 2-2. A summary of the three equations, values of constants, and approximate region of applicability are given in Table I.

Definition of symbols used in the equations of Table I are as follows:

M = Grain moisture content as a decimal, dry basis

M_m = Moisture content as a decimal, dry basis, required to form a unimolecular layer

c = A constant approximately equal to H_m/RT

H_m = Average net heat of desorption of the unimolecular layer, k cal per mole of water desorbed

R = Universal gas constant

T = Temperature, absolute

f = Relative vapor pressure, (relative humidity)

W = Grain moisture as a decimal, wet basis

W_b = Intercept in a plot of W versus ln (1-f)

W' = Slope of plot of W versus ln (1-f)

ln = Log to base e

n = Constant, slope of linear portion.

An equation was developed by Haynes (17) by fitting equilibrium moisture data to a general equation by means of the modified Doolittle technique.

The form of the general equation was:

$$Y = C + c_1X_1 + c_2X_2 + c_3X_2^2 + c_4X_1X_2, \qquad 2\text{-}3$$

in which Y = the log of the vapor pressure of seed moisture

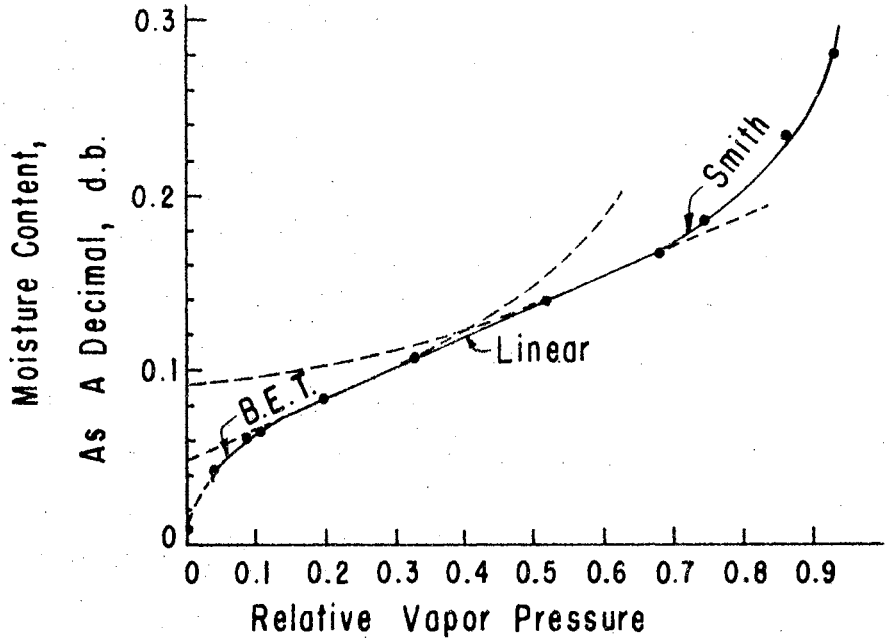

FIGURE 2-2. Desorption isotherm of wheat at 25 C illustrating portions which are described by the B.E.T., Linear, and Smith equations.

TABLE I

B.E.T., LINEAR, AND SMITH EQUATIONS AND REGIONS OF APPLICABILITY IN DESORPTION OF WHEAT

	Values Of Constants			Approx. Region Of Applicability	
Equation	Const.	25 C	50 C	25 C	50 C
$M/M_m = cf/(1-f)[1+(c-1)f]$	M_m	0.0780	0.0602	$0.04 < f > 0.30$	
B.E.T. (8)	c	22.9	15.1		
$M - M_0 = af$	M_0	0.0483	0.0278	$0.12 < f < 0.65$	
Linear	a	0.1715	0.1564		
$W - W_b / W' = \ell n (1/1-f)$	W_b	0.0845	0.0550	$0.50 < f < 0.95$	
Smith (32)	W'	0.0514	0.0595		

X_1 = the log of the vapor pressure of pure water at test temperature

X_2 = the seed moisture content, per cent dry basis

C and c_i are constants depending upon the material.

The constants were evaluated by using equilibrium moisture data obtained by the vapor-pressure method. For wheat, the constants were:

$C = -1.61379$

$c_1 = 1.26937$

$c_2 = 0.12543$

$c_3 = -0.00250$

$c_4 = -0.01182$.

Methods of Grain Drying Analysis

Theory of drying which is used in many fields of drying applications such as chemicals, paper, and stones can not always be directly applied to drying cereal grains since grain has some unique properties which influence the drying analysis. Some of these properties, such as presence of a seed-coat and manner in which the moisture is bound internally in the kernel, are inherent to the morphology of the kernel.

The vapor pressure theory of drying grain has been presented by several research workers. (15; p. 245). As the temperature of a product is increased, the vapor pressure inside the product increases. Thus, there results a potential for flow of moisture from zones of high vapor pressure to the lower vapor pressure of air surrounding the product. The flow of moisture is approximately proportional to the vapor pressure difference between the product and the surrounding atmosphere. Drying theory is influenced by the hygroscopic properties

of grain which were mentioned in the previous section. Several methods of approach to drying grain will be presented in this section.

Thin Layer Drying

Thin layer drying refers to drying of grain entirely exposed to air moving through the product. (15, p. 252). The resulting equation represents movement of moisture during the falling rate period. The two major periods of drying are the constant rate period and the falling rate period. In the constant rate period drying takes place from the surface of the grain and is similar to evaporation of moisture from a free water surface. The falling rate period is entered after the constant rate period and the critical moisture content occurs between the constant rate and falling rate periods. The critical moisture content is the minimum moisture content of the grain that will sustain a rate of flow of free water to the surface of the grain equal to the maximum rate of removal of water vapor from the grain under the drying conditions. For grain the initial moisture content is usually less than the critical moisture content so that all the drying occurs in the falling rate period. The critical moisture content for wheat is between 69 and 85 per cent dry basis. (31).

The equation which forms the basis for thin layer drying theory is:

$$M\text{-}M_o/M_o\text{-}M_e = e^{-k\theta} \qquad 2\text{-}4$$

in which M = moisture content at any time θ

M_e = equilibrium moisture content

M_o = original moisture content

k = drying constant, (the units are not clearly defined).

$M-M_o/M_o-M_e$ is referred to as the moisture content ratio.

Time of response terminology, similar to time of radioactive decay terminology, can be applied to moisture movement. Thus, the time of one-half response in a drying process would be the time necessary to obtain a moisture content ratio of one-half.

Thin layer theory is very important in the study of grain drying; but, since it was developed for grain entirely exposed to the circulated air, it is not an adequate method for use in drying grain in a deep layer as in deep bins.

Deep Layer Drying

Drying grain in a deep layer can be considered as drying in a series of thin layers in which the humidity and temperature of air leaving each layer varies with time depending upon the stage of drying. Equations, in addition to the thin layer drying equation, are needed for the deep layer drying analysis and were developed by Henderson and Perry (19).

Drying with heated air can be an adiabatic process, in which the energy for moisture evaporation is supplied by a reduction in temperature of the circulated air. The wet bulb (adiabatic humidification) lines of the psychrometric chart and the thin layer drying equation represent this process and can be used for calculating a drying heat and mass balance. Air at state "a", see Figure 2-3, is heated to state "b" and passed through the material to be dried. The process moves from state "b" up the wet bulb line, and the air exhausts at state "c". Equations were developed by Henderson and Perry for the rate of moisture removal and for the change in air humidity.

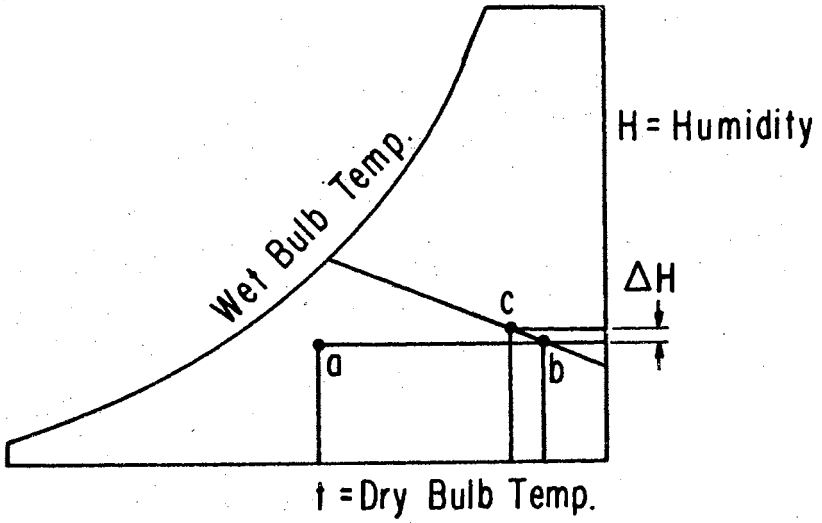

FIGURE 2-3. Skeleton psychrometric chart showing air state change, b to c for a drying process.

The deep layer conditions expressed in the above mentioned equations are based on the thin layer drying concept. This concept does not rigorously hold for deep layers (19, p. 287). However, an approximate solution can be obtained by a stepwise integration process considering thin layers through the grain depth. The stepwise integration is at best a laborious process and can yield only an approximate solution subject to limitations of the equations upon which the method is based.

Hukill's Method of Analysis

This also is a method for analysing the drying process in grain having greater depths than those for which the thin layer drying analysis applies.

The computed relationships between drying time, grain moisture, and grain depth units were generalized by Hukill (21) to make them applicable to various drying problems.

Descriptions of the above properties are given as follows:

Drying time - each time unit is the time of one-half response of grain fully exposed to the air entering the drying system.

Grain moisture - moisture is expressed as the moisture content ratio, $M-M_e/M_o-M_e$.

Grain depth - a depth factor is described as containing enough grain that if all the theoretically available heat could be used it would all dry to equilibrium in a period of time equal to the time of one-half response. The pounds of grain, G, in each depth is computed by use of the following heat balance equation:

$$(dQ/d\theta)c\Delta t = \Delta M\,(dw/d\theta)h_{fg} \qquad 2\text{-}5$$

in which $dQ/d\theta$ = volume of air, lb per hr

c = specific heat of air at constant pressure, approximately 0.24 btu per lb F

Δt = maximum temperature drop of the air in passing through the grain, F

ΔM = M_o-M_e, per cent dry basis

$dw/d\theta$ = moisture removed from volume under consideration, lb per hr

h_{fg} = latent heat of vaporization of moisture from grain, approximately 1170 btu per lb of water

G = $(dw/d\theta)\theta_{1/2}$.

With appropriate data the following information can be computed using Hukill's analysis for a drying problem at any desired time after drying has started:

moisture content at any depth;

pounds of moisture removed;

average rate of drying;

temperature and relative humidity of the exhaust air; and thermal efficiency of the drying operation.

Nelson's Batch Grain Drier Analysis

A prediction equation was developed by Nelson et al. (26) whereby the drying effect of air circulated through a bed or batch of grain can be calculated. The drying system considered was one that included a batch or bed of grain of uniform depth and dried by forced circulation of heated or unheated air at a uniform rate.

Theory of similitude and dimensional analysis were used in developing the equation relating variables such as average drying effect, bed depth, air circulation rate, elapsed time, grain moisture content, and entering air temperature and humidity. Constants appearing in the equation were evaluated from experimental data obtained with laboratory and full-size drying installations. The form of the prediction equation is:

$$E = C_1(\Delta M \Delta T/T_e)^n(1-e^{-C_2\lambda/V\phi}) \qquad 2\text{-}6$$

in which E = avg drying effect by air, lb of moisture removed from batch per lb of dry air circulated, lb/lb

ΔM = difference, initial grain moisture minus equilibrium moisture corresponding to entering air state, lb/lb

ΔT = difference, entering air dry bulb temperature minus "ideal" leaving air dry bulb temperature after a constant wet bulb process to equilibrium humidity for grain at initial moisture content, F

T_e = air dry bulb temperature entering grain, F absolute

λ = grain batch thickness or depth in direction of air flow, ft

V = air circulation rate through grain, cfm/sq ft

ϕ = elapsed time since start of drying process, min

e = base of natural logarithm system.

The above analysis can be used to estimate average and instantaneous drying effects during operation of batch grain drying systems, to plan and conduct experimental grain drying investigations, and to increase the scope of applications of grain drying experimental results.

A system of tables and charts from which the solution of equation 2-6 may be obtained for drying grain sorghum was developed by Day and Nelson (9). Alignment charts are used for the final solution of the equation. The system of analysis can be used to solve three basic types of problems in design or operation of grain drying systems. These include computing required circulation index, computing average grain moisture removed, and computing temperature of heated air.

Fluid Flow Through Porous Media

With regard to the system of forcing air through a bed of grain, the system is essentially one of fluid flow through a porous media. A development of some of the phases of this subject can contribute to analysing the air circulation system involved in grain drying installations.

For single spheres, it is immaterial in the study of resistance to flow whether the particle is falling and the fluid at rest, or the fluid in motion and the particle at rest. This fact has led several experimenters to believe that the resistance to the passage of fluids through static beds of irregular particles can be related to the laws of motion of a fluid past a single sphere, and that even the laws of resistance of suspension of particles will be capable of expression in terms of the resistance to motion of single spheres. Mott (24)

states that such a simplification has not yet met with general acceptance. However, the above mentioned laws are important to fluid flow through porous media and some of them will be briefly discussed.

According to Wadell (35), a body in steady motion through any real fluid, or at rest in a current of moving fluid, exhibits a resistance consisting in part of frictionless forces tangential to the surface of the body, and in part of pressure forces acting normal to the surface. If the velocity is constant (no acceleration) and if the fluid is incompressible (or if in a compressible fluid, the velocity does not approach the acoustic velocity so that the pressure changes are small and compressibility may be neglected), the resistance may depend mainly upon the relative velocity of fluid and body; on the density and viscosity of the fluid; on the volume, specific gravity, and shape of the body; and also upon the surface roughness of the solid. Newton (27) proposed a quadratic law of resistance in which resistance is directly proportional to the square of the fluid velocity, thus:

$$R = C_R A v^2 \rho_f$$

in which R = resistance to flow

C_R = coefficient of resistance

A = cross-sectional area perpendicular to flow

v = fluid velocity

ρ_f = fluid density.

Stoke's law showed that when a sphere moves slowly through a fluid, the resistance to motion is directly proportional to the velocity to the first power. Mott (24) points out that between the

ranges of velocity covered by Newton's law and Stoke's law the resistance is proportional to a power of the velocity intermediate between the quadratic of Newton's law and the first power of Stoke's law.

Shedd (30) experimentally arrived at fundamental data of the resistance to the flow of air at constant velocity throughout beds of grain of uniform depth. Plots by Shedd resulted in curves which are somewhat convex upward. If the plots were straight lines the pressure-flow relationship could be expressed by formulas of the form:

$$Q = aP^b \qquad 2\text{-}7$$

in which Q = air flow, cfm per sq ft of floor

P = pressure drop per ft depth of grain

a = Value of Q when P = 1

b = Slope of the curve.

Phenomena of hydrodynamics in porous media lead to differential equations and boundary conditions which make the analytical solution very difficult. Examples of such equations used to define phases of fluid flow are the Navier-Stokes equation and Laplace equation.

The Laplace equation occurs in many contexts in physical problems. Solutions of this equation can be obtained by performing suitable experiments which are themselves governed by the Laplace equation. In this manner it is often possible to set up an analogy to a certain problem of steady flow through porous media and thus to avoid the tedious job of solving the Laplace equation analytically. Orthogonal flow net problems described by the Laplace equation can be solved by using an electrical conductive sheet analogy. Karplus (22) and Soroka (33) give detailed instructions for using conducting

sheets to solve flow net problems with various boundary conditions.

Dimensional Analysis and Similitude

In a physical system involving many factors or variables which influence the system, methods of dimensional analysis and similitude offer a means of simplification achieved by combining the factors into a reduced number of dimensionless groups or parameters which facilitate experimental and analytical research. Dimensional analysis and similitude thus serve as a basis for planning and organization of experiments so that the maximum amount of useful information can be obtained from a minimum number of experiments. Dimensional analysis establishes the conditions for the validity of experiments with models and "the laws of comparison" of models with their prototypes.

To utilize dimensional analysis and similitude, the factors or variables considered to be pertinent to a physical system are chosen and analysed dimensionally. The factors are then grouped into independent dimensionless groups referred to as pi terms. The number of pi terms required for a set of pertinent factors can be determined by the Buckingham pi theorem which states that the number of independent and dimensionless products or pi terms that are required to express a relationship among the factors of the system is equal to the number of factors minus the number of dimensions in which the factors can be expressed (25). Langhaar (23) refined the pi theorem by showing that the number of pi terms required is always equal to the number of physical factors minus the rank of the dimensional matrix for the factors. The pi theorem makes no stipulation as to the most appropriate set of pi terms which can be formed from the factors but any

set consistent in number and form with the theorem is a valid set. However, no set is unique and other terms can be formed by multiplication or division of terms within the set.

The pi terms can be related by an equation of the type:

$$\pi_1 = f(\pi_2, \pi_3, \text{---}\pi_n) \qquad 2\text{-}8$$

which involves an unknown function f. In order to formulate a general prediction equation from equation 2-8, the nature of the function must be established. However, limited predictions can be made, from performance of a model system, to a prototype system without having evaluated the function if the model and prototype are operated so that each pi term of the prototype system is equal to the corresponding pi term of the model system.

The function in equation 2-8 cannot be determined by dimensional analysis alone but may be done from analysis of laboratory observations. Murphy (25) outlined a method for determining the type of the function and for evaluating it. The method consists of arranging the observations so that all of the pi terms, except one, involved in the function remain constant, and varying that one to establish a relationship between it and the dependent term. This arrangement can be referred to as a treatment schedule for the experiments. This procedure is repeated for each of the pi terms in turn, and the resulting relationships between the dependent pi term and the other individual pi terms, referred to as component equations, combined to give a general relationship. Generally the pi terms will combine by multiplication and if the component equations are of the power form, the general prediction equation will have the form:

$$\pi_1 = k_1 \pi_2^{k_2} \pi_3^{k_3} \text{ --- } \pi_n^{k_n}, \qquad 2\text{-}9$$

in which the k's are coefficients and exponents for the system. Power equations have the form:

$$\pi_1 = k \pi_2^{k_2} \qquad 2\text{-}10$$

and plot as straight lines on log-log paper.

Murphy (25) discusses conditions which are necessary or sufficient for combining the component equations by multiplication, addition, or a combination of the two methods.

CHAPTER III

EXPERIMENTAL DESIGN

General

The design of the research project "drying grain in deep cylindrical bins using cross-flow air circulation" was approached by using dimensional analysis and principles of similitude in which controlled laboratory experiments were performed using model grain drying systems. The project was divided into two major investigations: the air circulation system and the thermal drying system.

Models of deep cylindrical bins were used for the grain drying experiments using cross-flow forced circulation of air. Three types of cross-flow arrangements were chosen for the models as there seemed to be no "best" type of cross-flow configuration for terminal type grain storages. The selection of types of cross-flow arrangements was influenced by systems which would be feasible to add to existing structures as well as designs for future structures. In practice, air circulation systems might be combinations of cross-flow and vertical-flow, but the model bins were designed to study only cross-flow.

The three cross-flow configurations included: bin type I, one air inlet chamber or vertical plenum on one side of the bin with an exhaust plenum directly opposite on the other side of the bin; bin type II, two air inlets and two air exhausts with the inlet plenums

opposite each other and the exhaust plenums opposite each other; and bin type III, three air inlets and three air exhausts alternating at uniform spacings around the bin.

A set of miniature model bins, approximately six inches in diameter, was designed for use in an indoor laboratory where control of the installation was facilitated. The miniature bins were used to obtain the total or average drying effect; but the internal gradients of moisture content and static pressure were not studied in these models as the size was not adequate for measuring these properties.

A set of two-foot diameter bins was designed for use in an open shed and the internal pressure and moisture content gradients were measured in these bins. However, atmospheric air was used in these experiments and control of the system was limited.

Pertinent Factors and Dimensionless Groups

The pertinent quantities considered to influence the thermal drying system and a set of possible dimensionless groups, pi terms, formed from these quantities are listed in Table II. A general prediction equation relating the pi terms is as follows:

$$\pi_1 = f(\pi_2, \pi_3, \pi_4, \pi_5, \pi_6, \pi_7, \pi_8, \pi_9) \qquad 3\text{-}1$$

in which f denotes "a function of".

The pertinent quantities selected for the air circulation system are listed in Table III along with a possible set of dimensionless pi terms. A general prediction equation relating the pi terms is:

$$\pi_{11} = f(\pi_{12}, \pi_{13}, \pi_{14}, \pi_{15}) \qquad 3\text{-}2$$

TABLE II

PERTINENT FACTORS AND PI TERMS OF THE THERMAL DRYING SYSTEM

No.	Factor	Description	Dimension
1	M_R	Avg moisture removed from grain, % dry basis.	——
2	t	Elapsed time of dryer operation, min.	T
3	ΔM	Difference, $(M_g)_i - M_e$, lbs moisture per lb of dry grain; dry basis as a decimal. $(M_g)_i$ = Initial grain moisture content, dry basis as a decimal. M_e = Grain moisture content in equilibrium with air entering grain, dry basis as a decimal.	——
4	τ_e	Air dry bulb temp entering grain, F abs.	θ
5	$\Delta\tau$	Difference, $\tau_e - \tau_\ell$, F. τ_ℓ = Ideal temp of air leaving grain, F abs.	θ
6	τ_g	Initial grain temp, F abs.	θ
7	ρ_g	Bulk density of grain, $lb_{(M)}/ft^3$.	ML^{-3}
8	$\Delta\tau_w$	Difference, $\tau_e - \tau_o$, F. τ_o = Dry bulb temp of ambient air around bin, F abs.	θ
9	Q_a	Total air circulation rate through bin, $(ft^3$ of air/min$)/ft^3$ grain.	T^{-1}
10	ρ_a	Density of air entering grain, $lb_{(M)}/ft^3$.	ML^{-3}
11	c_a	Specific heat of air entering bin, $Btu/lb_{(M)}F$.	$HM^{-1}\theta^{-1}$
12	U	Bin wall overall heat transmission coef, Btu/min ft^2 F.	$HT^{-1}L^{-2}\theta^{-1}$
13	r	Hydraulic radius of cylindrical bin, ft.	L
14	S	Circumferential spacing of vertical cross-flow ducts, bin circumference/ No. of ducts, ft.	L

TABLE II (continued)

Dimensions: T = Time, θ = Temperature, M = Mass,
L = Length, H = Heat.

No. of pi terms required = 14-5 = 9

A possible set of pi terms is:

$\pi_1 = M_R$ $\quad \pi_4 = Q_a t$ $\quad \pi_7 = \Delta\tau_w / \tau_e$

$\pi_2' = \Delta M$ $\quad \pi_5 = \tau_e / \tau_g$ $\quad \pi_8 = \Delta\tau / \tau_e$

$\pi_2 = \Delta M \Delta\tau / \tau_e$ $\quad \pi_6' = U / \rho_a c_a Q_a r$ $\quad \pi_9 = \rho_g / \rho_a$

$\pi_3 = r / S$ $\quad \pi_6 = U\Delta\tau_w / \rho_a c_a Q_a r \tau_e$

TABLE III

PERTINENT FACTORS AND PI TERMS OF THE AIR CIRCULATION SYSTEM

No.	Factor	Description	Dimension
1	P	Static pressure head of air entering bin, ft of water.	L
2	Q_a	Total or volumetric air flow rate, $(ft^3$ of air/min)/ft^3 of grain.	T^{-1}
3	ρ_a	Air density entering bin, $lbs_{(M)}/ft^3$.	ML^{-3}
4	μ_a	Air absolute viscosity, $lb_{(F)}$ min/ft^2.	FTL^{-2}
5	d	Characteristic size of grain kernel, ft.	L
6	Z	Roughness coef of kernel surface.	——
7	r	Hydraulic radius of cylindrical bin, ft.	L
8	S	Circumferential spacing of vertical cross-flow ducts, bin circumference/No. of ducts, ft.	L
9	N_e	Newton's Second Law constant, $lb_{(F)}/lb_{(M)}$ ft/min^2.	$FM^{-1}L^{-1}T^2$

Dimensions: M = Mass, L = Length, T = Time, F = Force

No. of pi terms required = 9-4 = 5.

A possible set of pi terms is:

$\pi_{11} = P/r$ $\qquad$ $\pi_{14} = d/r$

$\pi_{12} = \rho_a r^2 Q_a N_e/\mu_a$ $\qquad$ $\pi_{15} = Z$

$\pi_{13} = r/S$

Discussion of Dimensionless Groups, Pi Terms

The laws of dimensional analysis and similitude do not specify the best or most appropriate set of pi terms which can be formed from a set of pertinent factors, but merely a valid set which are dimensionless and independent. To facilitate experimental and analytical research, it is helpful to judiciously select pi terms that are meaningful in the physical system. Some of the dimensionless groups will be discussed in this section. The factors and pi terms are defined in Tables II and III.

Drying Effect Parameter

M_R, moisture removed, per cent dry basis, was considered a convenient measure of the drying effect obtained in a drying system. The term can be converted to a ratio of the weight of moisture removed to the weight of dry air circulated by a method of an earlier study (9) such that:

$$E = M_R/(Q_a t)(\rho_a/\rho_g)100 \qquad 3\text{-}3$$

in which E = avg drying effect by the air, lb moisture removed per lb of dry air circulated, lb/lb.

Drying Potential Parameter

$\Delta M \Delta\tau/\tau_e$ was selected as the drying potential parameter. Although it would be desirable to directly use such properties as air temperature and moisture content and grain moisture content in the prediction equation, the psychrometric properties of the air and the hygroscopic properties of the grain would seem to be adequately characterized by the drying model described by Nelson (26). The

drying model is depicted in Figure 3-1 in which air at an initial temperature, τ_a, is heated to τ_e. In passing through the grain, moisture is added to the air at a constant wet bulb process until the process intersects the equilibrium humidity curve for the initial grain conditions and the air leaves the grain at a temperature τ_ℓ, $\Delta\tau = \tau_e - \tau_\ell$. This model may not be followed throughout the entire drying period but is the effect for a constant wet bulb process, and actual effect can be greater or smaller if actual process departs from a constant wet bulb process.

ΔM is computed as shown in Figure 3-2 for an isotherm at the temperature of the entering air, τ_e.

The product $\Delta M \Delta\tau/\tau_e, \pi'_2 \times \pi_8$, seems to be directly proportional to the drying potential of the entering air for a particular initial grain moisture content. A term to characterize the situation when the initial grain temperature is not the same as the temperature the air entering the grain was τ_e/τ_g.

Air Circulation Parameter

Some of the factors considered important to be characterized by the air circulation parameter were: velocity of air past a kernel, distance the air travels through the grain before it reaches some corresponding point in model and prototype, time of air travel, and air flow rate per volume of grain. The term selected was $Q_a t$.

The rate of air flow through an increment of bin height is:
for model

$$\text{flow rate} = (Q_a)_M V_M = (Q_a)_M \left[\pi (D_M)^2/4\right] y, \text{ cfm}$$

for prototype

$$\text{flow rate} = (Q_a)_P V_P = (Q_a)_P \left[\pi n^2 (D_M)^2/4\right] y, \text{ cfm}$$

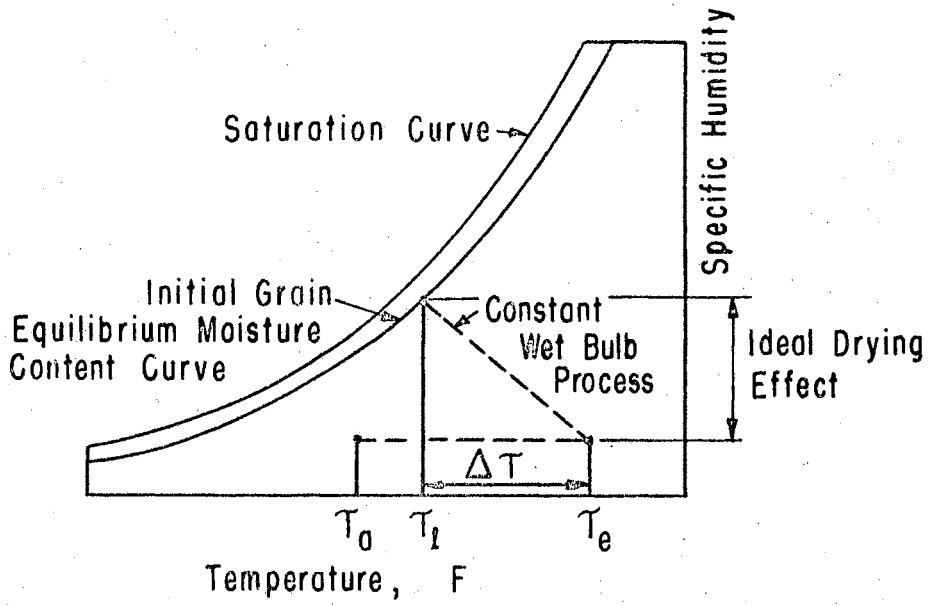

FIGURE 3-1. Skeleton psychrometric chart with a superimposed equilibrium grain moisture curve showing computation of ΔT.

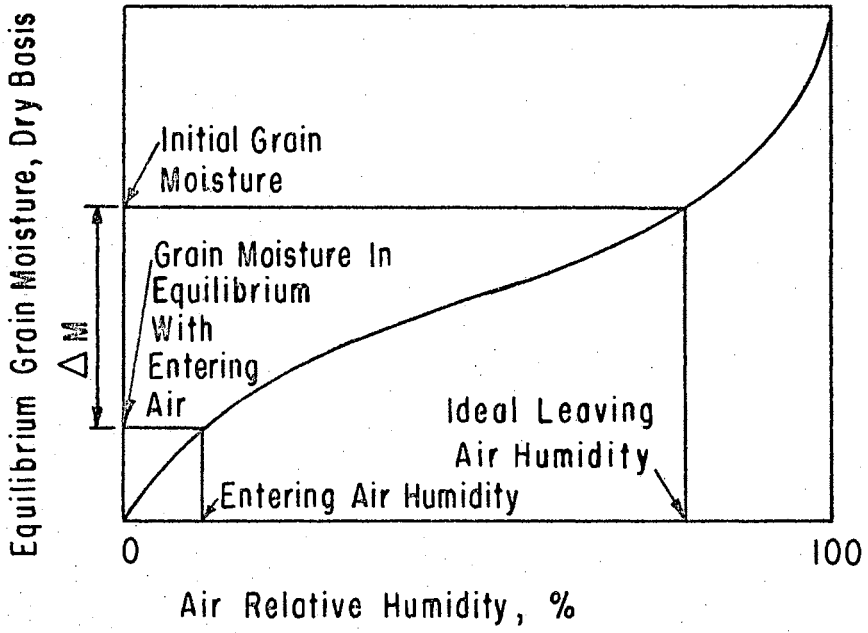

FIGURE 3-2. An equilibrium grain moisture isotherm showing computation of ΔM.

in which V = volume, ft^3

D = diameter, ft

y = increment of height, equal in model and prototype, ft.

The nominal air velocity is equal to the flow rate divided by the cross sectional area normal to flow at kernel location. The cross sectional area normal to flow is proportional to the width of the bin at a specified point times the height increment y, thus:

$$(v_n)_M = (Q_a)_M\left[\pi(D_M)^2 y/4\, c\, y\, \ell\right]$$

$$= (Q_a)_M\left[\pi(D)_M^2/4\, c\, \ell\right]$$

$$(v_n)_P = (Q_a)_P\left[\pi n^2 (D_M)^2 y/4c\, n\, \ell\, y\right]$$

$$= (Q_a)_P\left[\pi n (D_M)^2/4\, c\, \ell\right]$$

in which v_n = nominal air velocity, ft per min

D = bin diameter

c = proportionality constant

ℓ = width of bin at location of kernel being considered

The ratio of nominal velocities in model and prototype is:

$$(Q_a)_M\left[\pi(D_M)^2/4\, c\, \ell\right]/(Q_a)_P\left[\pi n (D_M)^2/4\, c\, \ell\right]$$

for equal volumetric flow rates in model and prototype, $(Q_a)_M = (Q_a)_P$:

$$(v_n)_P = n(v_n)_M.$$

Thus, for equal volumetric flow rates in model and prototype, the nominal air velocity past a kernel in respective positions in model and prototype is n times as great in the prototype as in the model.

The actual velocity would be much greater than the nominal velocity since the cross sectional area open to air flow is reduced by the amount of solid material present. However, for the same grain in model and prototype, it would seem the ratio of velocities past a kernel would be as the above analysis indicates.

The time of air travel to respective points in model and prototype was analyzed as follows.

Time for air to traverse bin = distance through bin/velocity of air

$$\text{Time through model bin} = (D)_M/(v_n)_M$$

$$= (D)_M/(Q_a)_M\left[\pi(D)_M^2/4\,c\,\ell\right]$$

$$= 4\,c\,\ell/(Q_a)_M\pi(D)_M$$

$$\text{Time through prototype} = (D)_P/(v_n)_P$$

$$= n(D)_M/(Q_a)_P\left[\pi n(D_M)^2/4c\,\ell\right]$$

$$= 4c\,\ell/(Q_a)_M\pi(D)_M$$

Thus for $(Q_a)_M = (Q_a)_P$, the time of air travel to respective points in model and prototype is equal in model and in prototype.

The air circulation pi term $Q_a t$ was thought to also fulfill the desired requirements of characterizing the amount of air the grain is exposed to and the length of path the air has been in contact with grain previous to arriving at some specified position in the grain mass. A term that fulfills these requirements in uniform grain depth drying systems is $V\phi/\lambda$, (26),

in which V = air circulation rate, cfm/sq ft

ϕ = elapsed time since start of drying process, min

λ = grain bed depth thickness, ft.

The term $Q_a t$ as related to cross-flow drying seems to be analogous to the term $V\phi/\lambda$ used in uniform drying as will be shown for a two duct system.

v = velocity of air = air flow rate/ cross sectional area normal to flow

let v_a = avg velocity at center of bin

thus, $v_a = (Q_a \pi D^2 Y/4)DY = Q_a \pi D/4$

now $v_a t/D = Q_a \pi Dt/4D$ which is proportional to $Q_a t$ since $\pi/4$ would be constant.

Parameter for Heat Transmission Through the Bin Wall

It was considered necessary to investigate the characteristics of heat transfer through the walls of model bins and prototype bins, especially when using heated air in model bins. It seemed reasonable to expect that heat loss from the model bin wall to the surrounding atmosphere could have a significant effect upon the results of drying grain in small model bins in which the ratio of exposed wall surface area to contained volume would be much higher for the model bin than for the full sized bin. The ratio was found to be:

$$(\text{Surface area/volume})_P = (1/n)(\text{Surface area/volume})_M$$

or $$(\text{Surface area/volume})_M = n(\text{Surface area/volume})_P .$$

Several of the dimensionless numbers prominent in heat transfer studies were considered such as Prandtl number, Nusselt number, and others. However, the parameter chosen, $U\Delta\tau_w/\rho_a c_a Q_a r \tau_e$, which is the

product of $\pi_6' \times \pi_7$ was thought to characterize the ratio of heat input to a bin to heat transmission through the bin wall.

Static Pressure Parameter

The pressure required to overcome the resistance offered to the flow of air by the grain was characterized by a pressure head unit P, as was done by Rose (29) in a study of fluid flow through porous media, instead of units of force per unit area. This was done to facilitate dimensional analysis and to have a unit which was similar to that used by blower manufacturers. The static pressure parameter was P/r.

Form of Reynolds Number

Previous investigations have shown that the head of fluid necessary to maintain a certain nominal velocity of flow through a bed of granular material is dependent in some way upon the density and the absolute viscosity of the fluid, upon the length of path of fluid travel, the diameter of the particles, and the diameter of the container of the particles (29, p 137). A form of Reynolds number, $\rho_a r^2 Q_a N_e / \mu$, seemed appropriate in the study of flow of air through a bed of grain, especially since viscous resistance could be characterized in this way and a direct term of air resistance was not employed.

Experimental Treatment Schedule

To facilitate experimental research, the general prediction equations 3-1 and 3-2, for the thermal drying system and air circulation system respectively, were reduced to manageable proportions

by considering a separate prediction equation for each type of grain and for each type of bin configuration. The form of the general prediction equation for the thermal drying system was reduced to:

$$\pi_1 = f(\pi_2, \pi_4, \pi_5, \pi_6). \qquad 3\text{-}4$$

The general prediction equation for the air circulation system was reduced to:

$$\pi_{11} = f(\pi_{12}, \pi_{14}). \qquad 3\text{-}5$$

A set of experiments was designed to evaluate the relationship of equation 3-4 and was designated as the treatment schedule for the thermal drying system, Table IV. The treatment schedule is to be repeated for each bin configuration and for each type of grain. A range of each pi term was planned so the prediction equation would be directly applicable to prototype installations without extrapolating the results from which the prediction equation was formulated. The approximate range to be covered for the terms was:

π_2,	0.0022	to	0.017
π_5,	1.00	to	1.17
π_6,	0.00036	to	0.0035
π_4,	0	to	12,000.

The results from "calibration of air flow rate" were used to evaluate the relationship of the prediction equation for the air circulation system. These experiments are reported in Chapter IV, Experimental Procedure.

TABLE IV

TREATMENT SCHEDULE FOR GRAIN DRYING EXPERIMENTS

π_1	π_2	π_5	π_6	π_4
Measure π_1 for each run	$(\pi_2)_1$ $(\pi_2)_2$ $(\pi_2)_3$ $(\pi_2)_4$ $(\pi_2)_5$	$\bar{\pi}_5$*	$\bar{\pi}_6$	$\bar{\pi}_4$
	$\bar{\pi}_2$	$(\pi_5)_1$ $(\pi_5)_2$ $(\pi_5)_3$ $(\pi_5)_4$ $(\pi_5)_5$	$\bar{\pi}_6$	$\bar{\pi}_4$
	$\bar{\pi}_2$	$\bar{\pi}_5$	$(\pi_6)_1$ $(\pi_6)_2$ $(\pi_6)_3$ $(\pi_6)_4$ $(\pi_6)_5$	$\bar{\pi}_4$
	$\bar{\pi}_2$	$\bar{\pi}_5$	$\bar{\pi}_6$	$(\pi_4)_1$ $(\pi_4)_2$ $(\pi_4)_3$ $(\pi_4)_4$ $(\pi_4)_5$

* Bar denotes constant value of pi term

Experimental Equipment and Instrumentation

Miniature Model Bins

The equipment used in the experiments with the miniature model bins will be listed under the headings of Calibration of Air Flow Rate and Grain Drying Experiments.

The equipment and instrumentation set up for calibration of air flow rate through the grain is shown in Figure 3-3. The component parts were:

1. Tank for compressed air.
2. Scales to weigh air tank. Toledo Balance scales, Serial No. 882309, Model 4032-Y, 0 to 5 lb capacity.
3. Air line hookup from air tank to plenum chamber consisting of: flexible air hose, air pipeline, valve, and pressure regulator.
4. Plenum chamber.
5. Pressure inclined manometer and pressure micromanometer. The inclined manometer was a Meriam draft gauge, Serial No. F-4, Model B-627, Type GP-4, single tube, pressure range of 0 to 2 inches water in 0.01 inch increments. The micromanometer was a Dwyer hook gauge manometer, Model 1420, pressure range of 0 to 2 inches of water with smallest division of 0.001.
6. Stop watch.
7. Model bins filled with grain. Details of the bins are included in the grain drying experiments.
8. Air wet and dry bulb temperature measuring psychrometer for ambient air before being compressed. A Friez hand-aspirated

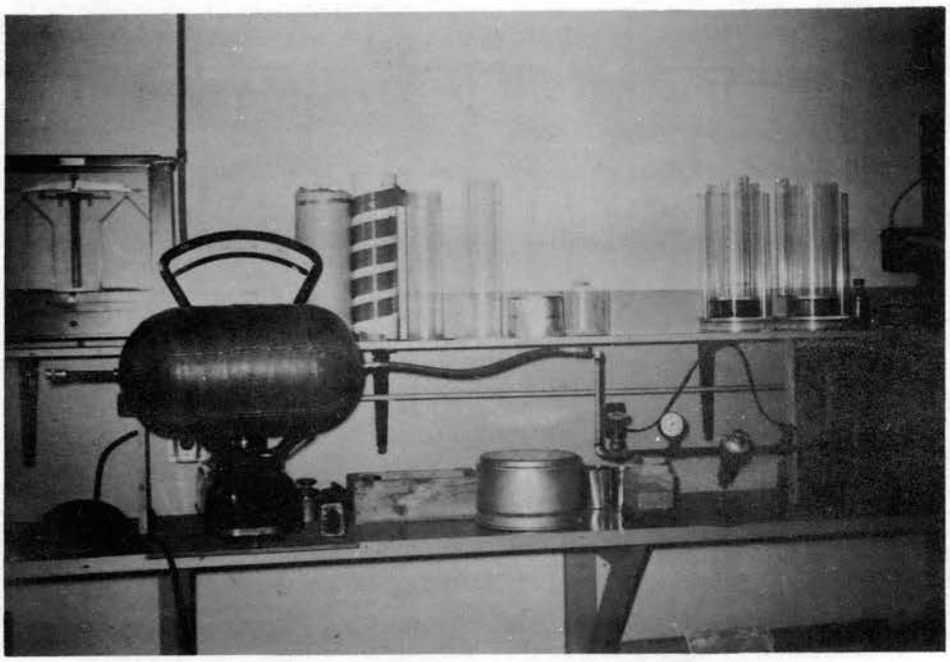

FIGURE 3-3 Equipment and instrumentation for calibration of air flow rate

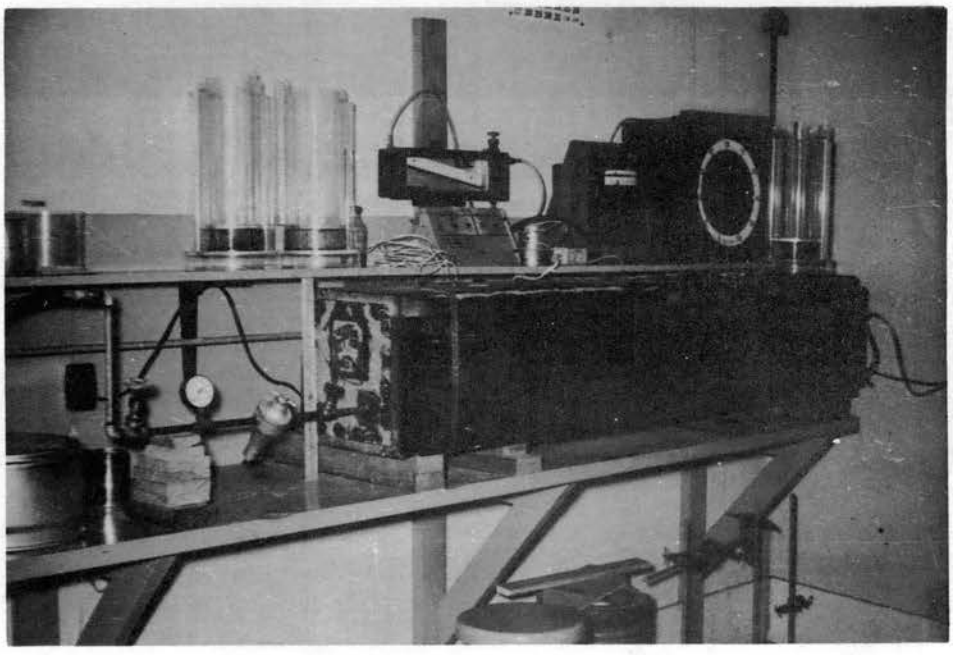

FIGURE 3-3 (continued)

psychrometer, Model HA-2.

9. Air dry bulb temperature thermocouple and indicator for air in plenum chamber. A Brown Electronik single point temperature recording potentiometer, Serial No. 605641, Model 152x13P-x-11 for iron constantan thermocouples, 0 to 200 F.
10. Air compressor for charging air tank.
11. Barometer. A Cenco mercurial barometer, Catalog No. 76878.

The equipment and instrumentation used in the grain drying experiments are shown in Figure 3-4. For the drying experiments, the plenum chamber was moved from the shelf, as used in the air flow calibration experiments, down to a platform near the floor so the scales could be mounted above the exhaust port of the plenum chamber.

The three miniature model bins with cross-flow configurations were built of clear lucite plexiglass according to Figure 3-5. Figure 3-6 is a photograph of the three miniature model bins. The bins were covered with two inch thick insulation and a cover of polyethylene plastic film was sealed around the insulation, as shown in Figure 3-7, in order to minimize error in change of weight of the bins during the experiment due to the hygroscopic properties of the insulation around the bins.

The model bins were set in place on a cradle which was attached to the scales at the top of the cradle and to a flexible tube connecting the bottom of the cradle with the exhaust port of the plenum chamber. By this arrangement, change of grain moisture content would be noted by the scale reading. An insulated outer chamber surrounded the cradle and bin. The flexible tubing connecting the cradle with the plenum exhaust port was very thin polyethylene

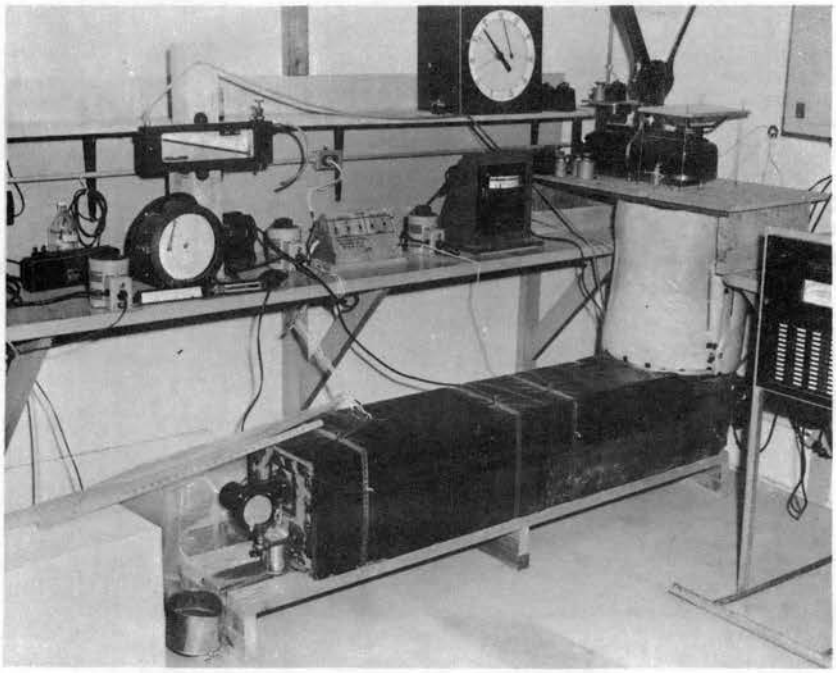

FIGURE 3-4 Equipment and instrumentation used in drying grain in miniture model bins.

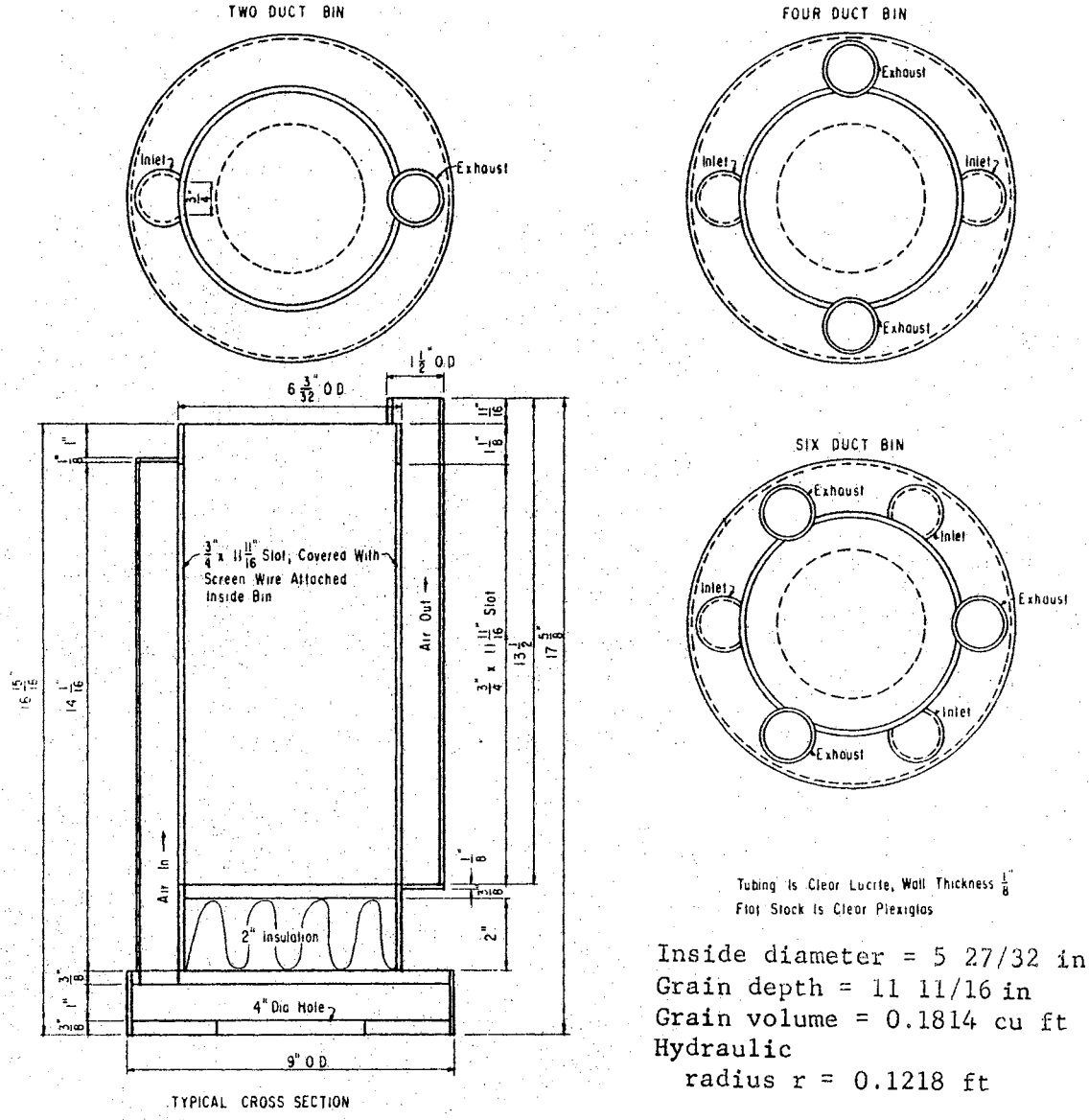

FIGURE 3-5. Design details of miniature model bins.

plastic film. The apparatus was sensitive to one gram when the extension of the tubing was maintained constant. The cradle inside the opened outer chamber is shown in Figure 3-8, the plastic tubing connecting the bottom of the cradle with the exhaust port of the plenum chamber is blocked from view by the bottom of the cradle.

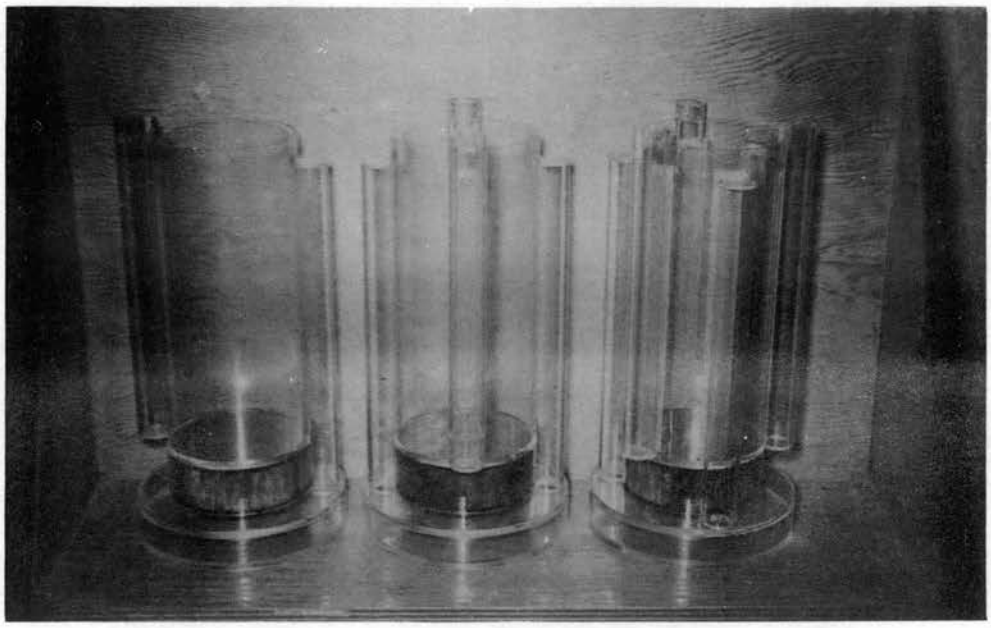

FIGURE 3-6 Three miniature cross-flow model bins built of plastic.

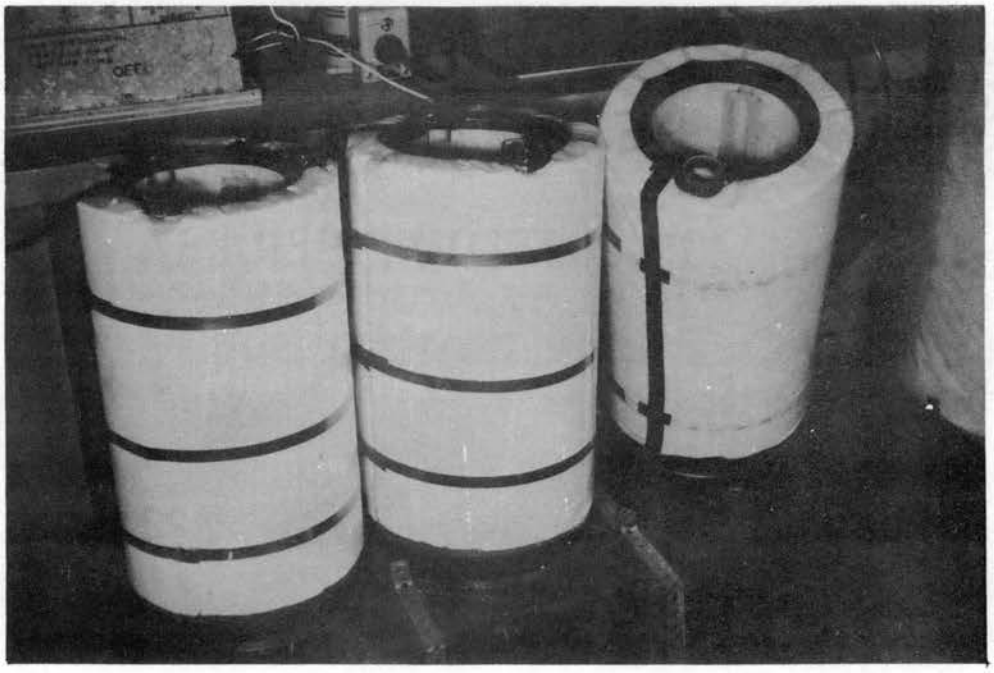

FIGURE 3-7 Miniature model bins with insulation.

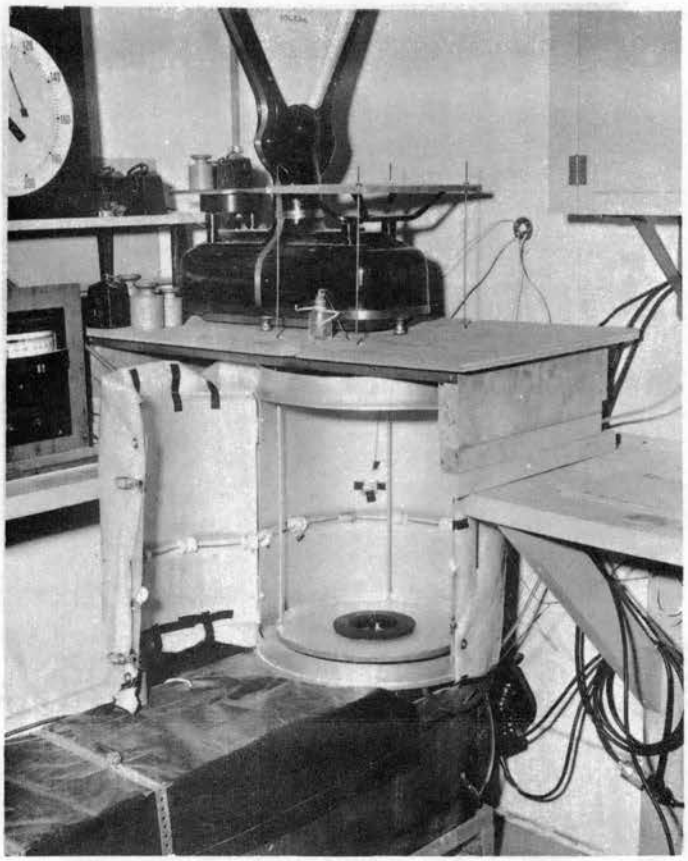

FIGURE 3-8 Opened outer chamber showing cradle on which the bin rests.

Figure 3-9 shows a bin in place resting on the rubber gasket on the bottom of the cradle.

A floating seal was used to cover the top surface of the grain when the bins were in use so that the seal followed the grain as the grain dried and shrank and prevented short circuiting of the cross-flow air. The floating seal consisted of covering the grain with a sheet of thin plastic film, placing a cone on the film as in Figure 3-10, and pouring dried sand over the cone so that the film was pressed tight against the bin wall. The exposed film was then folded over the sand so that the seal could slide down the inside of the bin as the grain shrank.

The component parts of the drying set up were:

1. Dehumidifier. A Coldspot automatic dehumidifier, Serial No. 1C369050, Model 106.614150.
2. Humidifier. A pan of water setting over an electric heating element with variable heat controller.
3. Air supply blower. A Fasco centrifugal blower, Serial No. 50748, Model J118, 100 cfm capacity at free delivery and 0.8 inch water cutoff pressure.
4. Plenum chamber with internal electrical heating elements and controls for the heater. The controller was a Brown Electronik temperature indicator and controller, Serial No. 561940, Model 105C4p22 for iron-constantan thermocouple sensing elements. See wiring circuit in Figure 3-11.
5. Cradle on which to suspend bins from weighing scales.
6. Weighing scales. Same as component part No. 2 in calibration set up.

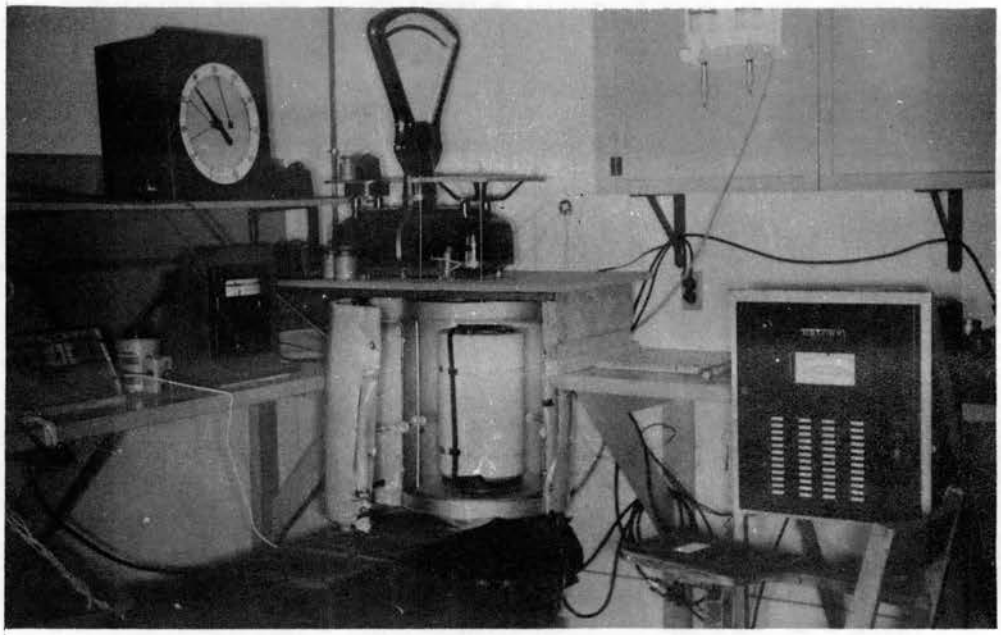

FIGURE 3-9 Opened outer chamber showing a bin in place.

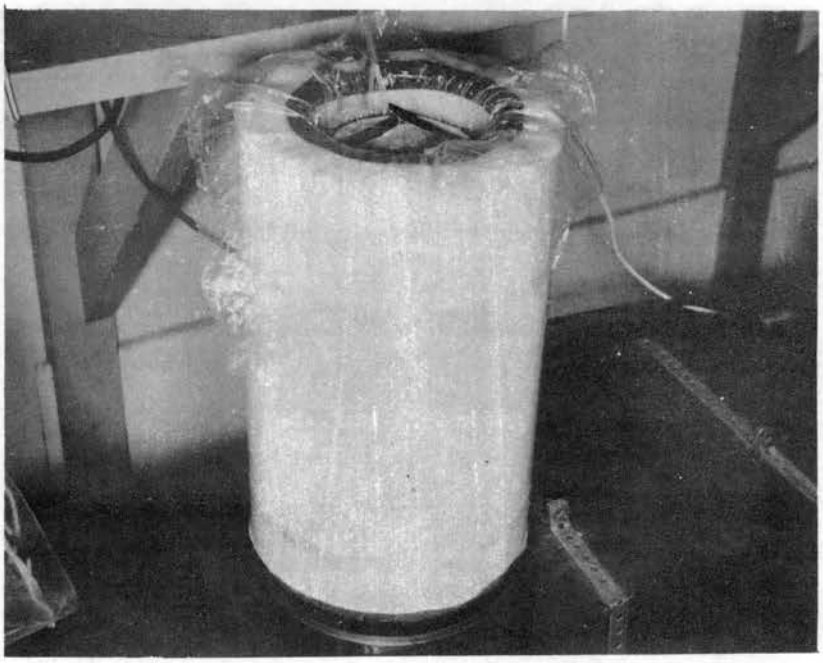

FIGURE 3-10 Cone and plastic film of floating seal used on miniature model bin.

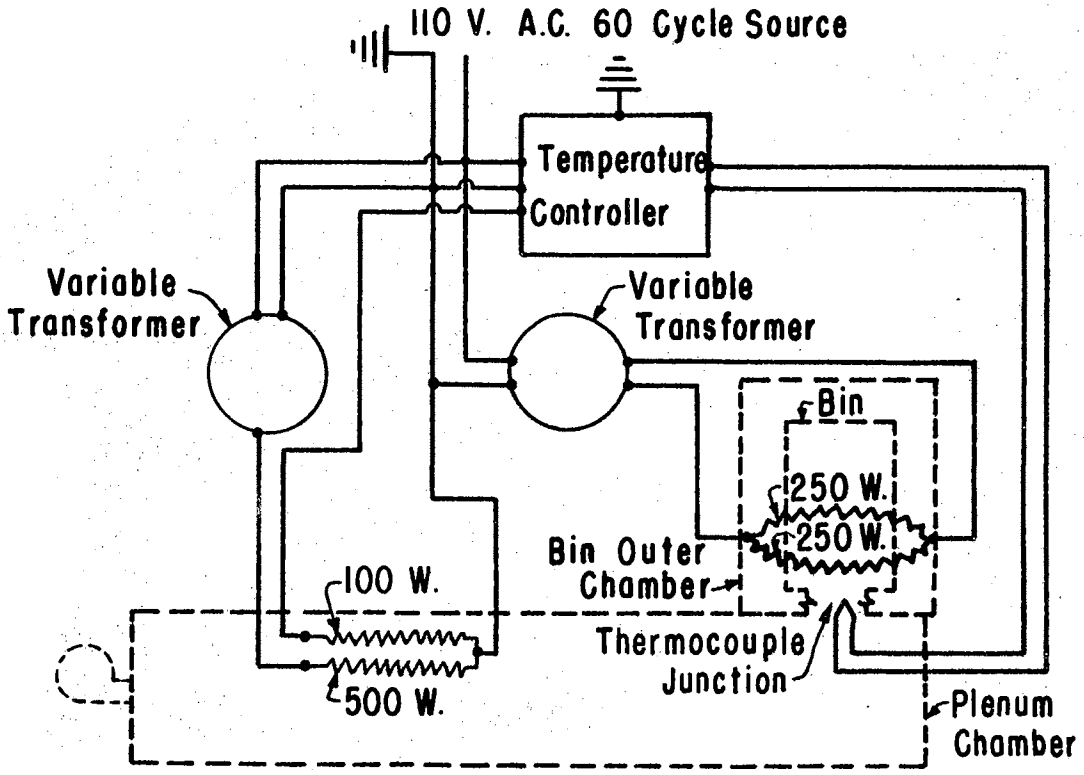

FIGURE 3-11. Electrical wiring circuit for heating elements in plenum chamber and in outer chamber.

7. Insulated outer chamber, around bin and cradle, with a built-in 500 watt heating element and variable heater control. See wiring circuit in Figure 3-11.

8. Model bins as described above and floating seal to cover exposed grain when bin is in place on cradle.

9. Inclined manometer and hook gauge for chamber pressure. Same as component part No. 5 of calibration set up.

10. Temperature thermocouples and indicating instrument for measuring temperature of:

    ambient air - wet and dry bulb;

    air entering grain - dry bulb; and

    exhaust air from bin - wet and dry bulb.

A Brown Electronik 48 point indicating potentiometer for iron-constantan thermocouple sensing elements, Serial No. 553140, Model 156 65Ps48, 0 to 300 F.

11. Grain supply contained in plastic film bags which were kept inside a refrigerated cold storage chest. The grain was "Kaw" variety hard red winter wheat of the 1961 harvest in a natural state of varying moisture contents from 21 per cent to 16 per cent, dry basis.
12. Drying oven and weighing scales for determining initial grain moisture content. The oven was a Precision Scientific Co., Serial No. 130-380, 800 watts with a temperature controller with 1 F sensitivity. The scales were Torsion Balance, Serial No. 42479, Model IL-6, 2 kg capacity with 0.1 gm divisions.
13. Instrument bench vibrator. A 1/4 hp electric motor was used as a bench vibrator to give increased sensitivity to the dial instruments.
14. Blower to circulate air around bin inside outer insulated chamber.
15. Timing watch.
16. Barometer. Component part No. 11 of calibration set up.
17. Therometer to measure initial temperature of bins and grain. A Taylor liquid in glass thermometer Model 208, 0 to 120 F with 1 F divisions.

Two-foot Diameter Model Bins

The two-foot diameter model bins were built on a length scale of 1/10 that of a hypothesized prototype 20 foot diameter by 100 foot

tall except the height of the models was further reduced. The model bins had inside dimensions of two-foot diameter by four-foot high and were built according to the plans of Figure 3-12. The test section, from which moisture content samples were taken, was the two-foot depth of grain located one foot from either end, see Figure 3-13. The test section of grain was thought to be representative of a unit depth of grain anywhere in the prototype except near the top or bottom due to end effects and except for the effect of grain compaction which might occur in the prototype.

The vertical ducts for air circulation across the bins extended six inches above and below the test section but lacked six inches of reaching the top or bottom of the bins. With this arrangement and by maintaining the bins in an almost full condition, it was believed that end effects and short circuiting of air, not passing through the full cross-flow path, were minimized.

The model bins had removable lids which were removed for filling, emptying, and for sampling the grain. A sampling lid was prepared with holes in it for taking samples of grain at desired positions using a miniature grain trier.

The air inlet, air exhaust, and bisector radials of each bin were designated as shown in Figures 3-14, 3-15, and 3-16. Positions 1, 2, and 3 were for samples from an air inlet radial; 4, 5, and 6 were from an air exhaust radial; 7, 8, and 9 were from a bisector radial; 10 was in the center of the bin; and 11, 12, and 13 were positions in the extra radials of bin type I. All these positions are also shown in Figures 3-14, 3-15, and 3-16 and from these figures it can be noticed that positions 1, 4, and 7 (of the radials except the extra radials of

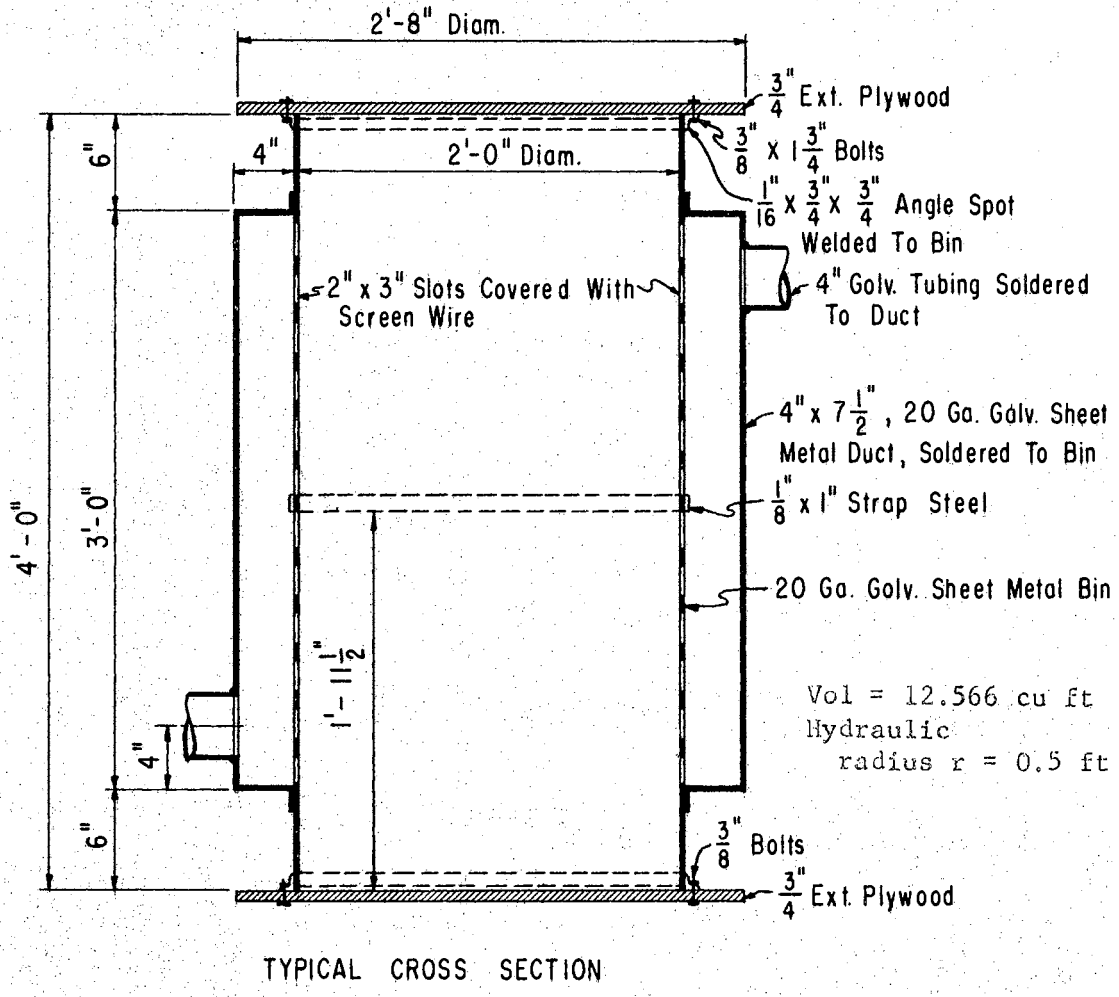

FIGURE 3-12. Design details of two-foot diameter model bins.

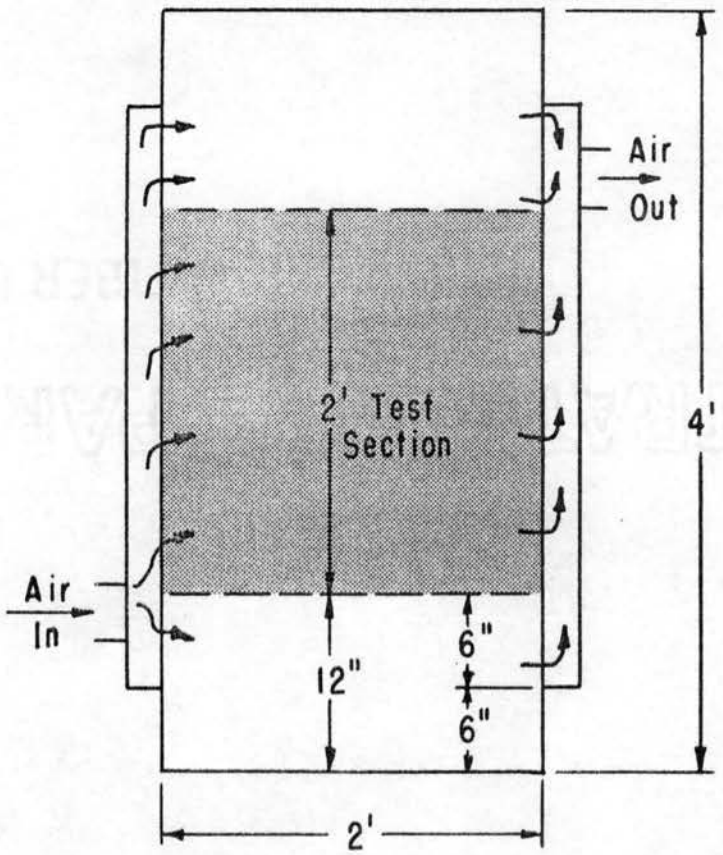

FIGURE 3-13. Test section of grain in two-foot diameter bins.

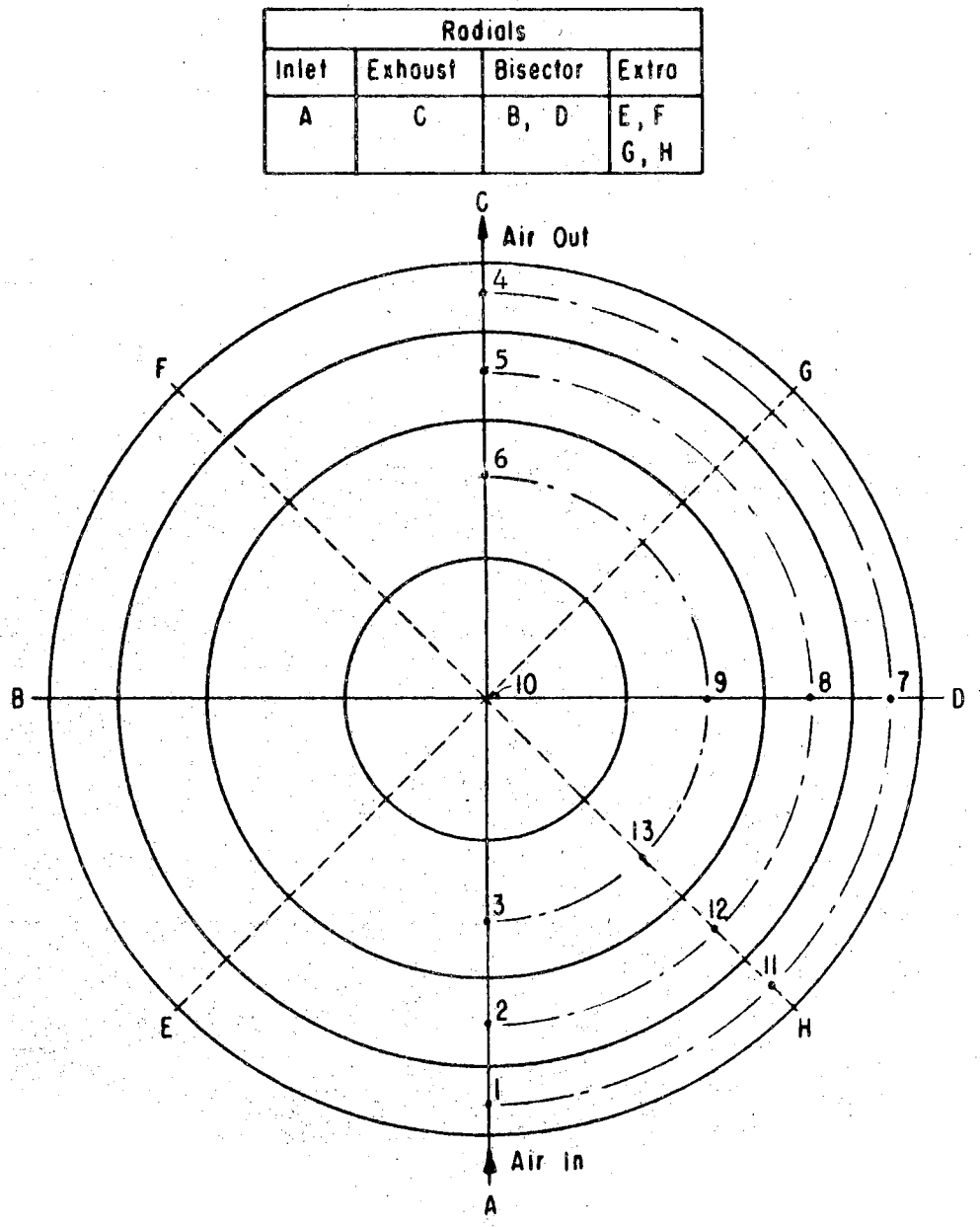

FIGURE 3-14. Designation of radials and sampling positions, two-foot diameter bin type I.

Radials		
Inlet	Exhaust	Bisector
A	C	B, D
E	G	F, H

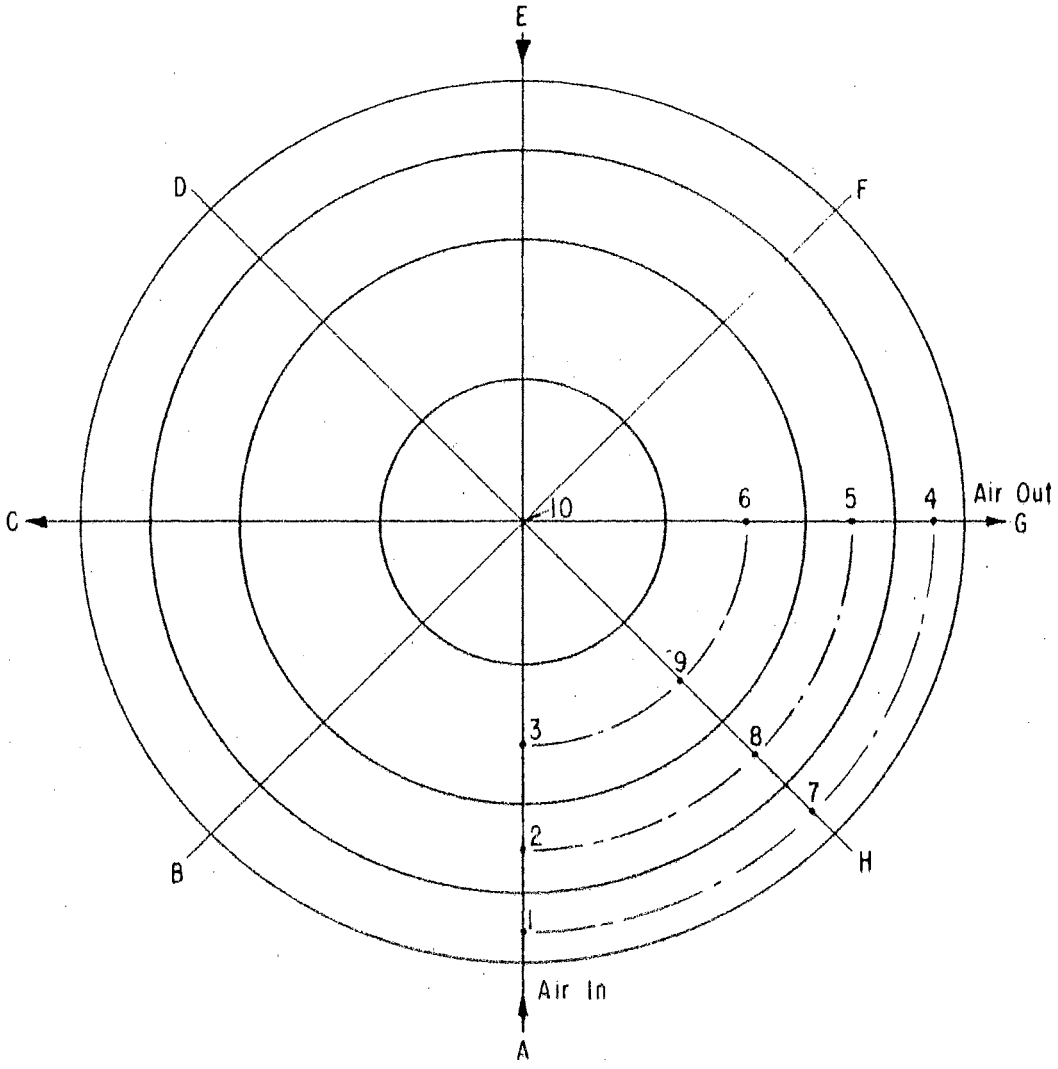

FIGURE 3-15. Designation of radials and sampling positions, two-foot diameter bin type II.

Radials		
Inlet	Exhaust	Bisector
A	C	B, D
E	G	F, H
I	K	J, L

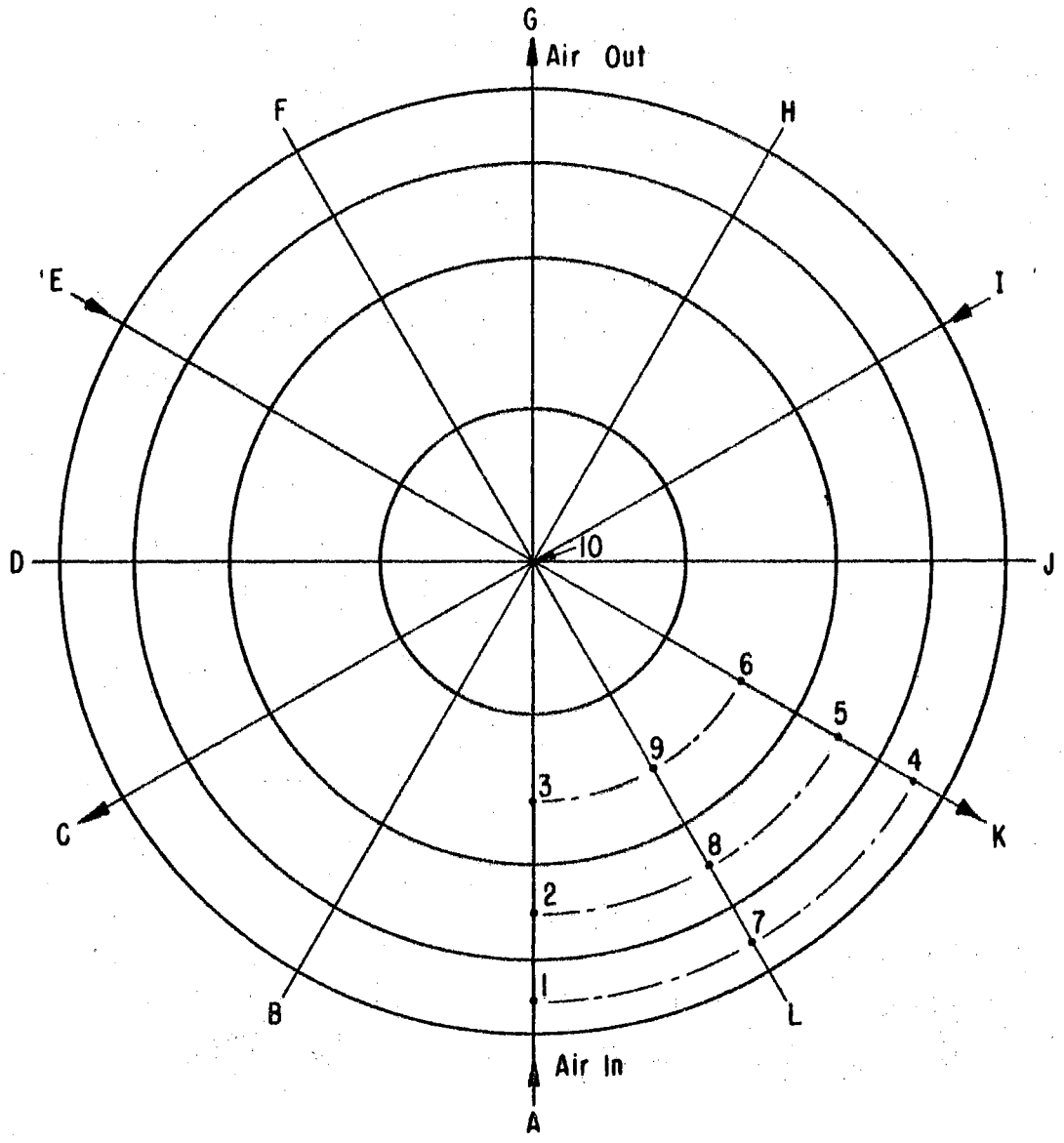

FIGURE 3-16. Designation of radials and sampling positions, two-foot diameter bin type III.

bin type I) are located at the mid-area of an outer concentric area. Also, positions 2, 5, and 8 are at mid-area of another concentric area, and positions 3, 6, and 9 are at mid-area of a third concentric area. These three areas are equal but the inner area which contains position 10 is only 1/3 as large as each of the three concentric equal areas. The above position layouts were for convenience in sampling the grain during the drying experiments.

An overall view of the three model bins and equipment is shown in Figure 3-17. Each model bin had an individual air blower, transition duct from blower to air straightening tube, air straightening tube in which to measure air flow rate, and inlet air and exhaust air manifolds and vertical plenum chambers spaced around the bin as required.

The blowers were Lau 7 inch wheel blowers with built-in motors. Capacity of the blowers was 725 cfm against a static pressure of 1/4 inch of water, operating from 115 volts 60 cycle a-c electrical source.

The air straightening tubes were 4 inch diameter aluminum tubes designed to meet diameter and length specifications required of a tube in which to measure air flow rate with a standard pitot-static tube. (2).

Air supply and exhaust manifolds and ducts were required on bins II and III as shown in Figures 3-18 and 3-19 respectively. The manifold air branching pieces were galvanized metal of the same size diameter as were the straightening tubes. Flexible ducts fabricated of 6 mil vinyl plastic film were used to connect the branching pieces to the vertical plenum chambers on the bins. Coiled wire shape maintainers were installed inside the plastic film ducts.

The other component parts of the experimental set up were:

1. Pitot-static tube and manometer for measurement of air

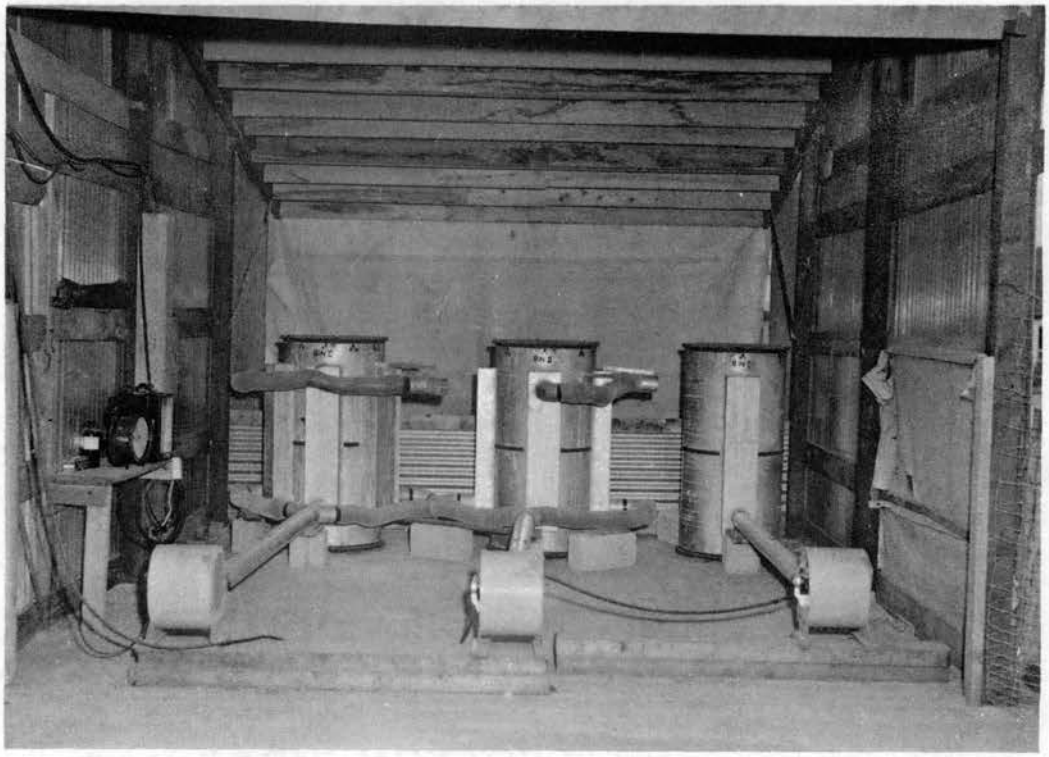

FIGURE 3-17 Two-foot diameter model bins and equipment. Front wind barrier removed, backdrop in rear of shed.

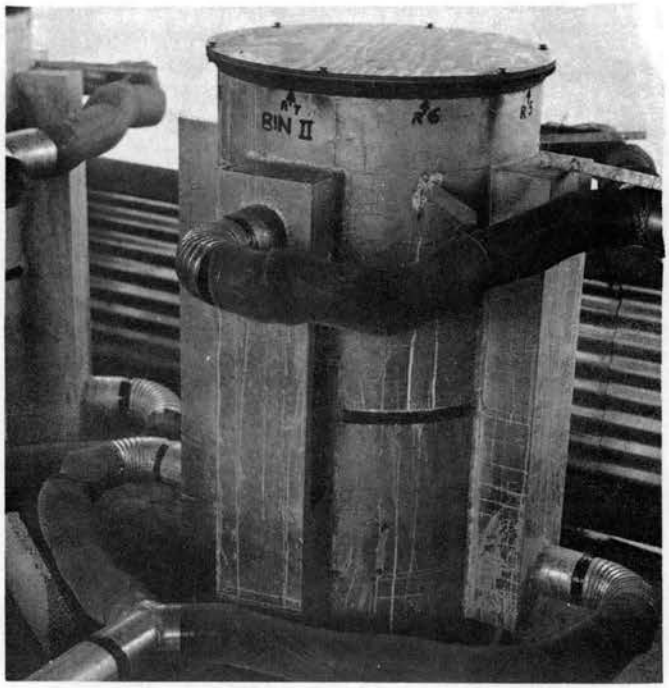

FIGURE 3-18 Air supply and exhaust manifolds and ducts of bin type II.

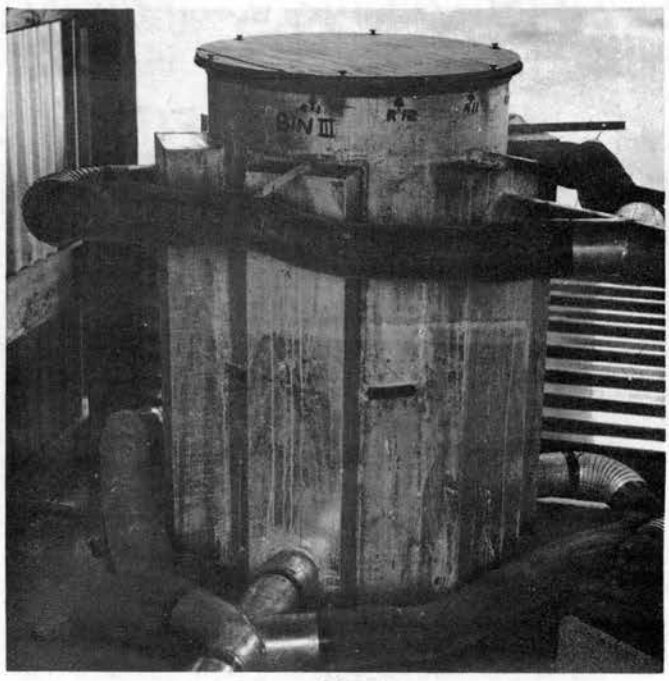

FIGURE 3-19 Air supply and exhaust manifolds and ducts of bin type III.

velocity and static pressures. The pitot-static tube was a Dwyer 5/16 inch diameter standard tube, 12 inches insertion length. The manometer, Figure 3-20, was shop built using alcohol with a specific gravity of 0.792 at standard temperatures and pressure and could be read to 0.001 inches of alcohol.

2. Thermohumidgraph for continuously recording ambient air temperature and relative humidity, Bristol, Serial No. F40691H.
3. Esterline-Angus recording watt-hour meter for recording blower operation time, Serial No. 111,100.
4. An upper limit air humidity switch which allowed the blowers to operate only when the ambient air humidity was below that of the switch setting. Minneapolis-Honeywell humidifier control type H44B.
5. Potentiometer calibration in F for use with an iron-constantan thermocouple junction for measuring temperature of air entering the grain and intergranular temperatures. Leeds and Northup, Serial No. 1157089.
6. Static pressure probe used with manometer listed in 1 above for measuring intergranular static pressure. The probe was built as in Figure 3-21.
7. Miniature grain trier, probe, for removing samples of grain for determining grain moisture conents. Seedburo bag trier, 30 inches long and 1/2 inch outside diameter. The trier was slightly modified in length to sample from the middle two-foot depth of the bins. Iron-constantan thermocouple leads were attached to the trier for taking intergranular temperatures mentioned in 5 above.

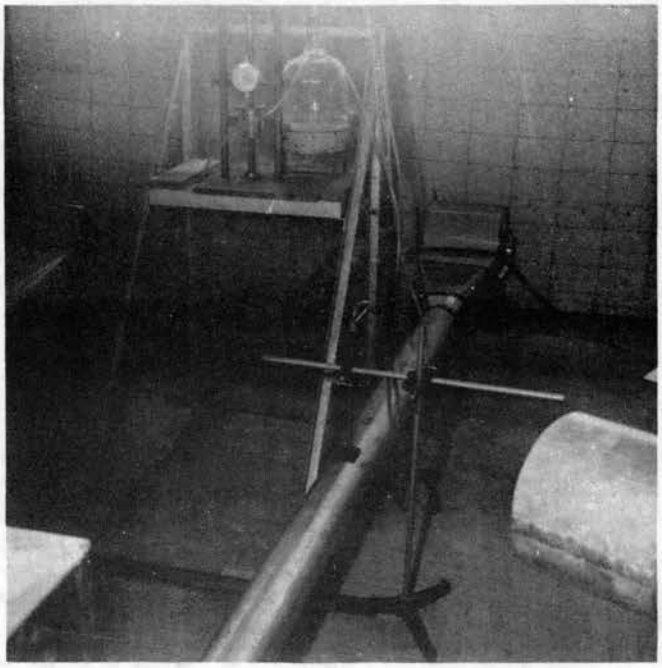

FIGURE 3-20 Manometer and pitot-static tube for measuring air flow rate.

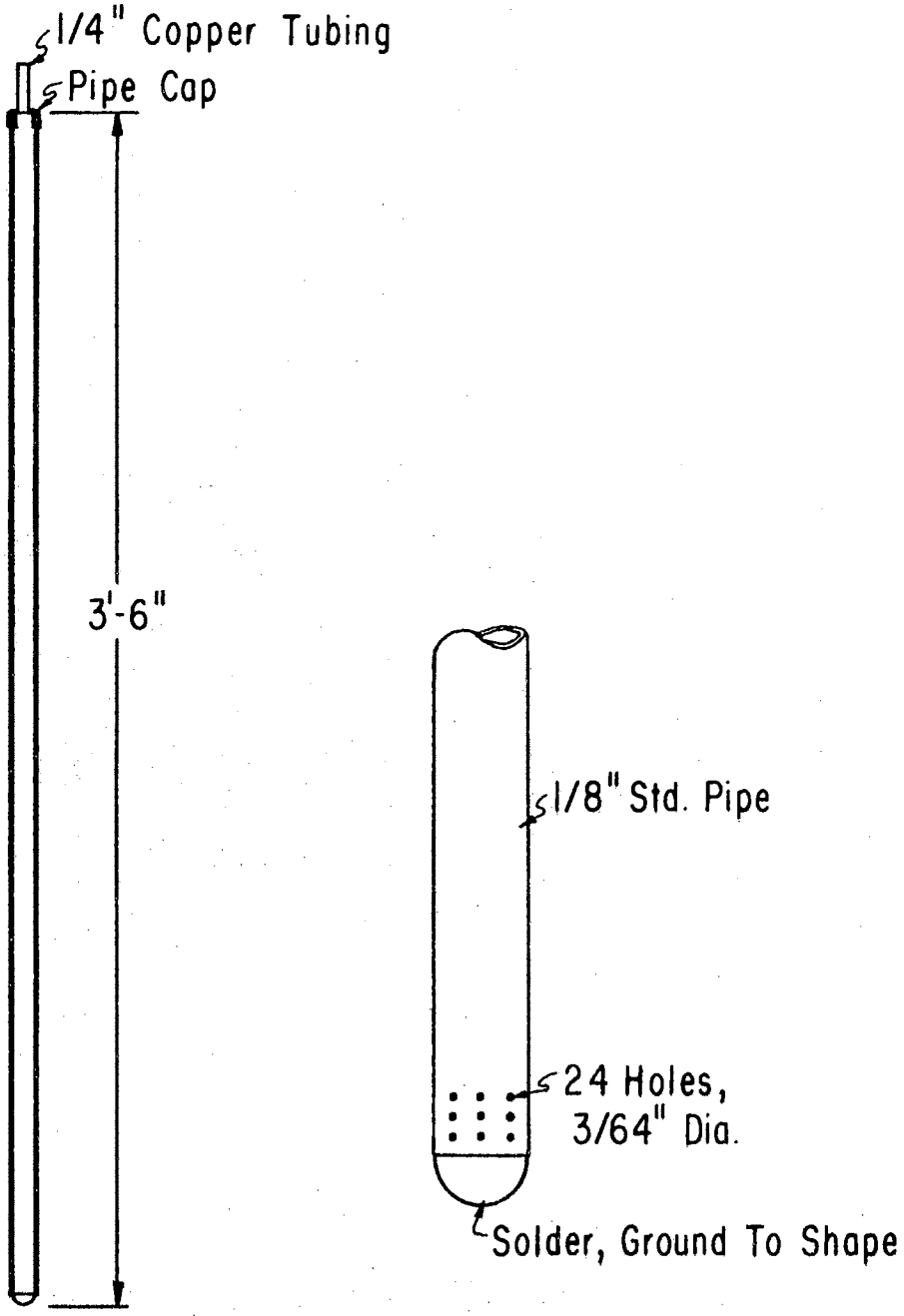

FIGURE 3-21. Probe for measuring intergranular pressures in two-foot diameter bins.

8. Drying oven in which to dry the grain samples to determine grain moisture content. The oven was modified to include forced air circulation and an automatic temperature controller which maintained the temperature within 2 F of the set point. The oven basic unit was a Precision Scientific Co., 800 watts, 115 volts, 60 cycle, Serial No. 130-380.
9. Scales to weigh samples of grain. Torsion Balance Style IL-6, Serial No. 42479, with 0.1 gram smallest scale division.
10. Hand aspirated Friez psychrometer for measuring ambient air and exhaust air wet and dry bulb temperatures.
11. Mercurial barometer, Cenco, Catalog No. 76878.
12. Air tight cans in which to briefly store and transport the grain samples to the weighing scales.

The two-foot diameter bins and equipment were set up in a shed with open front and back except that a three-foot high wind barrier was installed on front and back of the twelve-by-fourteen foot building to prevent wind from blowing directly on the blowers. The shed was orientated east and west with the bins aligned along the south side of the shed floor.

Due to the limited electrical current which can be carried by the recording watt-hour meter, the meter was connected to only one of the blowers, blower No. III. All three blowers were in series with the power relay which was controlled by the upper limit humidity switch. Thus, when the ambient air relative humidity was below the switch setting, the relay supplied power to the blowers simultaneously and blower No. III furnished a record of operating time of all three blowers through the recording watt-hour meter. The electrical circuit is shown in Figure 3-22.

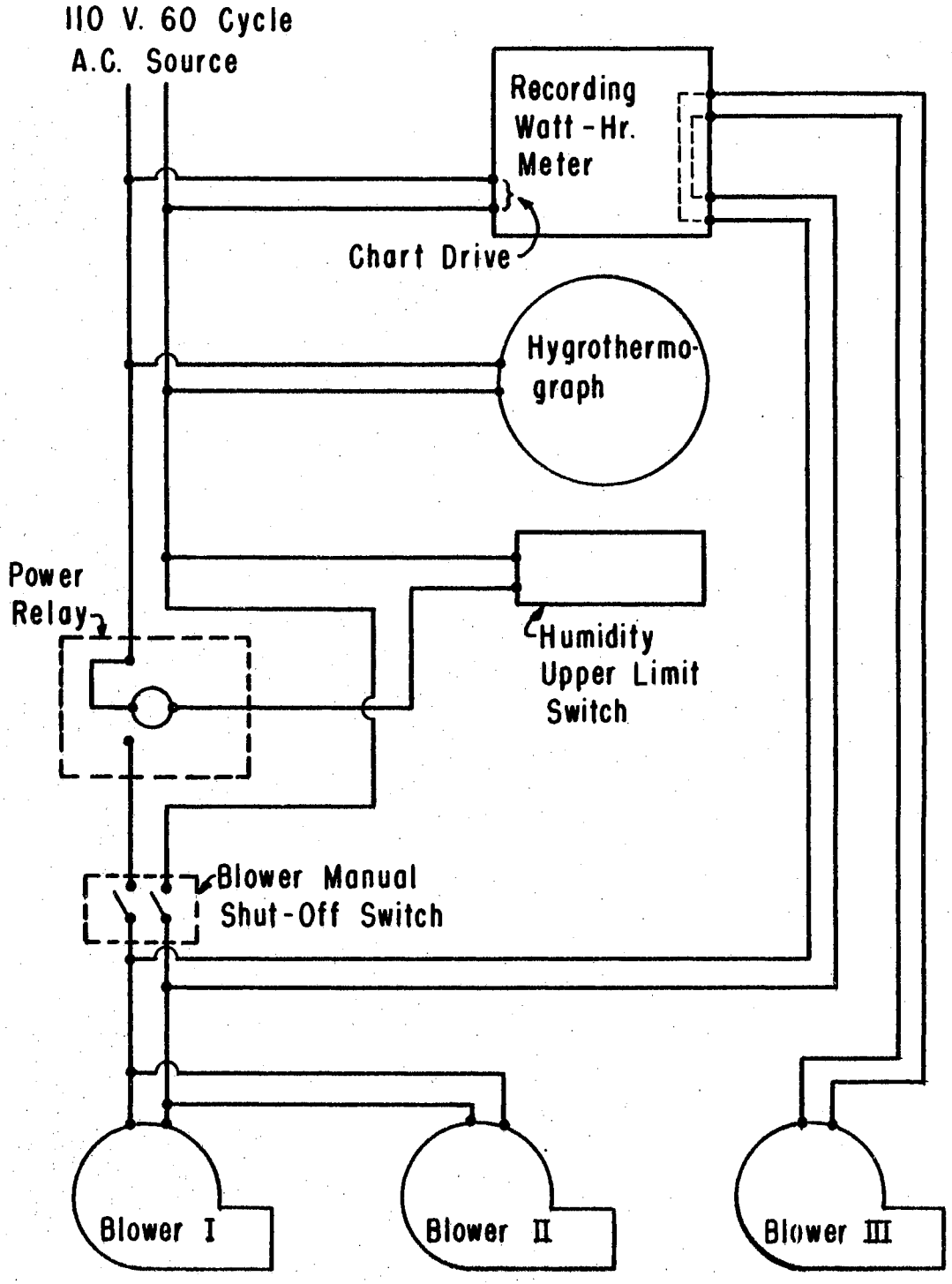

FIGURE 3-22. Electrical wiring circuit for instruments and blowers of two-foot diameter bins.

CHAPTER IV

EXPERIMENTAL PROCEDURE

Miniature Model Bins

The three miniature model bins, approximately six inches in diameter by twelve inches tall, having cross-flow configurations discussed in Chapter III under the heading, Experimental Equipment, were used one at a time in an indoor laboratory for drying of "Kaw" variety wheat.

The experimental procedure will be discussed under the headings of Air Circulation System and Thermal Drying System.

Air Circulation System

The equipment of Figure 3-3 was calibrated for air leakage rate with the plenum chamber exhaust port blocked. Then the port was opened and calibration of flow rate through the grain was made with a bin of grain in place over the exhaust port.

An air tank charged with compressed air was used as the air supply for determining the rate of air leakage from the plenum chamber at varying chamber static pressures. The general procedure was to adjust the pressure regulator to maintain a desired pressure in the chamber. The initial gross weight of the charged air tank and the starting time for each run were noted and after an experimental run, the gross weight of the air tank and the time were again

noted. The difference between the initial and final weights of the air tank gave the weight of moist air expended during the elapsed period of time. The chamber pressure was initially set by noting the reading of the inclined manometer. A more precise reading was taken from the micromanometer and the pressure regulator was adjusted if necessary.

Ambient air conditions were determined by measuring wet and dry bulb temperatures with a hand aspirated psychrometer before the air was compressed in an air compressor from which the air tank was periodically charged. Air moisture properties entering the chamber were corrected from ambient air conditions due to some moisture being condensed from the air in the compressor.

The range of pressure used in the leakage calibration was 0.10 to 1.00 inches of water. The runs were of 10 to 15 minutes duration and the air tank was recharged between runs to approximately 140 psi pressure.

The calibration of flow rate through the grain was similar to that used in calibration of the chamber for air leakage except the air outlet was not blocked and a bin filled with grain was in place over the exhaust port. Experimental runs of air flow rate through the grain were made as follows for the three bin types:

Bin type I - range of pressure from 0.02 to 0.2 inches water in 0.02 inch increments.

Bin type II - range of pressure from 0.01 to 0.07 inches water in 0.01 inch increments.

Bin type III - range of pressure from 0.01 to 0.06 inches water in 0.01 inch increments.

The above pressure ranges represent a range of flow rate from approximately 3 cfm per cu ft to approximately 25 cfm per cu ft.

The air tank would supply air at the above pressures for one to three minutes when initially charged to 140 psi pressure.

Thermal Drying System

The procedure followed in the drying experiments using the miniature model bins and equipment shown in Figure 3-4 will be presented in this section. In general, the procedure consisted of placing a bin of grain in the cradle over the plenum chamber exhaust port and forcing heated air through the grain. Moisture removed from the grain was reflected by a change of gross weight of the bin as shown by the weighing scale indicator. Control was exercised over: temperature, humidity, and flow rate of the air entering the bin; initial grain moisture content and grain temperature; initial temperature of the bin; and temperature of the air around the bin.

Detailed procedure will be listed as: A. Pre-run procedure; B. During run procedure; and C. Post-run procedure.

A. Pre-run procedure

1. Instruments and equipment

a. Zero manometer and micromanometer.

b. Plenum chamber exhaust port about 90 per cent closed.

c. Switch on plenum chamber blower. Monentarily switch blower off when bin of grain is placed on cradle, see 2-e below.

d. Switch on instrument bench vibrator.

e. Set plenum heater controls for desired temperature.

B. Procedure during run

1. Switch on plenum chamber blower, simultaneously starting timing watch.
2. Check scales from which bin is suspended. Add counter weights as necessary to bring and maintain dial reading about midscale.
3. Check plenum chamber static pressure from manometer and adjust blower output for approximate desired pressure. Refine adjustment from reading of micromanometer.
4. Take initial reading of:
   a. Gross weight of bin.
   b. Ambient air wet and dry bulb temperatures.
   c. Dry bulb temperature of air entering bin.
   d. Exhaust air wet and dry bulb temperatures.
   e. Dry bulb temperatures around bin.
   f. Plenum chamber pressure from micromanometer.
5. Make adjustments as necessary to maintain desired operating conditions.
6. Repeat readings of 4 at time intervals as prescribed by prearranged treatment schedule.

C. Post-run procedure

1. Remove bin from cradle and empty grain.
2. Shut down equipment as necessary.
3. Reweigh grain sample in oven after 72 hours of drying at 100 C.

Two-Foot Diameter Model Bins

The model bins and equipment shown in Figure 3-17 were used for drying grain sorghum, Hybrid R.S.-610 grain sorghum, dwarf yellow milo, in the fall of 1960 and Kaw variety hard red winter wheat in the summer of 1961. There were some alterations of the experimental procedure used for drying wheat from the procedure used to dry sorghum. These differences will be pointed out in the following discussion.

Before each experiment, the bins and ducts were checked for air leakage by measuring the air flow rate into and from each bin and comparing the results. The inflow and the outflow rates were simultaneously measured with individual pitot-static tubes. Although there was no grain in the bins during this check, the ends of the exhaust tubes were partially blocked to simulate the resistance to flow which would be encountered when the bins contained grain.

The procedure used during the drying experiments will be discussed under the following subjects: A. Filling the bins; B. Setting the equipment into operation; C. Measurements periodically taken; and, D. Sampling the grain for moisture content and temperature.

A. Filling the bins

1. The bins were filled with grain at the beginning of each experiment by using a grain auger. the discharge end of the auger was suspended at a fixed height above each bin successively. By this method, the grain was more uniformly distributed and compacted than if the grain had been scooped or poured in. Each bin held approximately 10 bushels but a total of 33 bushels was needed for each

experiment in order to have sufficient grain to maintain the bins in a full or almost full condition as drying progressed.

2. The grain was graded at the beginning and end of each experiment to detect any change in grade due to the drying process and to determine if there was any noticeable damage to the kernels.

B. Setting the equipment into operation

1. After the grain was placed in each bin at the beginning of each experiment, the blower manual shut-off switch (see Figure 3-22) was switched on and the upper-limit humidity switch set at 45 per cent relative humidity. The recording charts of the watt-hour meter and thermohumidigraph were set in operation and maintained with paper and ink throughout the experiment. A hand aspirated psychrometer was used to periodically check the ambient air temperature and humidity reading of the thermohumidigraph.

2. The humidity sensing element of the thermohumidigraph did not respond correctly to changes in the ambient air humidity so calibration graphs were plotted using humidity readings as measured by the psychrometer. These graphs are shown in Figures A-1 and A-2 for the sorghum and wheat drying experiments respectively.

3. Immediately after the blowers were set into operation at the beginning of each experiment, an attempt was made to achieve equal air flow rates to each bin. Since bin

type I offered the most resistance to air flow, the full output of blower I was allowed to flow through bin type I. This flow rate was measured using the pitot-static tube and manometer. The other two blowers were then adjusted to achieve the same air flow rate as in bin I by exhausting part of their output into the atmosphere. Complete equality of air flow rates in each bin was not achieved in the experiments due to difficulty in exhausting enough air from blowers II and III.

C. Measurements periodically taken

1. Barometric pressure and ambient air temperature at barometer location.
2. Ambient air wet and dry bulb temperatures.
3. Pressure measurements using pitot-static tubes in air straightening tubes from which to compute air flow rate to each bin.
4. Exhaust air wet and dry bulb temperatures.
5. Temperature of air in air straightening tubes. It was assumed that this was equal to the temperature of the air entering the grain.

The above measurements were taken often enough so that a reliable average of each measurement could be determined for each run except 4 above. Exhaust air wet and dry bulb temperatures were taken only just before switching off the blowers for end of run grain samplings when a complete set of the above measurements were taken.

D. Sampling the grain for moisture content and temperature

1. When the blowers had operated the desired length of time for each run, the blower manual shut-off switch was switched off and grain moisture samples and temperature measurements were taken as explained in the following discussion for one of the bins.
2. The bin lid was removed and the sampling lid placed on the bin. The marked radial on the sampling lid was aligned with an inlet radial of the bin according to a prearranged random schedule of sampling radials. Only one inlet radial, one exhaust radial, and one bisector radial was sampled except for the wheat experiment in which two extra radials were sampled in bin type I.
3. The thermocouple leads of the cable attached to the grain trier were connected to the potentiometer and the potentiometer adjusted according to self-contained instructions.
4. The grain trier was then inserted into the grain through the desired position holes in the sampling lid and a sample of grain taken into the trier. The grain entering the trier was from the test section, vertical middle two feet of the bin. The trier was then withdrawn one foot and a temperature measurement taken of the grain interspace at the vertical midpoint in the bin for the position being sampled, Figure 4-1. From previous trial experiments, it had been found that the equipment could

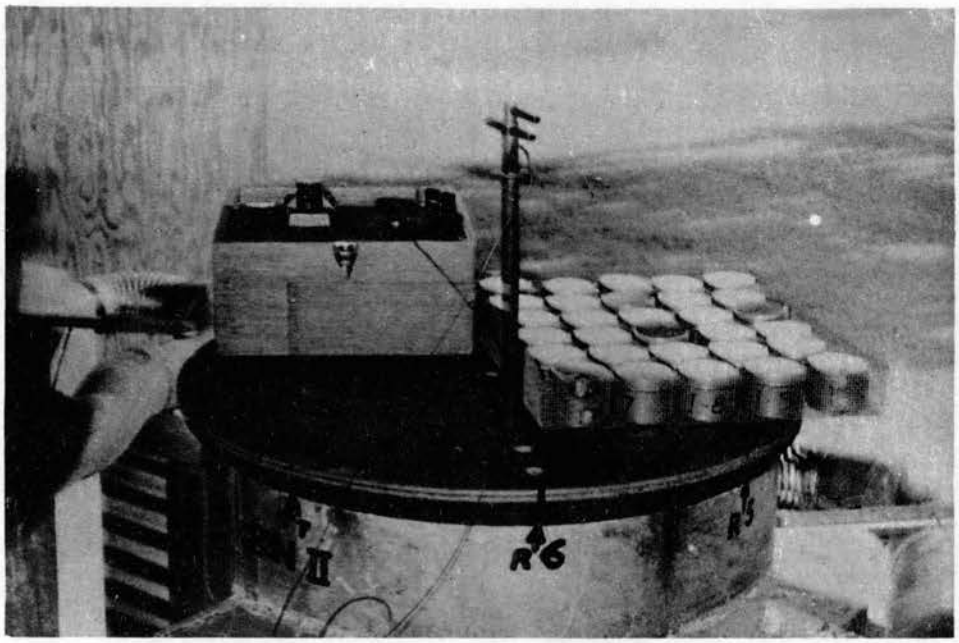

FIGURE 4-1 Sampling lid, grain trier, potentiometer, and grain sample containers.

not detect a vertical temperature gradient in the grain so the temperatures were subsequently taken at midpoint only. The trier was withdrawn from the bin and the samples of grain, approximately 34 grams, were emptied into a properly designated can and an air-tight lid placed on the can.

5. The other positions of the bin were sampled as above and the sampling lid was removed from the bin. Fresh grain was added to the bin to fill the space which resulted from grain shrinkage. Then the bin lid was reinstalled on the bin.

6. The other two bins were sampled as explained for the above mentioned bin. Ten samples were taken from each bin at the end of each run during the sorghum experiment and two additional samples from bin type I were taken during the wheat experiment. The extra samples from bin type I were for more adequate grain moisture and temperature gradient information and were not used in calculating average grain moisture.

7. After sampling, the equipment was returned to operation and the grain samples, contained in the air tight cans, were transported to a laboratory where the samples were weighed to the nearest half-tenth of a gram on Torsion Balance scales. The samples, with lids removed from the cans, were placed inside the drying oven where they were dried for 72 hours at 100 C. The samples were then reweighed so that the moisture content of each sample

could be computed.

During the wheat drying experiment, some grain moisture content and temperature measurements were taken after the blowers had been inoperative for a few hours subsequent to taking samples at the end of a run. The measurements were taken in the same positions that some of the end of run samples were taken in order to determine redistribution of grain moisture and temperature.

The static pressure measurements were taken of the bin horizontal cross sections at the end of the grain drying experiments. The pressure was taken using the manometer with the pressure probe inserted to the vertical midpoint of positions on the sampling lid for all radials of each bin and for the extra radials of bin type I.

By using the procedure for the drying experiments in the two-foot diameter bins, information was obtained whereby total or average drying effect could be evaluated as well as moisture content and pressure gradients across the bins.

CHAPTER V

ANALYSIS OF GRAIN HYGROSCOPICITY DATA

The equilibrium moisture properties for hard red winter wheat in the desorptive phase needed to be defined in order to evaluate certain properties of the thermal drying system. Much of the equilibrium moisture data in widespread use is for the adsorptive phase which does not seem appropriate for drying applications. Also, there is considerable variation in the data resulting from using equilibrium moisture equations presently available and actual equilibrium data for various temperatures as is illustrated in Figure 5-1 for the 77 F isotherm.

A search through technical literature revealed sets of wheat desorption data for eight temperatures ranging from 50 to 176 F. The data resulted from research projects in England, Germany, Canada, and the United States. The data are listed in Table V along with source information of the data. The data included several varieties of wheat but it was predominantly hard red winter and hard red spring wheat. The sigmoid shape of the hygroscopicity isotherms as well as the temperature effect can be noted from Figure 5-2 which shows plots of a typical or average set of equilibrium data from each of the eight temperatures covered by the data of Table V.

An expression relating equilibrium moisture content, air relative humidity, and air and grain temperature was developed as will be

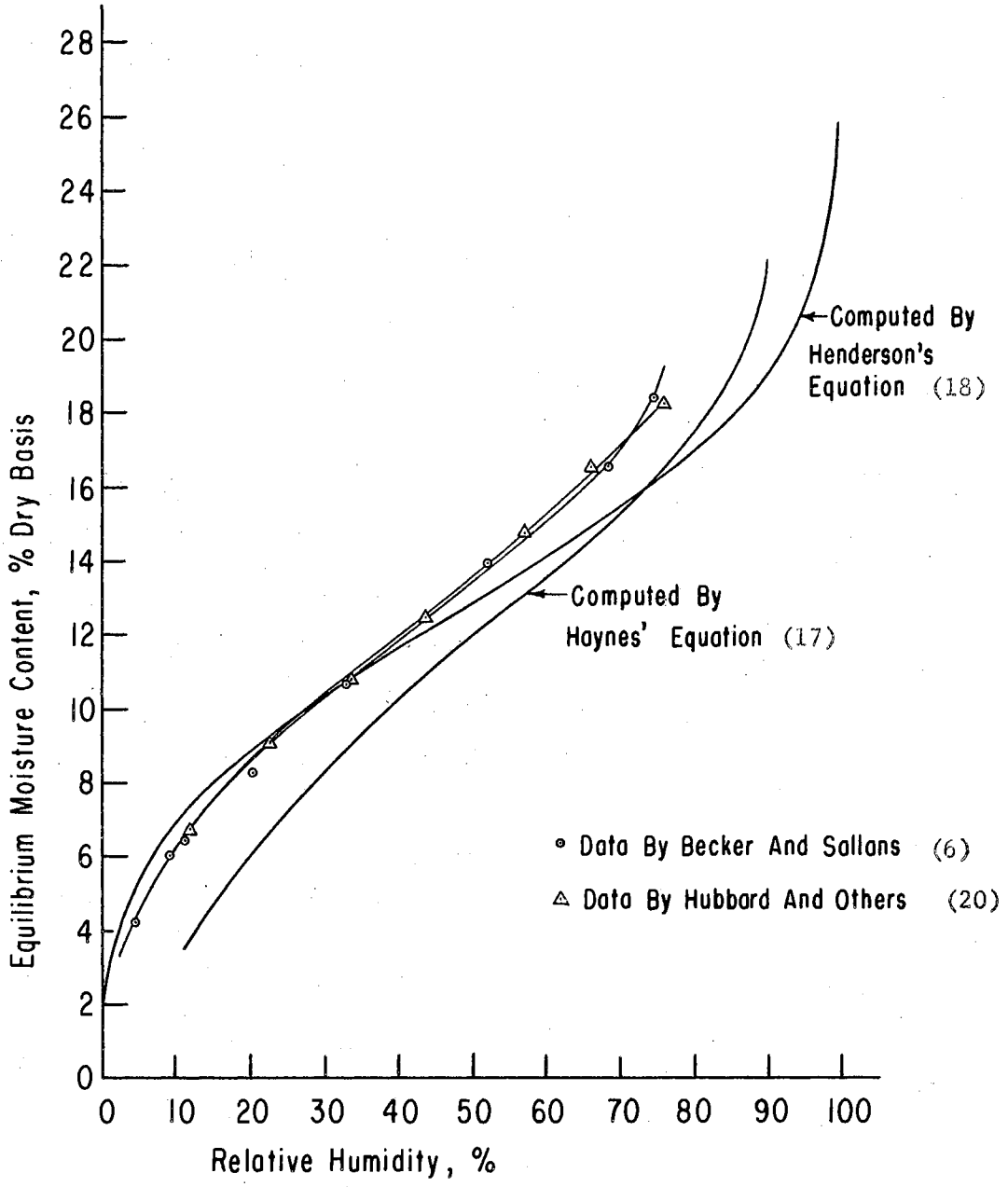

FIGURE 5-1. 77 F Isotherms by equations and from observed data.

TABLE V

WHEAT DESORPTION HYGROSCOPICITY DATA

DATA SET NO.	TEMP F	EQUILIBRIUM MOISTURE % DRY BASIS	RELATIVE HUMIDITY %
1	50	7.7	10.
		12.0	30.
		15.3	50.
		18.0	70.
		20.5	80.
2	50	8.1	10.
		11.7	30.
		14.2	50.
		16.7	70.
		19.6	80.
3	50	7.3	10.
		11.9	30.
		15.2	50.
		16.7	70.
		19.9	80.
4	68	7.2	10.
		11.1	30.
		14.3	50.
		19.7	80.
5	68	5.9	10.
		7.5	20.
		9.0	30.
		10.7	40.
		12.2	50.
		13.8	60.
		15.6	70.
		17.6	80.
6	77	4.21	4.5
		6.02	9.0
		6.46	11.1
		8.30	20.3
		10.68	32.8
		13.95	52.0
		16.60	68.3
		18.52	74.7
7	77	7.01	12.0
		9.36	22.6
		10.98	33.2
		12.68	43.8
		15.04	57.0
		16.73	66.0
		18.74	75.8
8	77	6.53	12.0
		8.77	22.6
		10.45	33.2
		12.18	43.8
		14.40	57.0
		15.86	66.0
		18.05	75.8
9	77	6.77	12.0
		9.05	22.6
		10.79	33.2
		12.51	43.8
		14.76	57.0
		16.55	66.0
		18.34	75.8
10	86	6.61	11.8
		8.93	22.0
		10.74	32.8
		12.44	43.5
		14.46	56.3
		16.25	64.6
		18.37	75.6
11	86	6.13	11.8
		8.30	22.0
		10.10	32.8
		11.81	43.5
		13.87	56.3
		15.39	64.6
		17.47	75.6
12	86	6.55	11.8
		8.89	22.0
		10.68	32.8
		12.35	43.5
		14.00	56.3
		15.15	64.6
		17.22	75.6
13	86	6.36	11.8
		8.73	22.0
		10.57	32.8
		12.42	43.5
		14.14	56.3
		15.49	64.6
		16.99	75.6
14	86	6.52	11.8
		9.12	22.0
		10.66	32.8
		12.38	43.5
		14.39	56.3
		16.10	64.6
		18.09	75.6
15	86	6.44	11.8
		8.75	22.0
		10.50	32.8
		12.15	43.5
		14.16	56.3
		15.85	64.6
		17.90	75.6
16	86	6.47	11.8
		8.65	22.0
		10.44	32.8
		12.22	43.5
		14.23	56.3
		15.85	64.6
		17.81	75.6
17	95	6.09	11.7
		7.98	21.0
		9.84	32.5
		11.84	43.4
		13.07	54.6
		14.48	63.2
		16.81	75.5
18	95	5.80	11.7
		7.64	21.0
		9.46	32.5
		11.22	43.4
		12.93	54.6
		14.30	63.2
		16.32	75.5
19	104	4.6	10.
		6.5	20.
		8.0	30.
		9.5	40.
		11.0	50.
		12.5	60.
		14.2	70.
		16.5	80.
20	122	4.71	12.7
		6.09	20.6
		6.98	28.6
		9.07	39.
21	176	2.5	10.
		3.8	20.
		5.0	30.
		6.0	40.
		7.2	50.
		8.7	60.
		10.8	70.
		13.0	80.

TABLE V (continued)

SOURCE OF DATA

SET NO	RESEARCHER AND COUNTRY	TEMP C	TEMP F	KIND OF WHEAT
1	Gane (13), England	10	50	Weak, White English
2	"	10	50	Medium, Plate
3	"	10	50	Strong, No. 3 Pacific Manitoba
4	"	20	68	Weak, White English
5	Pichler (28), Germany	20	68	Unknown
6	Becker and Sallans (6), Canada	25	77	Thatcher, Western Canadian*
7	Hubbard, et. al. (20), U.S.A.	25	77	Elgin Soft White
8	"	25	77	Stewart, Durum
9	"	25	77	Pawnee**
10	"	30	86	Elgin, Soft White
11	"	30	86	Stewart, Durum
12	"	30	86	Pawnee**
13	"	30	86	Pawnee**
14	"	30	86	Pawnee**
15	"	30	86	Pawnee**
16	"	30	86	Mida*
17	"	35	95	Mida*
18	"	35	95	Stewart, Durum
19	Pichler (28), Germany	40	104	Unknown
20	Becker and Sallans (6), Canada	50	122	Thatcher, Western Canadian*
21	Pichler (28), Germany	80	176	Unknown

* Hard Red Spring
** Hard Red Winter

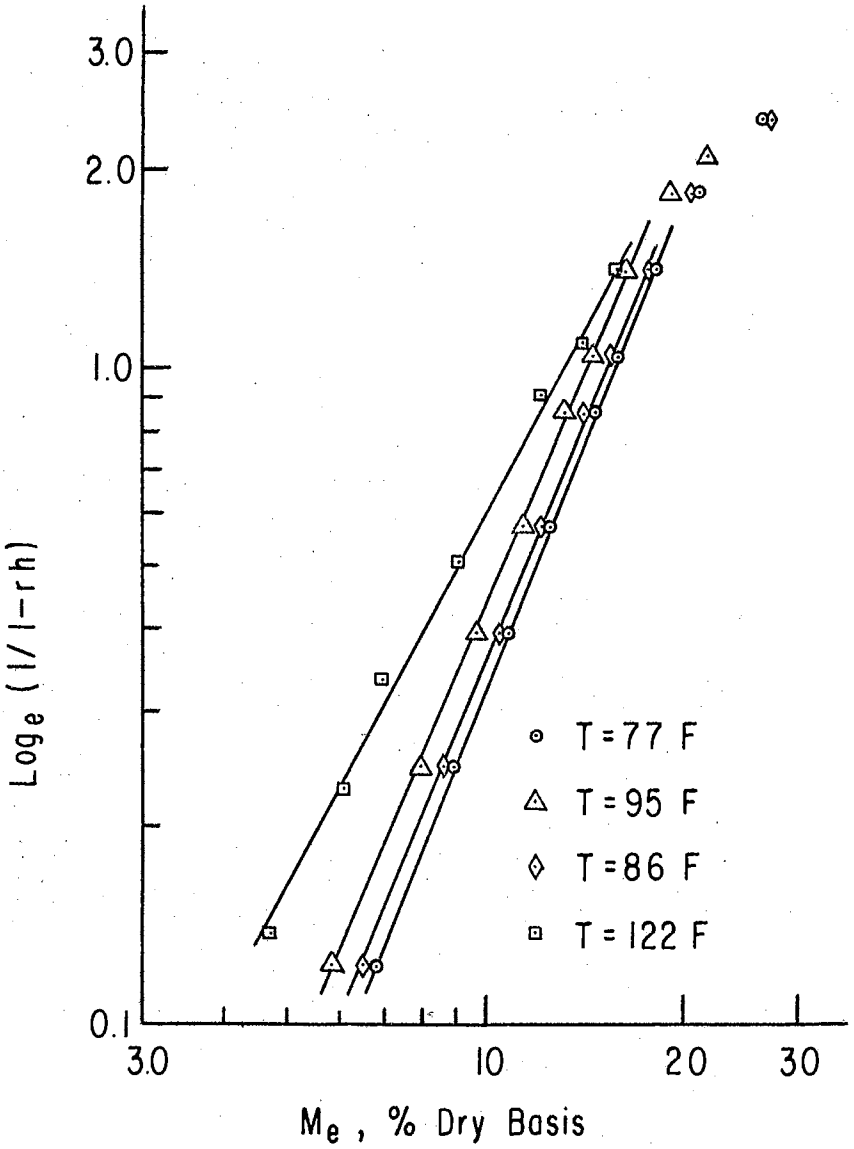

FIGURE 5-3. Typical isotherms illustrating the straight line relationship of equation 5-2.

each temperature level were evaluated by simultaneous solutions of the equation using appropriate sets of equilibrium data from Table V. The best fit for each temperature level was obtained by a method of least squares as computed by an IBM-650 electronic computer using part of the program in Table A-I. The Y intercepts and regression coefficients so obtained are listed in Table VI.

A definite trend between the Y intercept and temperature and between the regression coefficient and temperature was noticed, so these properties were plotted versus temperature as shown in Figures 5-4 and 5-5 respectively. The plots of Figures 5-4 and 5-5 appeared as straight lines on log-log paper so the form of the relationships was:

$$a = P_1 T^{P_2}$$

or $$\log a = \log P_1 + P_2 \log T, \qquad 5\text{-}4$$

and $$b = P_3 T^{P_4}$$

or $$\log b = \log P_3 + P_4 \log T. \qquad 5\text{-}5$$

T, temperature F, was used in the above equations. Absolute temperatures could have been used but would have resulted in an extreme value of P_1, in the order of 10^{-75}. Equations 5-4 and 5-5 were linear in the logarithmic form so the method of least squares was used to evaluate the respective Y intercepts and regression coefficients. An IBM-650 electronic computer and the rest of the program of Table A-I was utilized to compute the following values:

$$P_1 = 5.7336 \times 10^{-10}$$

TABLE VI

Y INTERCEPTS AND REGRESSION COEFFICIENTS
OF EQUATION 5-2 FOR EIGHT
TEMPERATURE LEVELS

Temp F	Y intercept, a	Regression coef, b
50	0.00028598	2.8973
68	0.0013370	2.4378
77	0.0014121	2.3744
86	0.0014243	2.3947
95	0.0018794	2.3521
104	0.0040649	2.1425
122	0.0059575	2.0330
176	0.024561	1.6565

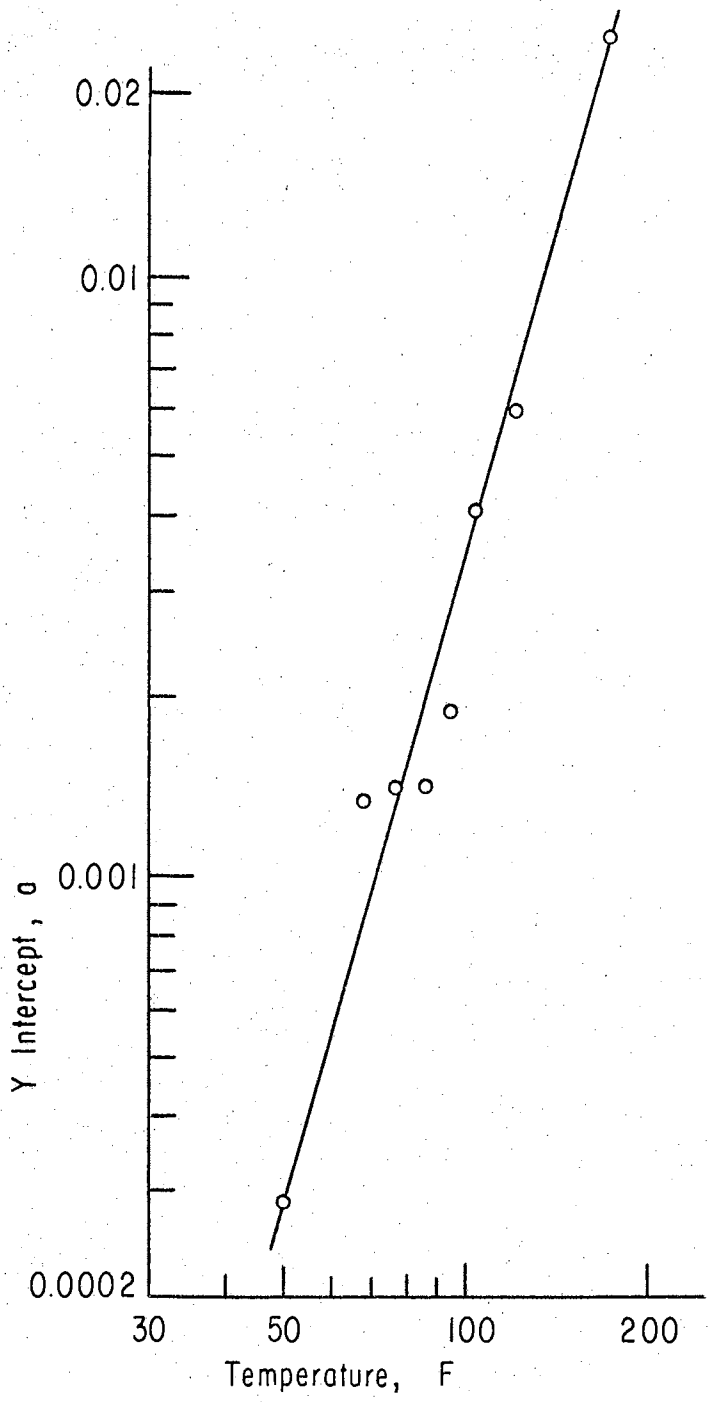

FIGURE 5-4. Plot of Y intercept of equation 5-2 versus temperature.

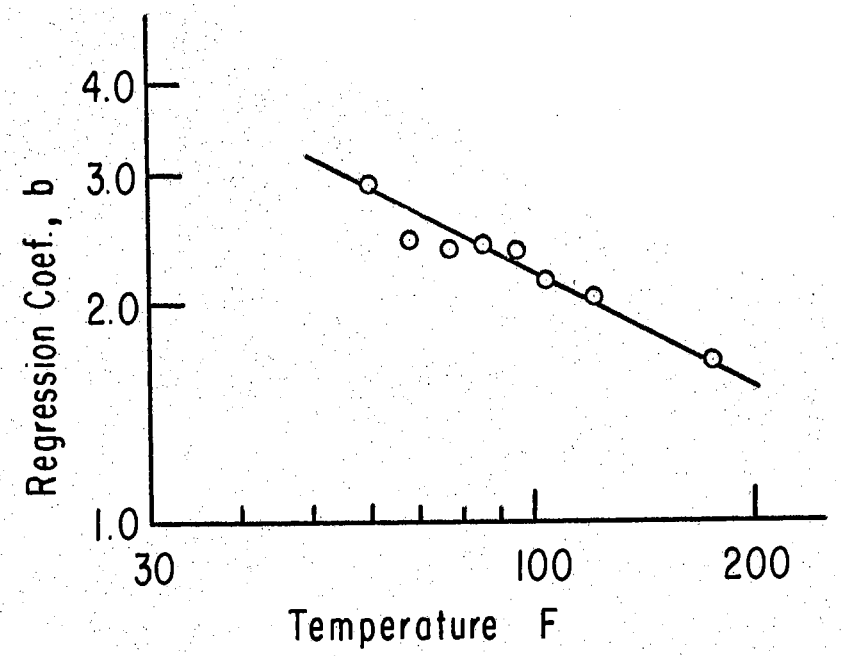

FIGURE 5-5. Plots of regression coefficients of equation 5-2 versus temperature.

P_2 = 3.3718

P_3 = 14.863

P_4 = -0.41733

A modified form of Henderson's equation was thus obtained of the form:

$$1\text{-}rh = e^{-P_1 T^{P_2} M_e^{P_3} T^{P_4}}, \qquad 5\text{-}6$$

in which rh = air relative humidity, decimal

e = 2.718 · · ·

T = air and grain temperature, F

M_e = wheat desorptive equilibrium moisture content, per cent dry basis.

P_1, P_2, P_3, P_4, constants evaluated as listed above.

Equation 5-6 was used to evaluate rh corresponding to a level of T for a range of M_e. These computations were performed using the IBM-650 electronic computer. The results of these computations were used to plot M_e versus rh for a range of temperatures from 30 F to 180 F in increments of 5 F as illustrated in Figure 5-6 for six isotherms.

The plots of Figure 5-6 reveal that the equilibrium moisture content increases asymptotically as the relative humidity approaches 100%. This increase of equilibrium moisture content does not appear to be in agreement with the physical phenomenon as shown in Figure 5-7 in which each isotherm has a definite maximum value of equilibrium moisture content at a relative humidity of 100%. (28).

Values of the maximum equilibrium moisture content, $(M_e)_{max}$, for an isotherm were approximated from the plots of Figure 5-8 which show $(M_e)_{max}$ for several levels of relative humidity from data in Table V. Linear regression analysis of the data of Figure 5-8 transformed into logarithmic form resulted in the following:

rh	Y intercept	Regression Coefficient	Correlation Coefficient, r
0.30	4.953×10^{10}	-4.270	-0.952
0.50	4.491×10^{8}	-3.489	-0.988
0.70	2.478×10^{5}	-2.265	-0.947

The plot for $(M_e)_{max}$ for rh = 1 was drawn using the three values of Figure 5-7 and the linear trend of the slopes, regression coefficients, of the 0.30, 0.50, and 0.70 rh plots of Figure 5-8. The slope of $(M_e)_{max}$ for rh = 1.0 was estimated as -1.33.

The plots of equilibrium moisture versus relative humidity using the modified form of Henderson's equation were altered on the upper

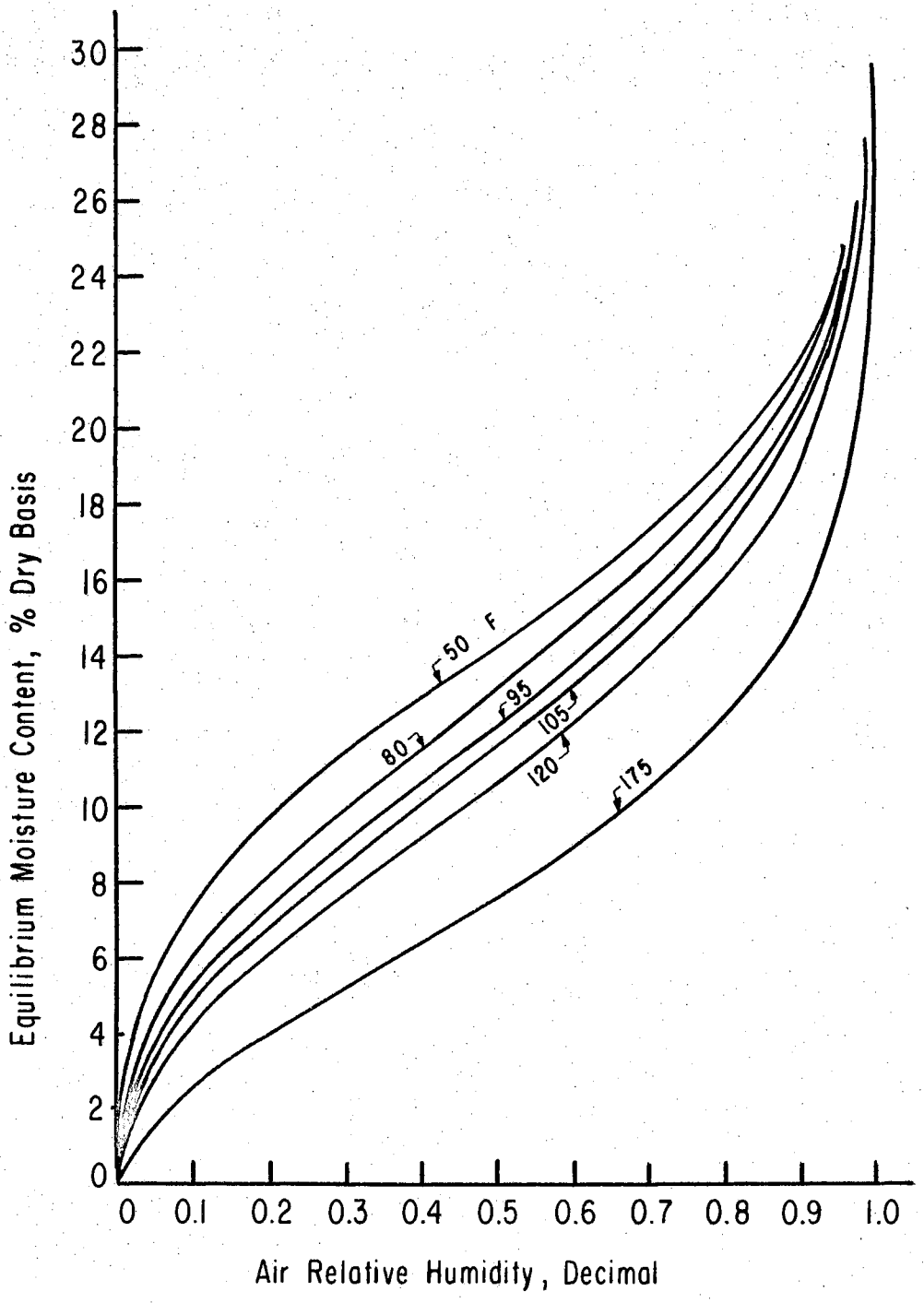

FIGURE 5-6. Plot of six isotherms using equation 5-6.

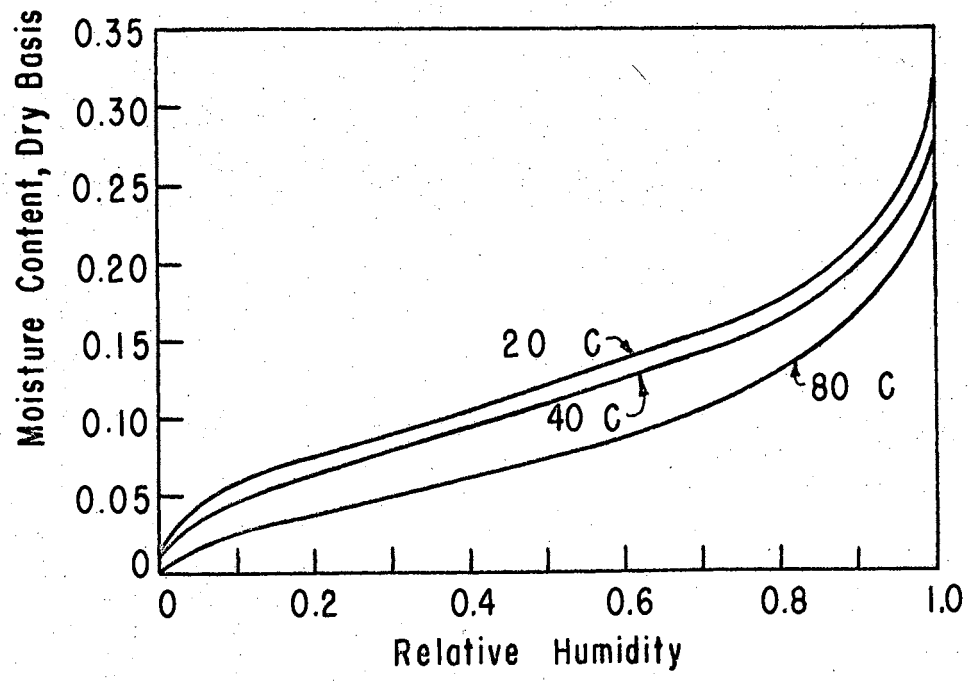

FIGURE 5-7. Wheat desorption isotherms showing maximum value of equilibrium grain moisture content, dry basis as a decimal.

end by drawing a smooth curve from rh = 0.70 to $(M_e)_{max}$ as shown for a few of the isotherms in Figure 5-9. Values were taken from these altered isotherm plots for relative humidity and temperature corresponding to constant equilibrium moisture contents as listed in Table VII. The values from Table VII were used to plot constant equilibrium wheat moisture content lines superimposed upon a psychrometric chart, Figure 5-10. Figure 5-10 was used to facilitate wheat drying analyses.

It would seem that a more appropriate relationship of equilibrium moisture content than that expressed by equation 5-6 could be developed since the equation is dimensionally non-homogeneous and not in accordance with the physical situation in the range of relative humidities above about 70 per cent.

A form of a dimensionally homogeneous equation for an isotherm was hypothesized to be:

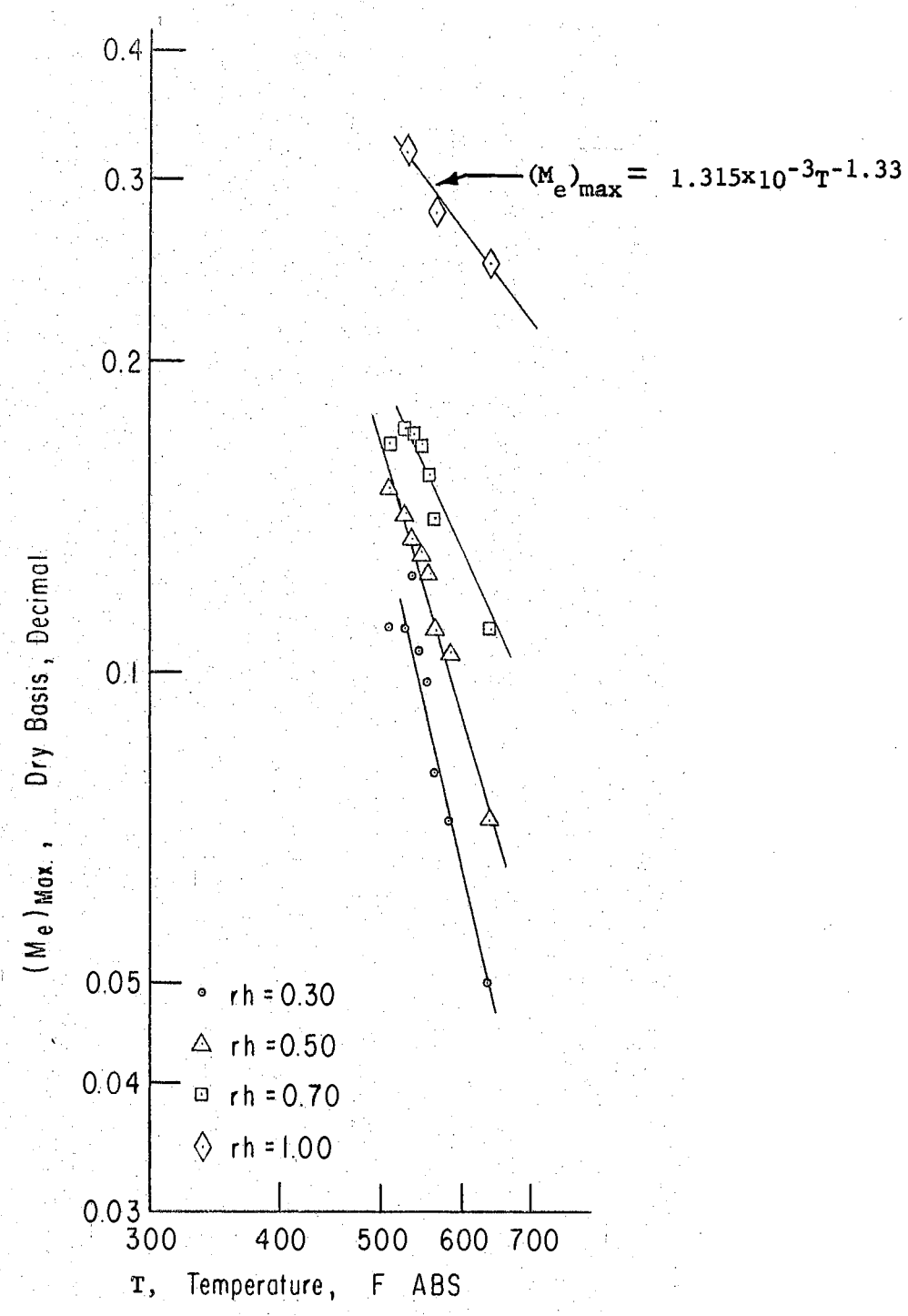

FIGURE 5-8. Plots of maximum equilibrium moisture content versus temperature.

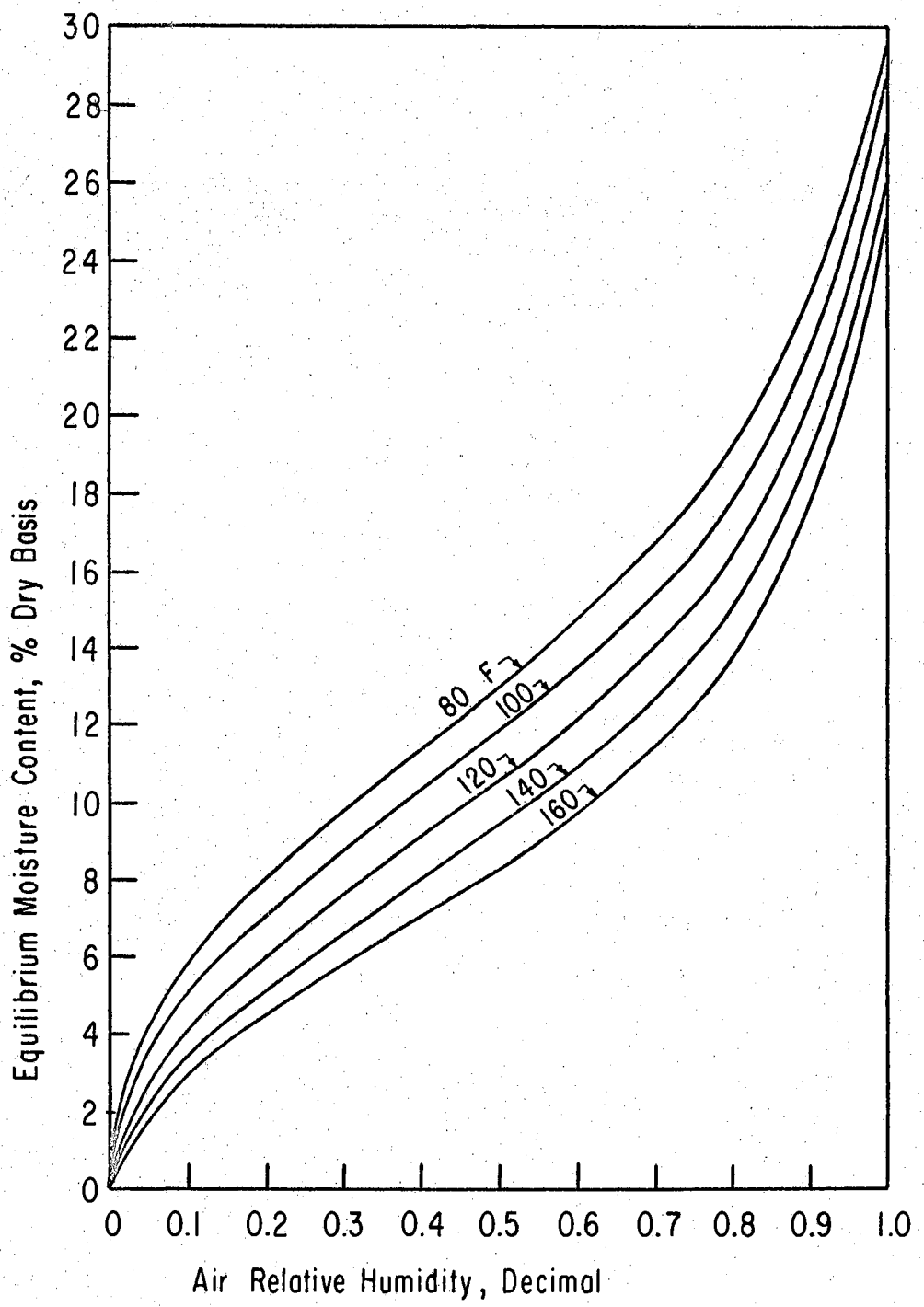

FIGURE 5-9. Plots of computed equilibrium moisture isotherms for wheat altered on upper end to go through estimated $(M_e)_{max}$.

TABLE VII

AIR RELATIVE HUMIDITY, DECIMAL

Wheat Moisture Content % dry basis	Temperature, F												
	60	65	70	75	80	85	90	95	100	105	110	115	120
10.0	0.244	0.258	0.273	0.289	0.306	0.323	0.341	0.360	0.378	0.397	0.417	0.436	0.456
11.0	0.296	0.320	0.326	0.348	0.370	0.383	0.405	0.410	0.432	0.460	0.475	0.495	0.519
12.0	0.366	0.381	0.398	0.414	0.431	0.450	0.468	0.487	0.507	0.526	0.546	0.565	0.585
13.0	0.421	0.442	0.450	0.475	0.500	0.512	0.530	0.540	0.560	0.590	0.604	0.620	0.634
14.0	0.500	0.511	0.526	0.541	0.557	0.575	0.592	0.610	0.628	0.646	0.664	0.681	0.699
15.0	0.557	0.562	0.580	0.600	0.610	0.630	0.645	0.656	0.672	0.700	0.712	0.725	0.745
16.0	0.628	0.637	0.648	0.661	0.674	0.688	0.695	0.710	0.730	0.740	0.753	0.765	0.780
17.0	0.670	0.676	0.692	0.710	0.715	0.732	0.742	0.753	0.770	0.780	0.787	0.800	0.813
18.0	0.738	0.732	0.740	0.753	0.757	0.770	0.780	0.790	0.802	0.810	0.818	0.827	0.841
19.0	0.776	0.772	0.780	0.790	0.792	0.803	0.823	0.820	0.832	0.840	0.845	0.865	0.867
20.0	0.808	0.810	0.812	0.820	0.823	0.833	0.842	0.850	0.860	0.865	0.869	0.878	0.889
21.0	0.837	0.838	0.841	0.850	0.850	0.859	0.866	0.873	0.882	0.887	0.891	0.900	0.908
22.0	0.864	0.865	0.868	0.874	0.875	0.882	0.890	0.896	0.903	0.906	0.910	0.918	0.926

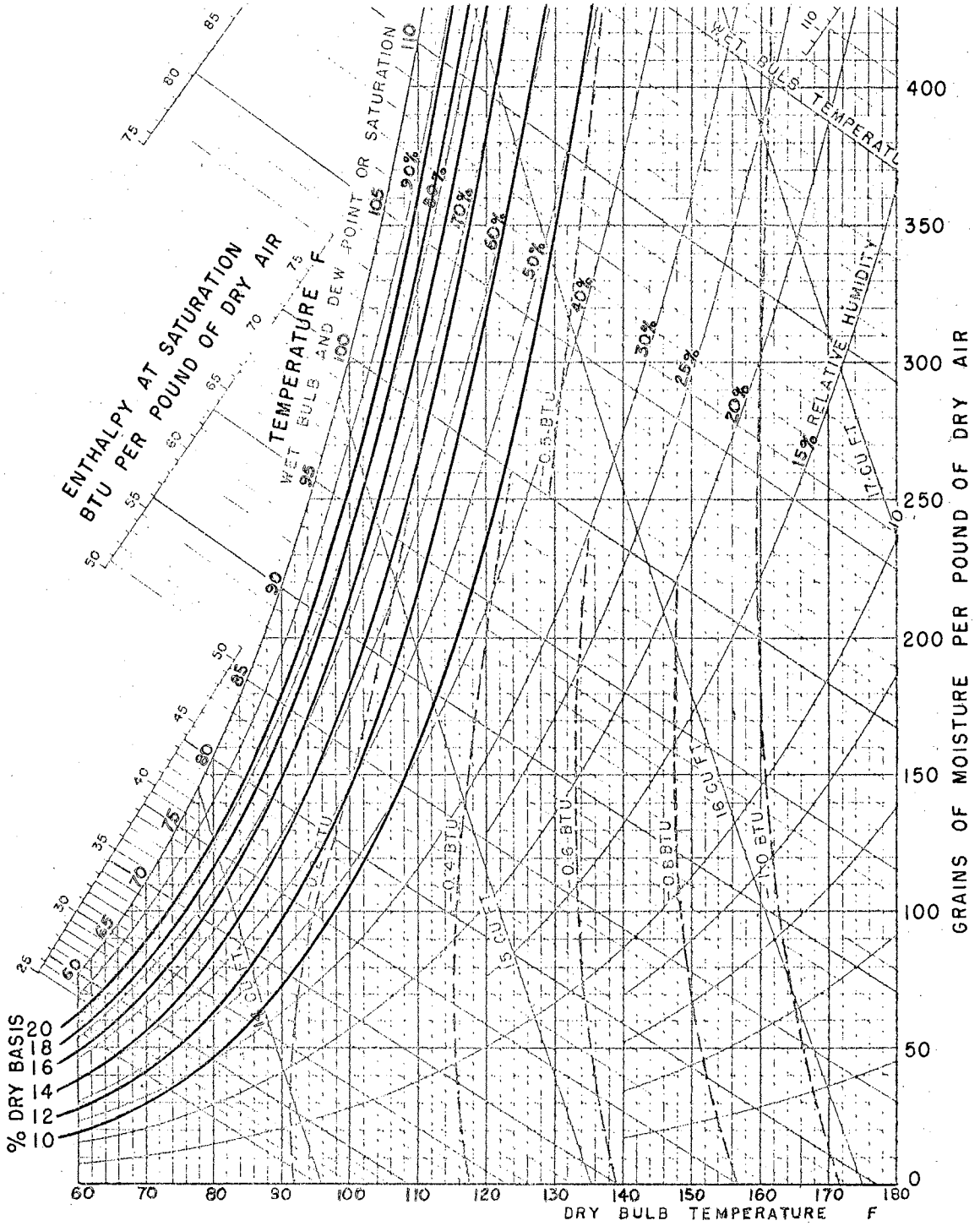

FIGURE 5-10. Wheat equilibrium moisture content lines superimposed upon a psychrometric chart.

$$M_e = (M_e)_{max}\, c_1 \left[1-e^{-c_2(rh)^{c_3}}\right] \qquad 5\text{-}7$$

in which M_e = equilibrium moisture content, dry basis as a decimal

$(M_e)_{max}$ = equilibrium moisture content at 100% relative humidity

rh = relative humidity, decimal.

Preliminary investigation revealed that $(M_e)_{max}$ and c_3 appear to be functions of H/RT of the power form so that equation 5-7 can probably be written as:

$$M_e = k_1(H/RT)^{k_2}\left[1-e^{-k_3(rh)^{k_4(H/RT)^{k_5}}}\right] \qquad 5\text{-}8$$

in which H = average heat of adsorption, cal per mole

R = univeral gas constant

T = air and grain temperature, F abs

k_i = constants.

Becker and Sallans (6) list some limited data of values of H for wheat.

A satisfactory method of evaluating the constants of equation 5-8 was not found although a method of simultaneaous solutions of non-linear equations was tried extensively using an IBM-650 electronic computer. (14). The method was even modified to incorporate Hartley's (16) method of convergence.

CHAPTER VI

ANALYSIS OF EXPERIMENTAL DATA

The data discussed are those resulting from the flow rate and drying experiments using the miniature model bins and the two-foot diameter bins. The data transformed into dimensionless groups, pi terms, are listed in Appendix B.

Symbols and pi terms are defined in Tables II and III. Additional definitions are listed where required.

Air Circulation System

The form of the general equation relating the factors involved in the air circulation system was equation 3-2. For the particular system of flow of air through a specified kind of grain in a certain cross-flow bin configuration, the equation was reduced to equation 3-5:

$$\pi_{11} = f(\pi_{12}, \pi_{14}).$$

By this approach, a separate equation was required for each kind of grain and for each cross-flow bin arrangement.

π_{12} was considered as representative of a Reynolds number and equation 3-5 was thus a relation between static pressure and Reynolds number. The data for calibration of air flow rate through wheat was used to evaluate the function of equation 3-5 since a substantial

variation in the range of π_{12} was obtained with the range of pressures used in the calibration data. π_{14} was not varied in the procedure, but it could not be omitted for the particular system since a geometric distortion factor was introduced by the term when considering a model and prototype system.

The calibration data of air flow rate through wheat were transformed into values of π_{11} and π_{12} and plotted as shown in Figures 6-1, 6-2, and 6-3 for bins type I, II, and III respectively. To evaluate π_{12}, a value of $N_e = 1/(32.2)(60^2)$ was used. Air absolute viscosity was taken from Figure A-3 and converted to the proper time units. (10). Air density was corrected for local barometric pressure and temperature. The data are listed in Table B-I.

The data of Figures 6-1, 6-2, and 6-3 plotted as straight lines on log-log paper so that a linear regression analysis could be made of the data in logarithmic form. Results of the regressions including correlation coefficients r are included on the figures.

The equations included in Figures 6-1, 6-2, and 6-3 are prediction equations for static pressure drop as related to air flow rate for wheat, but the equations are limited to the miniature bin systems since the function involving π_{14} was not evaluated. The prediction equations were extended in scope of application by the following analysis for the effect of π_{14}.

The distortion factor arising from π_{14} was characterized by considering the miniature bins as the model system and any other bin as the prototype system. The length scale ratio of model to prototype is:

$$n = r_P/r_M = D_P/ D_M, \qquad 6\text{-}1$$

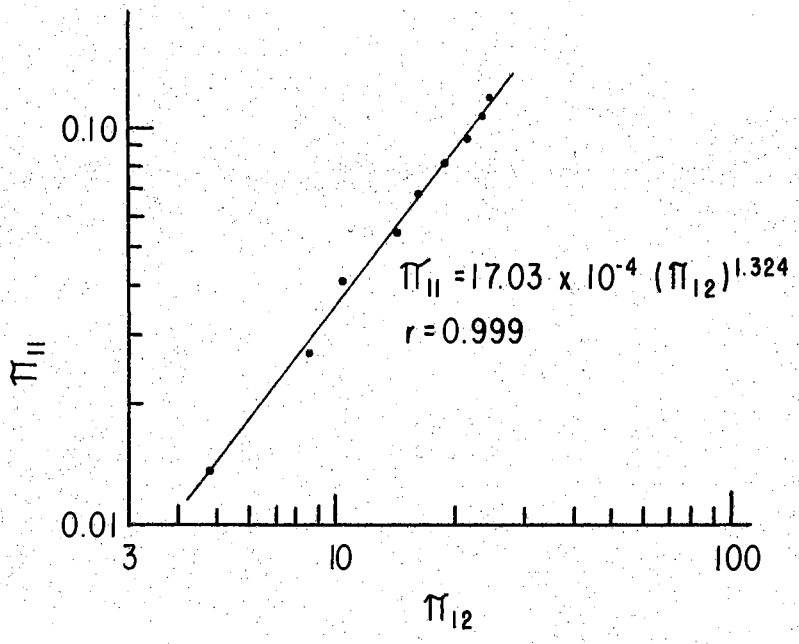

FIGURE 6-1. π_{11} versus π_{12}, air circulation system for miniature bin type I.

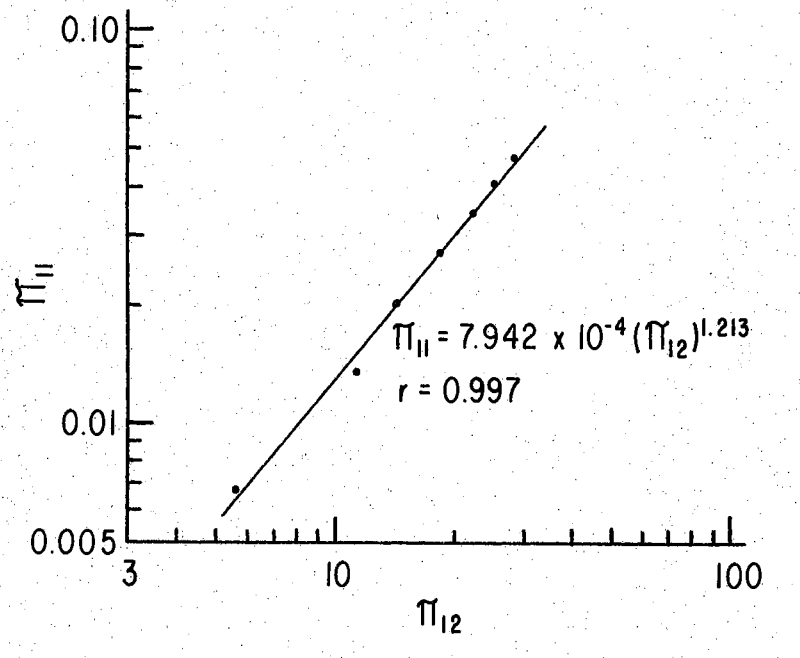

FIGURE 6-2. π_{11} versus π_{12}, air circulation system for miniature bin type II.

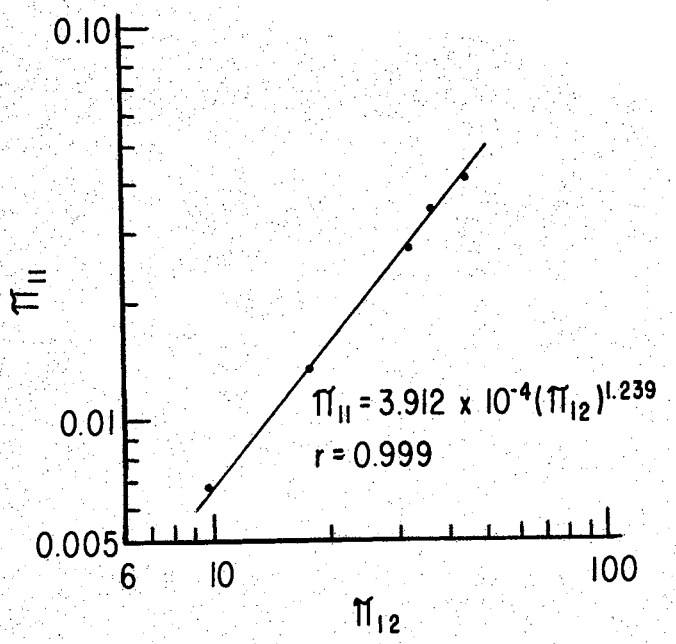

FIGURE 6-3. π_{11} versus π_{12}, air circulation system for miniature bin type III.

in which D = bin diameter, ft

subscript M = prototype

subscript P = model .

The geometrical distortion factor α is defined by Murphy (25) as the ratio of a pi term of the model system divided by the corresponding pi term of the prototype system. Since the characteristic size of the grain kernel, d, is the same in model and prototype, the distortion factor of π_{14} is:

$$\alpha = (\pi_{14})_M/(\pi_{14})_P = (d_M/r_M)/(d_P/r_P)$$

or $$\alpha = n. \qquad 6\text{-}2$$

If it is hypothesized that the unknown function of π_{14} can be

accounted for by including the distortion factor to the first power, the prediction equation including the distortion effect can be written as:

$$n\pi_{11} = f(\pi_{12}),$$

or
$$n\pi_{11} = A\pi_{12}^{B} \qquad 6\text{-}3$$

A and B are evaluated for each bin type in Figures 6-1, 6-2, and 6-3.

The distortion effect as presented in equation 6-3 can be visualized by noting that the characteristic grain kernel size with respect to the bin size is n times as great in the model as in a prototype which results in a relatively greater resistance offered to air flow in the model than in a larger prototype. Therefore, the pressure drop in a prototype is only 1/n of the value of that for the model for an equal value of π_{12} in model and prototype.

The two-foot diameter bins were considered a prototype system and equation 6-3 checked as listed below.

$D_p = 2.0$

$D_M = 0.487$

$n = 4.11$

π_{11} and π_{12} from Table B-II.

BIN TYPE	$n\ \pi_{11}$	$A\ \pi_{12}^{B}$
I	0.4090	0.4572
II	0.2035	0.1437
III	0.1082	0.08135

To extend the range of π_{12}, it was assumed that resistance of grain to air flow is approximately linearly proportional to length of air travel and to air flow rate. This approximation can be verified

from Shedd's curves (30) for small increments of air velocity. A limited prediction equation from which to predict pressure drop can be written as:

$$(p/R\ Q_a)r^2 = f(r/S,\ r/Y)$$

in which p = air pressure drop across bin, $lb_{(F)}/ft^2$

R = resistance of grain to air flow, $(lb_{(F)}/ft)/ft^3$ air/min

Y = bin height, ft

Other symbols in Table III.

or,
$$\left[(p/R\ Q_a)r^2\right]_P = \left[(p/R\ Q_a)r^2\right]_M \left[\frac{f(r/S,\ r/Y)_P}{f(r/S,\ r/Y)_M}\right] \qquad 6\text{-}4$$

For a model operated such that $(R)_P = (R)_M$ and r, S, and Y of the prototype are respectively equal to nr, nS, and nY of the model, equation 6-4 can be reduced to:

$$(p)_P = n^2\left[(Q_a)_P/(Q_a)_M\right](p)_M . \qquad 6\text{-}5$$

The static pressure and flow rate data for the wheat experiment using the two-foot diameter bins were used as the model system for computing predicted pressures in a twenty-foot diameter prototype system by using equation 6-5. The pressure and flow rate data from the two-foot bins and as predicted by equation 6-5 for a twenty-foot diameter bin were transformed into values of π_{11} and π_{12} and plotted along with the miniature bin data for wheat in the three type bins, Figure 6-4. The plots of Figure 6-4 appear to be appropriate for estimating pressure drop in a prototype system although the data for values of π_{12} beyond that for the two-foot diameter bins have not been verified in actual installations.

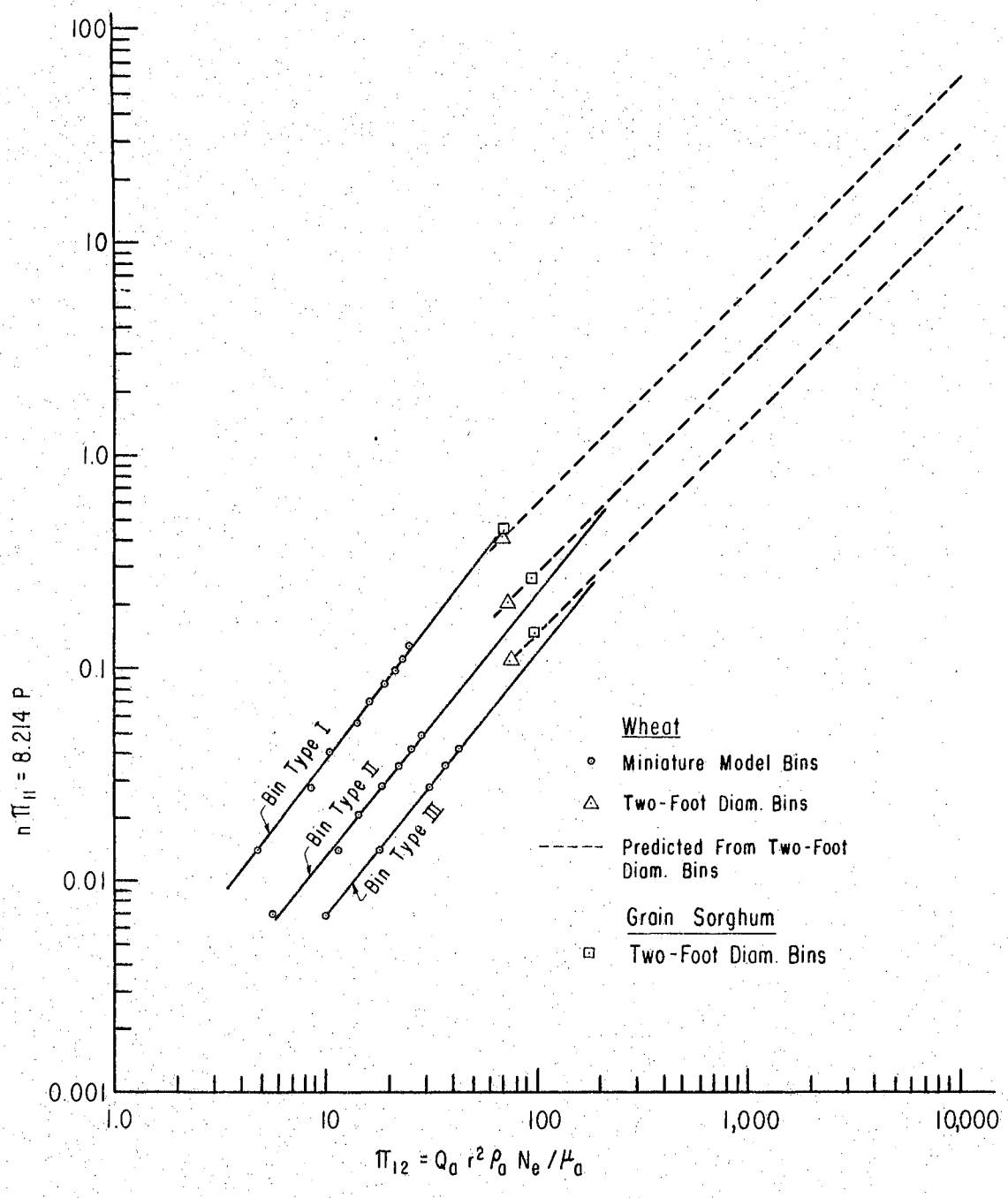

FIGURE 6-4. Graph for estimating pressure drop in prototype installations.

For estimating pressure drop in a prototype system from Figure 6-4, computations can be facilitated since:

$$n = D/0.487$$

$$r = D/4$$

thus, $$n\pi_{11} = (8.214)P \qquad 6\text{-}6$$

in which P = static pressure of air entering bin, ft of water.

For a desired flow rate in a drying set up, π_{12} can be computed and by referring to the appropriate graph of Figure 6-4, (8.214)P can be read from which the pressure drop P can be calculated. Conversely, if P is known, the flow rate can be estimated.

Data for grain sorghum in the two-foot diameter bin, Table B-II, are also included on Figure 6-4.

The internal static pressure distributions for the three cross-flow configurations of the two-foot diameter bins are shown in Figures 6-5 and 6-6 for the sorghum and wheat experiments respectively. The pressure distributions were measured near the end of each experiment using the static pressure probe and sensitive manometer.

The static pressure patterns for sorghum and wheat, Figures 6-5 and 6-6, agree very closely with patterns predicted by application of linear potential flow theory to forced air circulation through porous material. The pressure midway between the air inlet and exhaust area was about half the inlet pressure and symmetry existed in the patterns between pairs of inlet and exhaust areas. A noticeable exception to the linear pressure drop pattern occurred for wheat in bin type I, Figure 6-6, as there was considerably more pressure drop in the air inlet half of the bin than in the air exhaust half. The pressure

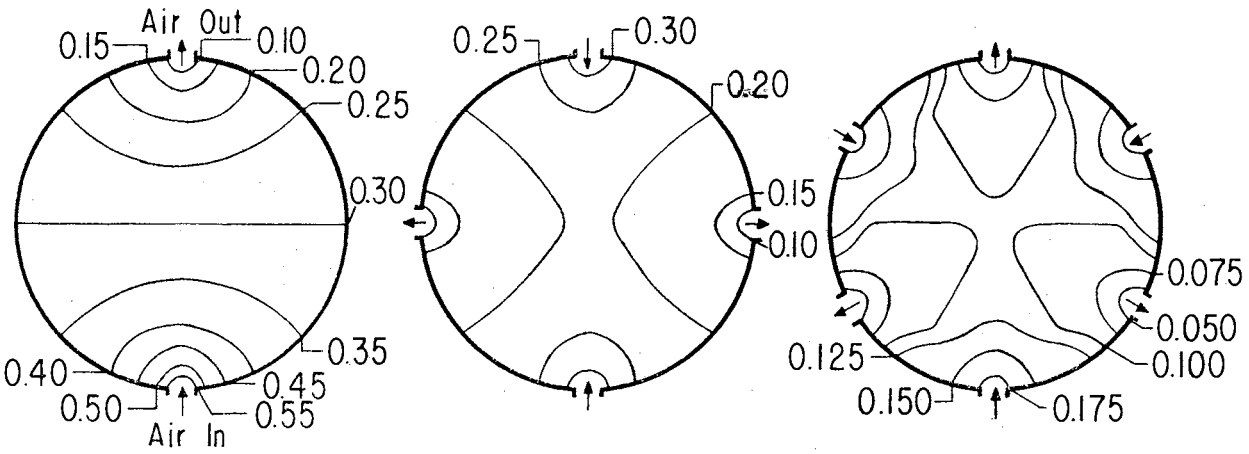

	BIN TYPE I	BIN TYPE II	BIN TYPE III
Static Pressure =	0.64	0.39	0.21
Flow Rate =	2.98 cfm/cu ft	4.02	4.10

FIGURE 6-5. Static pressure distributions, inches water, for grain sorghum in two-foot diameter bins.

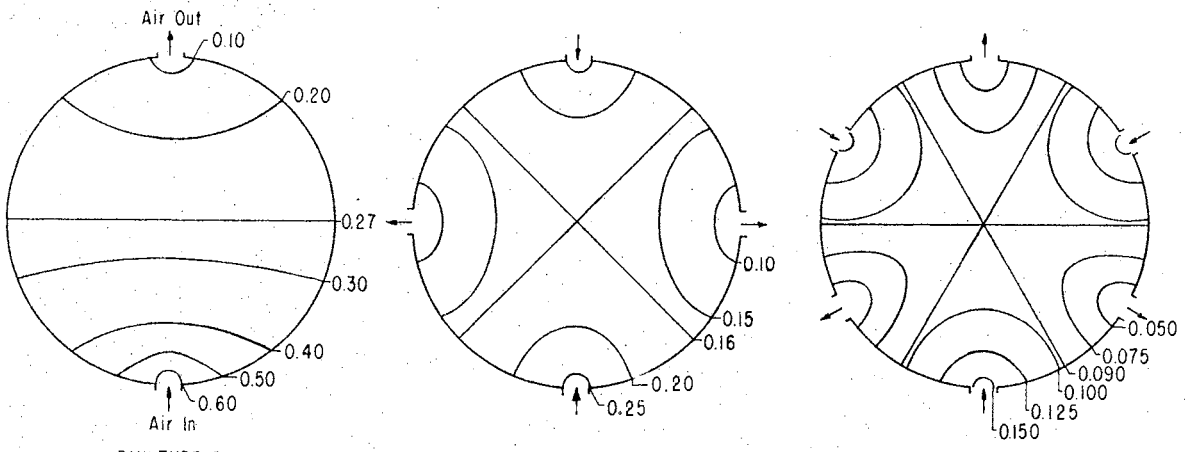

BIN TYPE I BIN TYPE II BIN TYPE III

Static Pressure =	0.60	0.30	0.16
Flow Rate =	3.01 cfm/cu ft	3.19	3.26

FIGURE 6-6. Static pressure distributions, inches water, for wheat in two-foot diameter bins.

gradients along the bisector radials are evaluated in Figure 6-6.

Thermal Drying System

Prediction Equation

The approach used to formulate a general prediction equation for drying wheat in deep cylindrical bins with cross-flow air circulation was to develop component equations from the data of the treatment schedule followed in the experimental research using the miniature model bins. The component equations were then combined into a prediction equation relating the amount of moisture removed to the factors which influenced the drying system. Estimates of the constants in the prediction equation were made from the analysis of the component equations. An electronic computer was used in the final evaluations of the constants. After the prediction equation was formulated, the correspondence between observed and calculated was determined for miniature bin data and the data from the two-foot diameter bins for wheat.

The general form of the prediction equation was equation 3-1. For the particular drying system of forcing air through a specified kind of grain in a certain cross-flow bin configuration, equation 3-1 was reduced to equation 3-4:

$$\pi_1 = f(\pi_2, \pi_4, \pi_5, \pi_6)$$

This type of equation would be limited to the above conditions of kind of grain and type of cross-flow bin arrangement, but it would be general in nature as concerns the other factors which are involved in the drying process. By this approach, a separate prediction

equation would be required for each kind of grain and for each bin configuration.

In developing the component equations, π_1 was considered to be the dependent term and the other pi terms of equations 3-1 were considered as the independent terms. π_1 versus each of the other pi terms, one at a time, was considered in the analysis using the data of the treatment schedule in which one independent term at a time was varied while the other pi terms were held constant or approximately constant.

Results of the drying experiments using the miniature model bins were used to compute the values of the pi terms of equations 3-4 and are indexed in the treatment schedule, Table VIII. Values of the pi terms are listed in Tables B-III, B-IV and B-V respectively for bins type I, II, and III for drying of wheat. The values are listed in the floating decimal point system which is explained at the beginning of Appendix B. Experiments to obtain a complete treatment schedule using bin type III were not performed. Table IX gives the average values of several of the quantities which make up the pi terms for each experimental run for bins type I, II, and III.

Plots of computed wheat desorption equilibrium moisture data, Figure 5-9, and constant grain moisture curves superimposed upon a psychrometric chart, Figure 5-10, were used to evaluate π_2 by the method illustrated in Figures 3-1 and 3-2.

For use in computation of some of the pi terms, the following values were used:

U for miniature bins = 0.00193

$N_e = 1/(32.2)(60^2)$.

TABLE VIII

TREATMENT SCHEDULE FOR EXPERIMENTS
OF MINIATURE MODEL BINS

π_1	π_2	π_5	π_6	π_4	RUN NUMBER		
					BIN TYPE I	BIN TYPE II	BIN TYPE III
Measure π_1 for each run	$(\pi_2)_1$	$\bar{\pi}_5^*$	$\bar{\pi}_6$	$(\pi_4)_1$----------$(\pi_4)_8$	1	15	
	$(\pi_2)_2$				2	16	
	$(\pi_2)_3$				3	17	
	$(\pi_2)_4$				4	18	
	$(\pi_2)_5$				5	19	29
	$\bar{\pi}_2$	$(\pi_5)_1$	$\bar{\pi}_6$	$(\pi_4)_1$----------$(\pi_4)_8$	6	20	
		$(\pi_5)_2$			7	21	
		$(\pi_5)_3$			8	22	30
		$(\pi_5)_4$			1	15	
		$(\pi_5)_5$			9	23	
	$\bar{\pi}_2$	$\bar{\pi}_5$	$(\pi_6)_1$	$(\pi_4)_1$----------$(\pi_4)_8$	10	24	
			$(\pi_6)_2$		11	25	
			$(\pi_6)_3$		1	15	
			$(\pi_6)_4$		12	26	
			$(\pi_6)_5$		13	27	
			$(\pi_6)_6$		14	28	

* Bar denotes constant value of pi term.

TABLE IX

VALUE OF SOME OF THE FACTORS INVOLVED IN THE PI TERMS OF THE THERMAL DRYING SYSTEM AS USED IN THE MINIATURE MODEL BIN EXPERIMENTS

BIN TYPE	RUN NO.	τ_e	W*	τ_g	Q_a	$(M_g)_i$
I	1	559.6	0.00821	504.6	16.35	0.1669
	2	559.6	0.00647	500.6	16.35	0.1933
	3	579.6	0.00896	516.6	13.11	0.2048
	4	599.6	0.00823	533.6	13.67	0.1990
	5	619.6	0.01167	552.6	13.95	0.1976
	6	559.6	0.00844	559.6	16.35	0.1628
	7	559.6	0.00890	535.6	16.35	0.1628
	8	559.6	0.00886	519.6	16.35	0.1655
	9	559.6	0.00897	491.6	16.35	0.1641
	10	559.6	0.00944	499.6	16.35	0.1641
	11	559.6	0.00777	499.6	16.35	0.1641
	12	559.6	0.00714	499.6	16.35	0.1628
	13	559.6	0.00849	499.6	16.35	0.1682
	14	559.6	0.00926	497.6	16.35	0.1641
II	15	559.6	0.00848	499.6	17.00	0.1696
	16	559.6	0.00548	502.6	16.85	0.2048
	17	579.6	0.00713	516.6	12.11	0.2041
	18	599.6	0.00593	534.6	13.05	0.1912
	19	619.6	0.00913	550.1	13.79	0.1898
	20	559.6	0.00860	561.6	16.75	0.1751
	21	559.6	0.00879	538.1	16.75	0.1772
	22	559.6	0.00890	518.6	16.75	0.1758
	23	559.6	0.00831	490.6	16.73	0.1737
	24	559.6	0.00971	500.6	17.02	0.1730
	25	559.6	0.00835	500.6	16.75	0.1758
	26	559.6	0.00868	500.6	17.15	0.1703
	27	559.6	0.00846	500.1	16.95	0.1696
	28	559.6	0.00845	500.6	16.95	0.1723
III	29	619.6	0.00838	550.6	13.47	0.2048
	30	559.6	0.00900	519.6	16.55	0.1765

* W = humidity ratio of air entering bin, lb moisture per lb dry air.

Air absolute viscosity was taken from Figure A-3 and converted to the proper time units.

Preliminary experimental runs, Figure 6-7, using the miniature model bin set up revealed that a plot of weight of moisture removed versus elapsed time would be a growth rate type of curve with a maximum value of moisture removed which is determined by the drying air properties and initial grain condition. However, depending upon the relative value of initial grain temperature and entering air temperature, value of π_5, the curve is not well defined in the initial stages of drying. If the initial grain temperature was as low as the air dew point temperature, condensation on the grain would occur resulting in an initial moisture gain by the grain mass. Plots of π_1 versus π_4 gave the same shape curves as the plots of grams of moisture removed versus elapsed drying time. Figure 6-8 is a run for $\pi_5 = 1.0$ and Figure 6-9 is a run when $\pi_5 = 1.138$

Plots of π_1 versus π_2 are shown in Figures 6-10 and 6-11 respectively for bins type I and II. Since the plots were straight lines on log-log paper, equations for the plots were of the form:

$$\pi_1 = a\pi_2^{\,b} \quad . \tag{6-7}$$

Equation 6-7 can be transformed into the linear form:

$$\log \pi_1 = \log a + b \log \pi_2 \quad . \tag{6-8}$$

The component equations involving π_2 were evaluated by linear regression analyses of the transformed equations. The component equations are listed in Figures 6-10 and 6-11 with their respective correlation coefficients r.

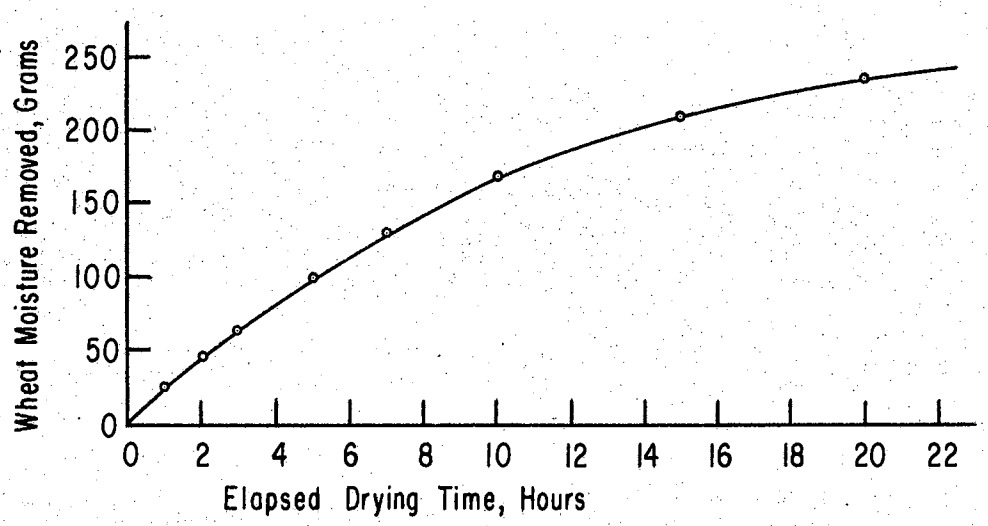

FIGURE 6-7. Characteristic shape of drying curve.

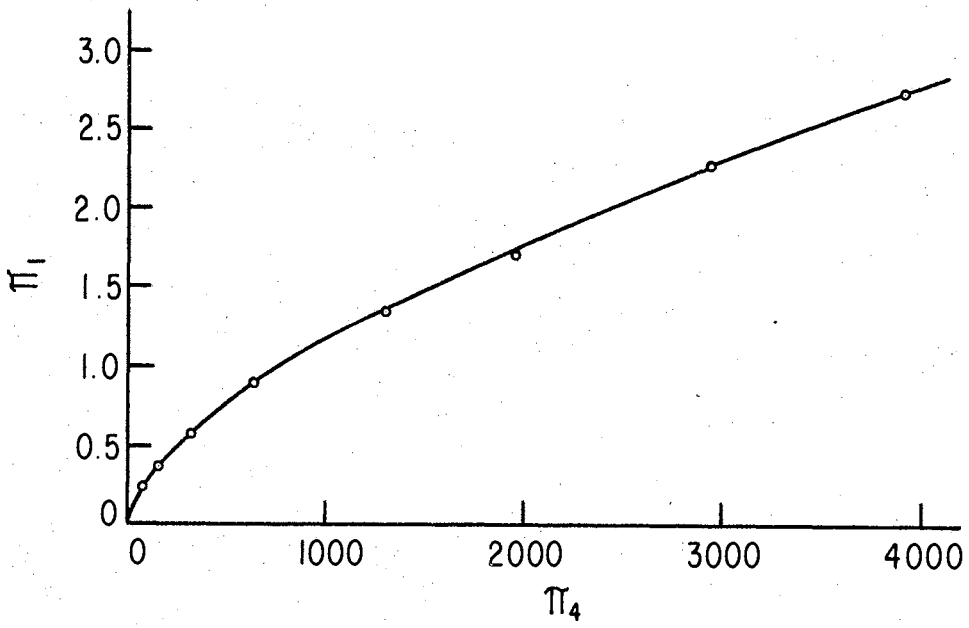

FIGURE 6-8. Plot of π_1 versus π_4 for $\pi_5 = 1.00$. Bin type I, run 6.

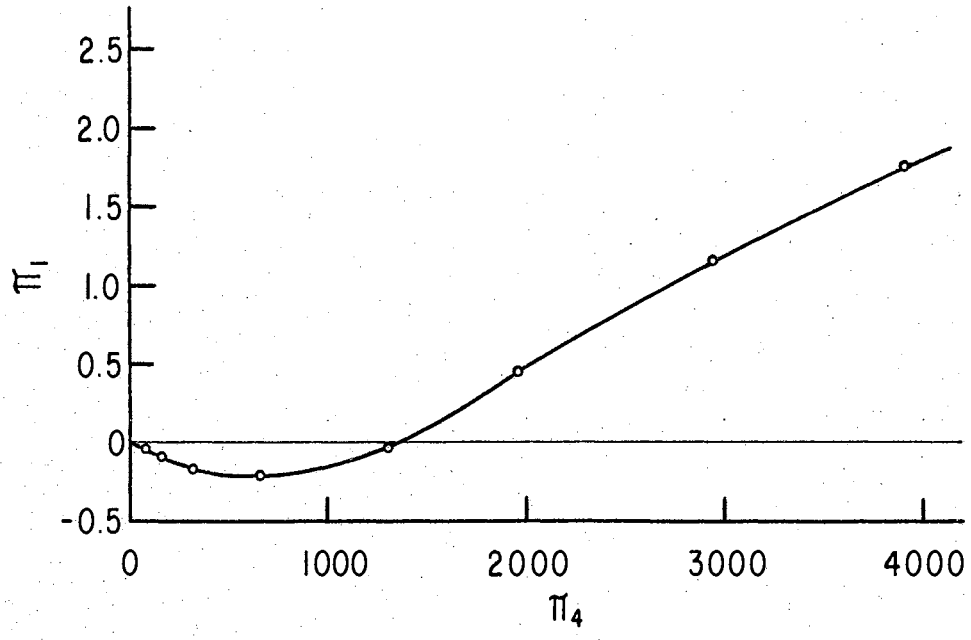

FIGURE 6-9. Plot of π_1 versus π_4 for $\pi_5 = 1.138$. Bin type I, run 9.

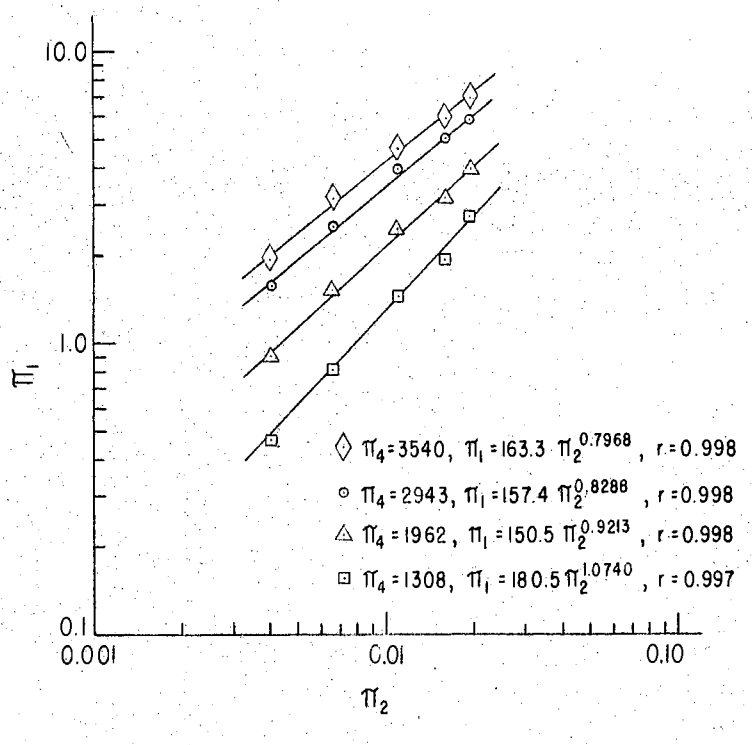

FIGURE 6-10. Graphs of component equation, π_1 versus π_2 for bin type I.

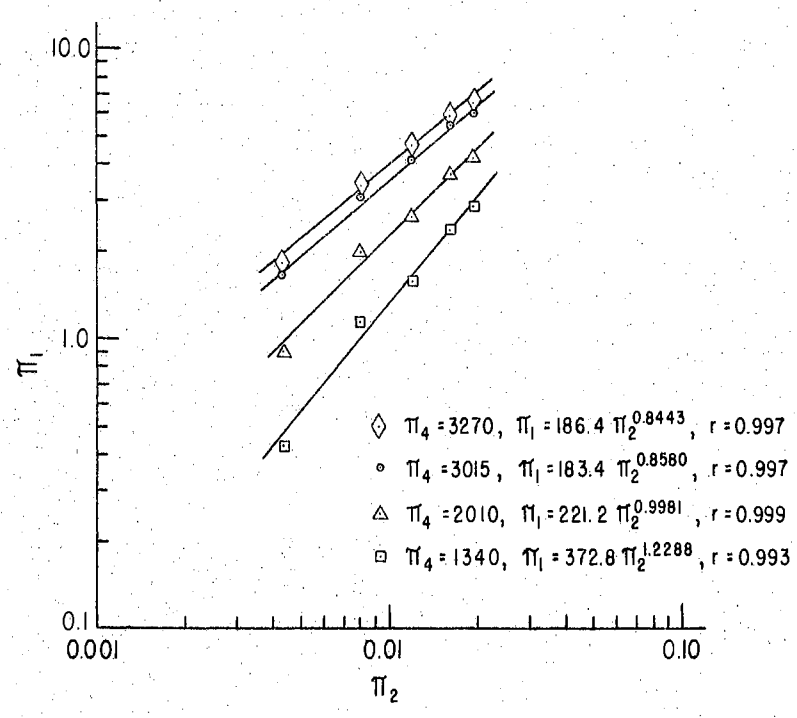

FIGURE 6-11. Graphs of component equation, π_1 versus π_2 for bin type II.

The plots of Figures 6-10 and 6-11 revealed that the relationships of π_1 versus π_2 appeared to be dependent upon π_4 since the slopes of the plots are not constant for each bin type. However, further analysis indicated that the relationships were influenced by the transient effect of a thermal diffusivity term rather than by π_4. The thermal diffusivity term was not incorporated in the experimental treatment schedule, but by using additional data of grain thermal conductivity, specific heat, and density, the term could be evaluated. (1, p. 105). The term was:

$$\pi_{10} = c_g \rho_g r^2 / k_g t \qquad 6\text{-}9$$

in which c_g = grain specific heat, btu/lb$_{(M)}$F, $HM^{-1}\theta^{-1}$

k_g = grain thermal conductivity, btu ft/ft^{2}min F, $HL^{-1}T^{-1}\theta^{-1}$.

The other terms are defined in Table II. Values of π_{10} are included in Tables B-I, B-II, and B-III for wheat in the miniature bins and in Table B-VIII for wheat in the two-foot diameter bins.

Plots of π_1 versus π_5 are shown in Figures 6-12 and 6-13 for bin type I and II respectively. The component equations involving π_5 are listed in the Figures with their respective correlation coefficients r for the data in linear logarithmic transformation. As with π_1 versus π_2, the component equations involving π_5 appeared to be dependent upon π_4. This dependency was also considered to be actually upon π_{10} rather than upon π_4.

Plots of π_1 versus π_6, Figures 6-14 and 6-15 for bins type I and II respectively, revealed no consistent relationship. Consequently, π_6 was eliminated from the analysis. Linear regressions of π_1 versus π_6, in logarithmic transformations, were made and the lines plotted as

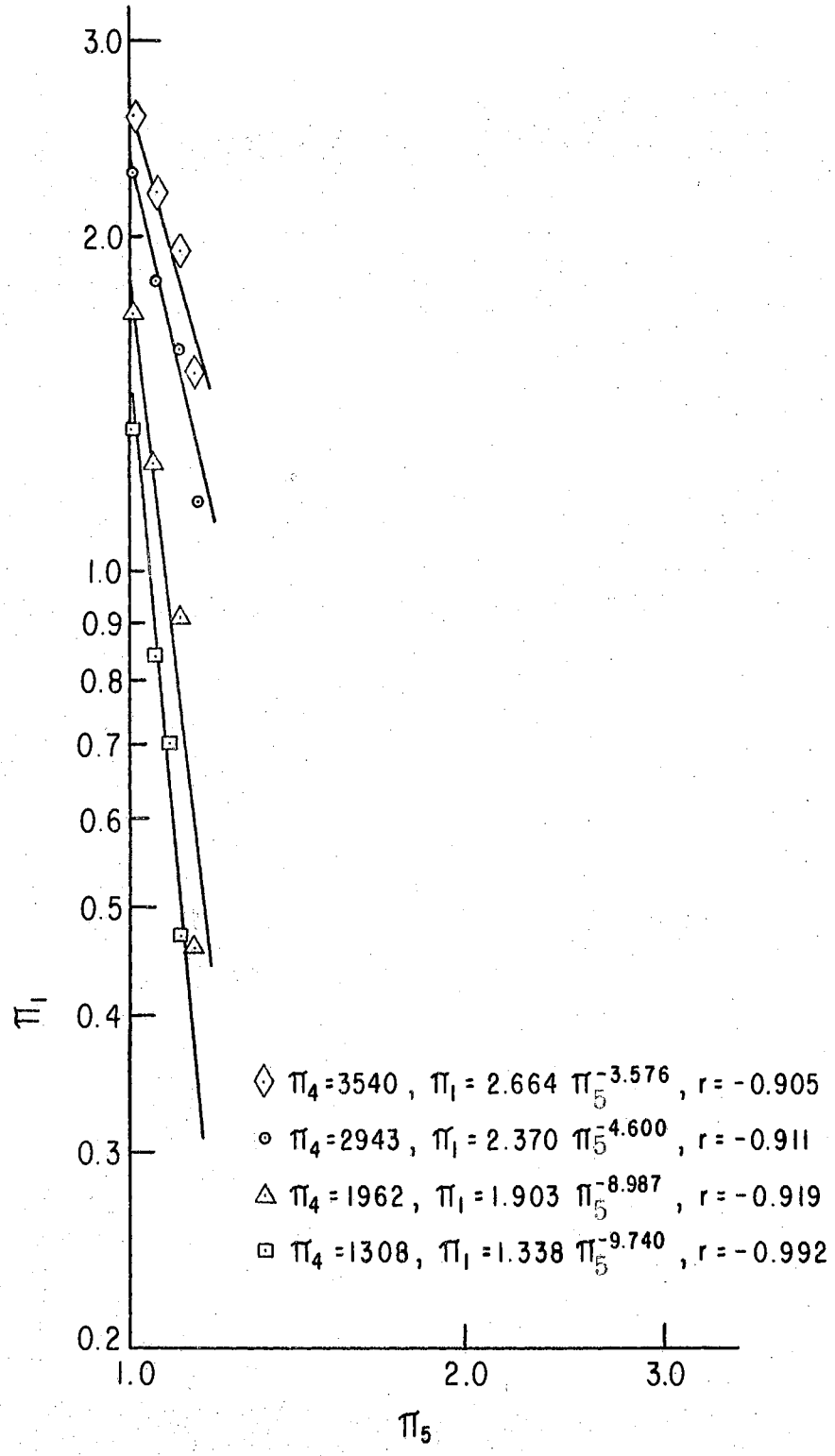

FIGURE 6-12. Graphs of component equation, π_1 versus π_5 for bin type I.

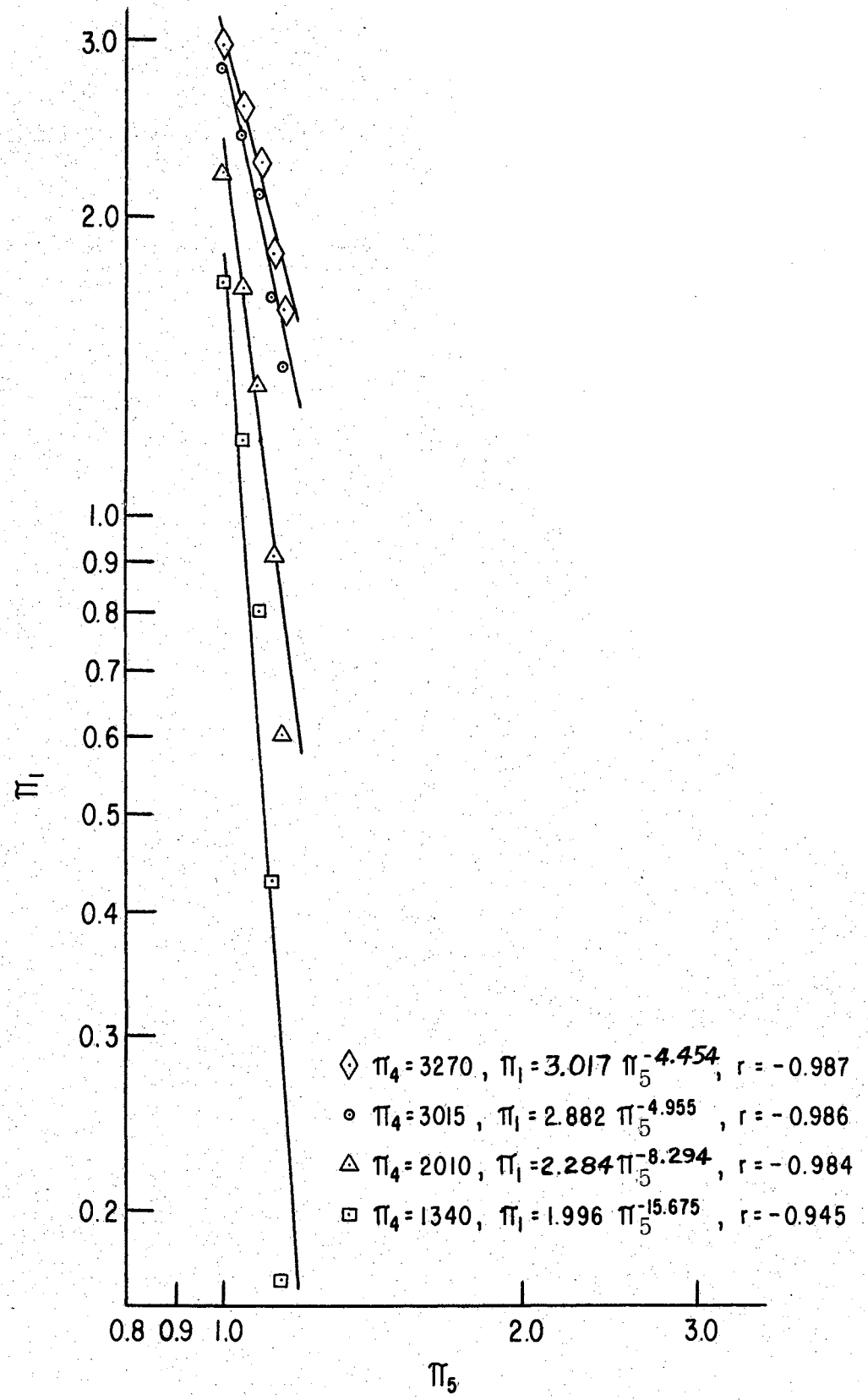

FIGURE 6-13. Graphs of component equation, π_1 versus π_5 for bin type II.

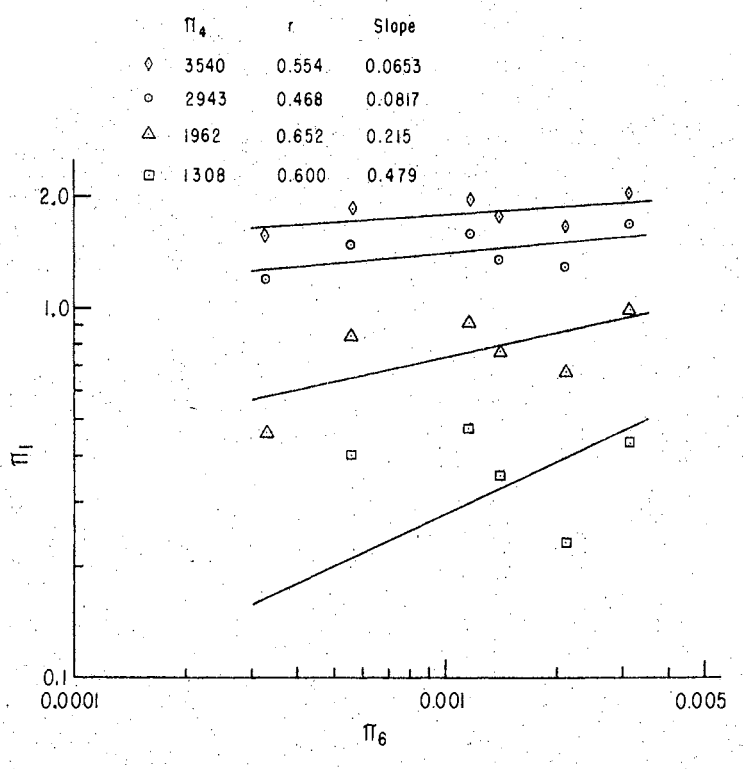

FIGURE 6-14. Plots of π_1 versus π_6 for bin type I.

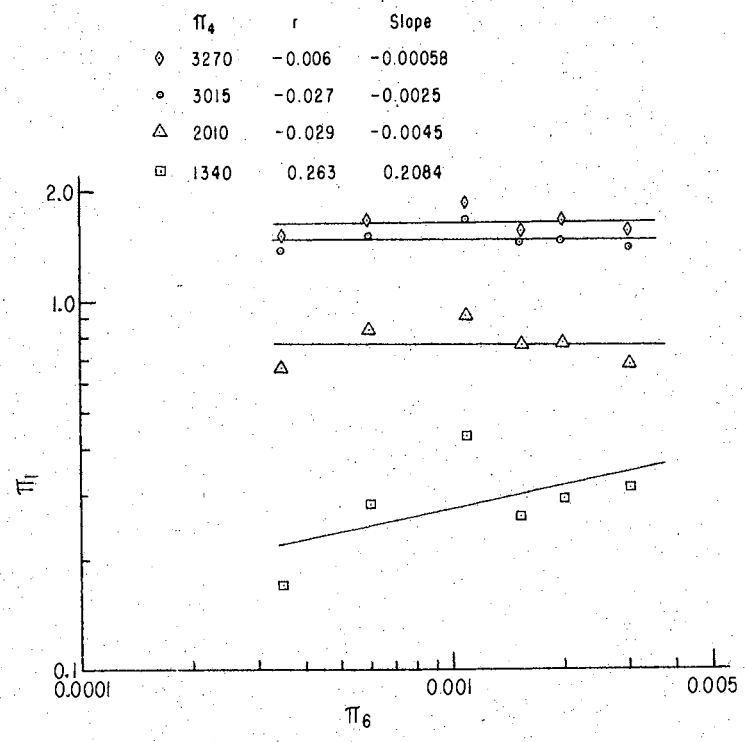

FIGURE 6-15. Plots of π_1 versus π_6 for bin type II.

shown in Figures 6-14 and 6-15. Regression coefficients, slopes of lines, and correlation coefficients are included in the Figures.

A relationship between π_1 and π_4 was hypothesized which had an asymptote and included the effects of π_2, π_5, and π_{10}. The relationship was of the form:

$$\pi_1 = k_1(1-e^{-k_2 \pi_4}) \qquad 6\text{-}10$$

in which $k_1 = f(\pi_2)$

$k_2 = f(\pi_5, \pi_{10})$.

For values of $\pi_5 > 1$, the results during an increment of π_4 from the beginning of the experiment were erratic and in some cases a moisture gain was experienced by the grain mass, see Figure 6-9. That is, when $\pi_5 > 1$ a drying effect, reduced from what would occur if $\pi_5 = 1$, occurred during an increment of π_4 from the beginning of the experiment. For $\pi_5 < 1$, a drying effect greater than if $\pi_5 = 1$ would be indicated for an initial increment of π_4. For $\pi_5 \neq 1$, a plot of π_1 versus π_4 could be approximated by a plot for $\pi_5 = 1$ if the $\pi_5 = 1$ plot were displaced an increment of π_4 to the right for $\pi_5 > 1$ and to the left for $\pi_5 < 1$. The increment of π_4 that the $\pi_5 = 1$ curve was displaced shall be referred to as δ. Thus it was hypothesized that the drying effect would be altered by an increment of π_4, δ, in addition to the effects included in equation 6-10. The mathematical model for the drying curve was now hypothesized to be of the form:

$$\pi_1 = C_1 \pi_2^{C_2}\left[1-e^{-C_3 \pi_{10}^{C_4} \pi_5^{C_5} (\pi_4-\delta)}\right].$$

The δ increments were determined by superimposing the π_1 versus π_4 drying curves for $\pi_5 = 1$ upon the curves for varying values of

π_5 at a constant value of π_2. The δ increments were plotted versus π_4, Figures 6-16 and 6-17 for bins type I and II respectively. The resulting relationships between δ and π_5 appeared linear on Cartesian coordinates such that:

$$\delta = -k_1+k_1 \pi_5 \quad . \qquad 6\text{-}11$$

Additional analysis indicated that δ would be reduced for a value of $\pi_5 > 1$ if π_2 were increased above the values from which equation 6-11 was formulated. The graphical superposition method was further applied to evaluate points on Figures 6-16 and 6-17 for different levels of π_2. A straight line was fitted to these points. The slopes of the δ versus π_5 plots were plotted versus π_2, Figure 6-18, to determine the relationship among δ, π_5, and π_2. The plots in Figure 6-18 also appeared linear on Cartesian coordinates so that the form of the equation for δ became:

$$\delta = -C_6-C_7 \pi_2+C_6 \pi_5+C_7 \pi_2 \pi_5 \qquad 6\text{-}12$$

or, $$\delta = (\pi_5-1)(C_6+C_7 \pi_2)$$

The resulting form of the prediction equation was:

$$\pi_1 = C_1 \pi_2^{C_2} \left[1-e^{-C_3 \pi_{10}^{C_4} \pi_5^{C_5} (\pi_4+C_6+C_7 \pi_2-C_6 \pi_5-C_7 \pi_2 \pi_5)}\right] \qquad 6\text{-}13$$

in which C_i are coefficients and exponents depending upon type of grain and bin configuration.

Several methods were used to determine the most suitable values for the C_i in equation 6-13. One method was to evaluate C_2 and C_5 from

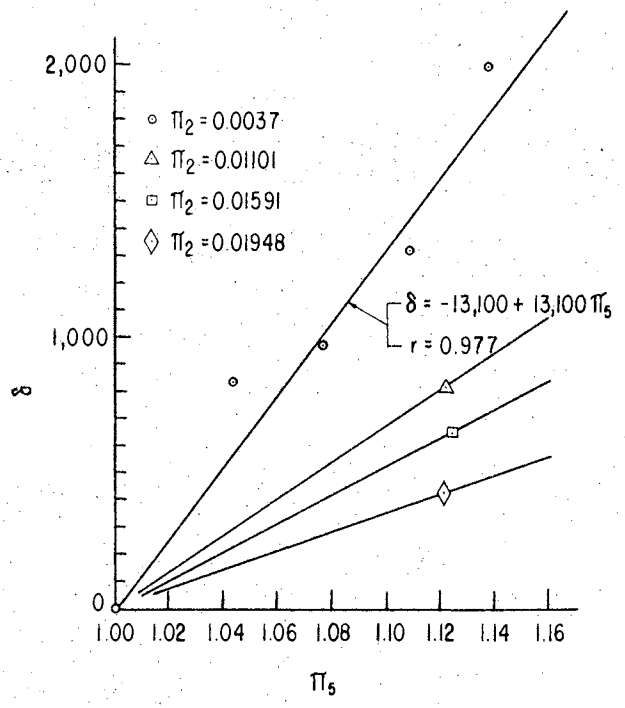

FIGURE 6-16. Determination of δ, an increment of π_4, bin type I.

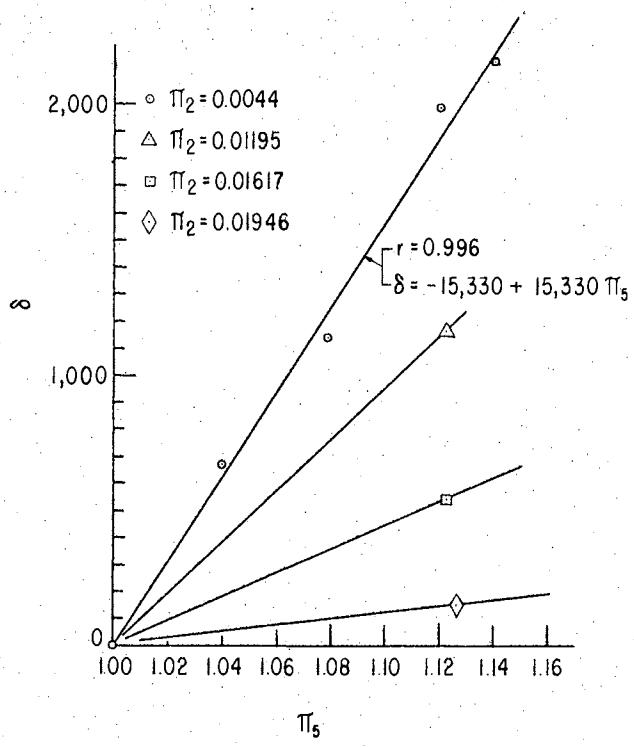

FIGURE 6-17. Determination of δ, an increment of π_4, bin type II.

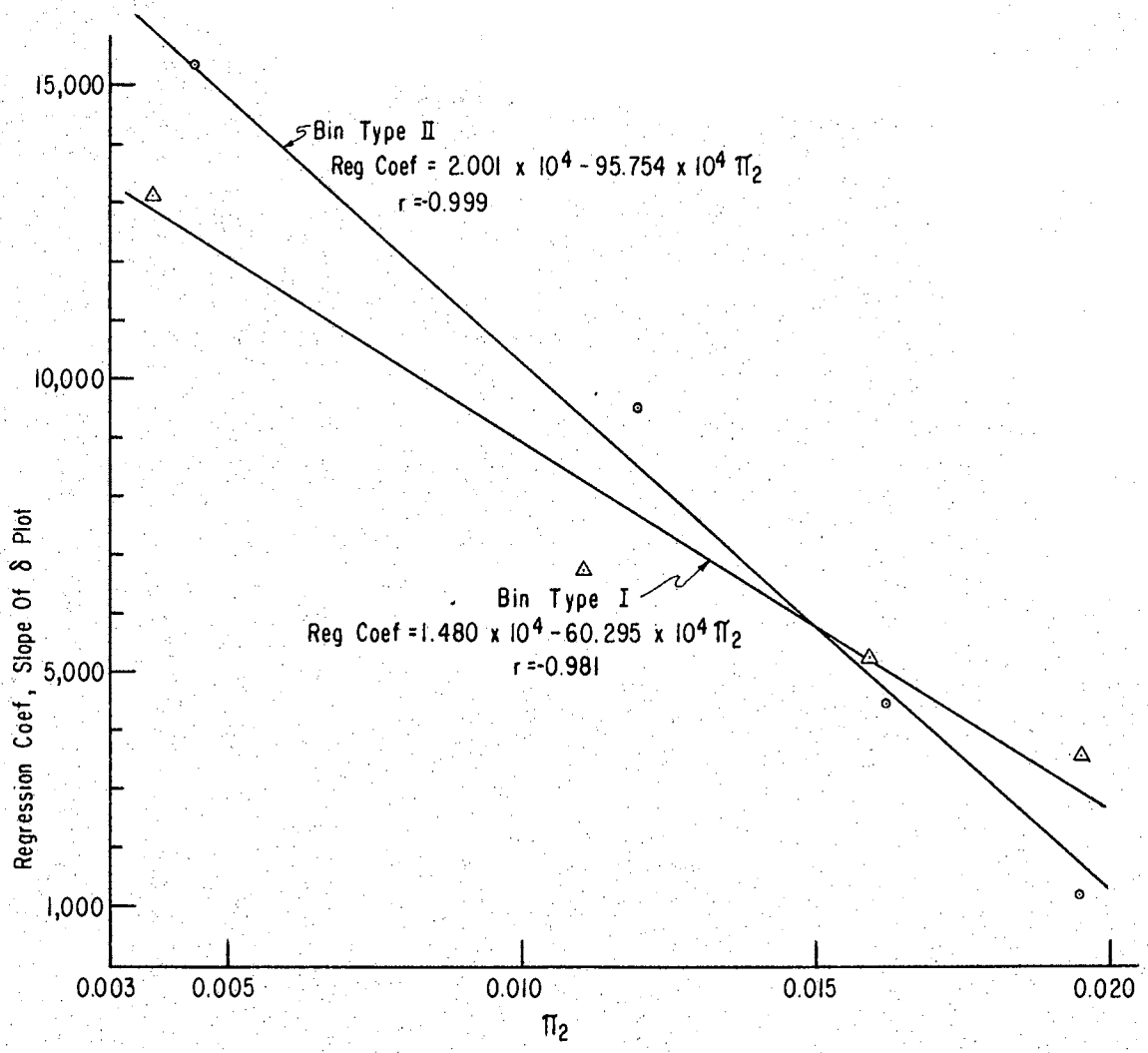

FIGURE 6-18. Slope of the δ plots versus π_2.

the component equations, disregarding the values when π_4 was small. C_6 and C_7 were evaluated from Figure 6-18. C_4 was estimated to make the equation valid when π_4 was small and $\pi_5 = 1$. Estimates for C_1 and C_3 were made from a simultaneous solution of equation 6-13 and the first partial derivative of the equation with respect to π_4 which was: (δ not expanded)

$$\partial\pi_1/\partial\pi_4 = C_1C_3\pi_2^{C_2}\pi_{10}^{C_4}\pi_5^{C_5}e^{-C_3\pi_{10}^{C_4}\pi_5^{C_5}(\pi_4-\delta)} . \qquad 6\text{-}14$$

The simultaneous solution of equations 6-13 and 6-14 led to a graphical solution of linear and an exponential curve as follows:

From equation 6-13, (δ not expanded),

$$C_1\pi_2^{C_2}e^{-C_3\pi_{10}^{C_4}\pi_5^{C_5}(\pi_4-\delta)} = C_1\pi_2^{C_2} - \pi_1$$

or,

$$e^{C_3\pi_{10}^{C_4}\pi_5^{C_5}(\pi_4-\delta)} = C_1\pi_2^{C_2}/C_1\pi_2^{C_2} - \pi_1 = 1/(1-\pi_1/C_1\pi_2^{C_2}) \qquad 6\text{-}15$$

From equation 6-14,

$$C_1 = (\partial\pi_1/\partial\pi_4)e^{C_3\pi_{10}^{C_4}\pi_5^{C_5}(\pi_4-\delta)}/C_3\,\pi_2^{C_2}\,\pi_{10}^{C_4}\,\pi_5^{C_5} \qquad 6\text{-}16$$

Substitute the value of C_1 from equation 6-16 into equation 6-15,

Thus:

$$e^{C_3\pi_{10}^{C_4}\pi_5^{C_5}(\pi_4-\delta)} = 1/1-\pi_1C_3\pi_{10}^{C_4}\pi_5^{C_5}/(\partial\pi_1/\partial\pi_4)e^{C_3\pi_{10}^{C_4}\pi_5^{C_5}(\pi_4-\delta)}$$

or,

$$e^{C_3\pi_{10}^{C_4}\pi_5^{C_5}(\pi_4-\delta)}\left[1-C_3\pi_1\pi_{10}^{C_4}\pi_5^{C_5}/(\partial\pi_1/\partial\pi_4)e^{C_3\pi_{10}^{C_4}\pi_5^{C_5}(\pi_4-\delta)}\right] = 1$$

Finally:

$$e^{C_3\pi_{10}^{C_4}\pi_5^{C_5}(\pi_4-\delta)} = \left[C_3\pi_1\pi_{10}^{C_4}\pi_5^{C_5}/(\partial\pi_1/\partial\pi_4)\right]+1 \quad . \qquad 6\text{-}17$$

An example of the graphical solution of C_3 is shown in Figure 6-19. C_3 was then substituted into either of equations 6-13, or 6-14 and C_4 evaluated.

A second method was to compute C_1 and C_2 from the wheat hygroscopicity relationships since the asymptotes of the drying curves, π_1 versus π_4, were directly proportional to $C_1\,\pi_2^{C_2}$. Values of $(\pi_1)_{max}$, equal to $\Delta M \times 100$ by definition for a constant wet bulb process, were plotted versus π_2, Figure 6-20, from which C_1 and C_2 were evaluated. C_5, C_6, and C_7 were evaluated as in the previous method of approach. By evaluating C_1, C_2, C_6, and C_7, equation 6-13 could be transformed into a linear form so that a linear regression would yield simultaneous solutions of C_3 and C_4. The linear transformation of equation 6-13 was derived as follows: (δ not expanded)

$$\pi_1/C_1\pi_2^{C_2} = 1-e^{-C_3\pi_{10}^{C_4}\pi_5^{C_5}(\pi_4-\delta)}$$

$$1/(1-\pi_1/C_1\pi_2^{C_2}) = e^{C_3\pi_{10}^{C_4}\pi_5^{C_5}(\pi_4-\delta)}$$

$$\log_e 1/(1-\pi_1/C_1\pi_2^{C_2}) = C_3\pi_{10}^{C_4}\pi_5^{C_5}(\pi_4-\delta)$$

$$\log_{10}\left\{\log_e\left[1/(1-\pi_1/C_1\pi_2^{C_2})\right]\right\} = \log_{10}C_3+C_4\log_{10}\pi_{10}+C_5\log_{10}\pi_5+\log_{10}(\pi_4-\delta)$$

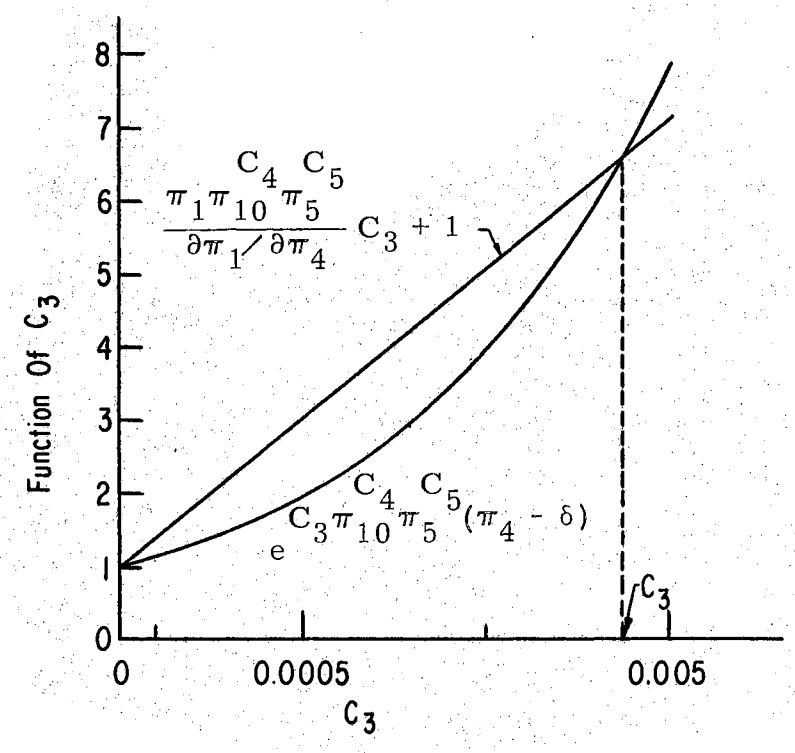

FIGURE 6-19. Graphical Solution of Simultaneous Equations for C_1 and C_3.

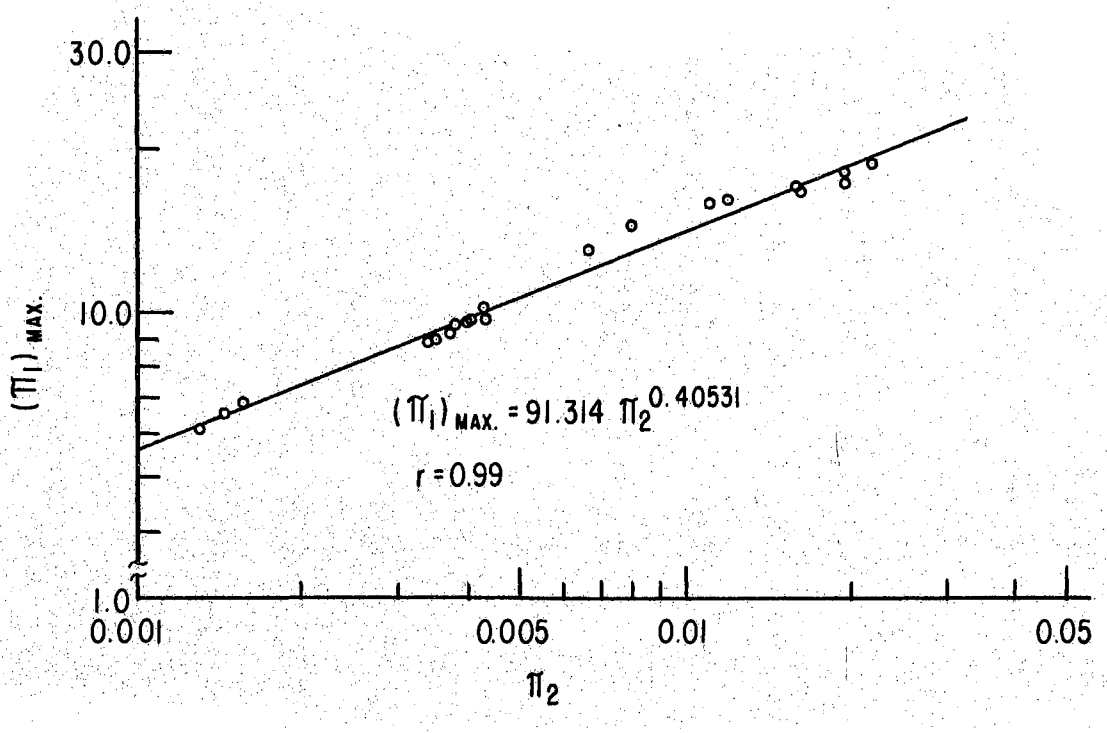

FIGURE 6-20. Graph of $(\pi_1)_{max}$ versus π_2.

Finally,

$$\log_{10}\left\{\log_e\left[1/(1-\pi_1/C_1\pi_2^{C_2})\right]/(\pi_4-\delta)\pi_5^{C_5}\right\} = \log_{10}C_3+C_4\log_{10}\pi_{10} \quad . \qquad 6\text{-}18$$

Equation 6-18 is of the linear form:

$$Y = A+BX$$

in which $Y = \log_{10}\left\{\log_e\left[1/(1-\pi_1/C_1\pi_2^{C_2})\right]/(\pi_4-\delta)\pi_5^{C_5}\right\}$

$X = \log_{10}\pi_{10}$

$A = \log_{10}C_3$, C_3 = antilog A

$B = C_4$.

A third method was using a program on an I.B.M. 650 electronic computer which simultaneously solved for the C_i. The program format used was program I by Granet and Edwards (14) for linear and nonlinear regression calculations. The regression procedure derives least square estimates for parameters (constants) of any analytic function for which the first derivatives with respect to the parameters exist. The procedure depends on the fact that a criterion function can be stated which is a linear combination of the partial derivatives with respect to the parameters. Original estimates for each of the parameters are included in the program and by an iterative procedure, increments are added algebraically to the original estimates until the program converges on the best combination of values of the parameters by a method of reducing the sum of squares of residuals between observed and predicted to a minimum.

It was found that an unrealistic asymptote resulted if the program were allowed to solve simultaneously for all seven of the C_i.

A more appropriate solution resulted by using C_1 and C_2 as evaluated from the $(\pi_1)_{max}$ versus π_2 relationship and solving simultaneously for C_3, C_4, C_5, C_6, and C_7.

The partial derivatives of the dependent term π_1, with respect to the C_i for use in the computer program were as follows: (δ not expanded)

Let: $Y = \pi_1$ $\quad P_1 = C_3$

$X_1 = \pi_2$ $\quad P_2 = C_4$

$X_2 = \pi_5$ $\quad P_3 = C_5$

$X_4 = \pi_4$ $\quad P_4 = C_6$

$X_5 = \pi_{10}$ $\quad P_5 = C_7$

Thus, $$D_1 = \partial Y/\partial P_1 = C_1 X_1^{C_2} X_5^{P_2} X_2^{P_3} (X_4-\delta) e^{-P_1 X_5^{P_2} X_2^{P_3} (X_4-\delta)}$$

$$D_2 = \partial Y/\partial P_2 = (P_1 \log_e X_5) D_1$$

$$D_3 = \partial Y/\partial P_3 = (P_1 \log_e X_2) D_1$$

$$D_4 = \partial Y/\partial P_4 = C_1 X_1^{C_2} P_1 X_5^{P_2} X_2^{P_3} (1-X_2) e^{-P_1 X_5^{P_2} X_2^{P_3} (X_4-\delta)}$$

$$D_5 = \partial Y/\partial P_5 = X_1 D_4$$

The computer program in Fortran statements is listed in Table A-II. The program was processed for machine use by compiling the program using Fortransit II-s with the appropriate sub-routines.

The computer program was very sensitive and would result in over-flow and underflow errors for some combinations of the original estimates. Data for π_4 less than estimated δ were removed for the iterations. Run 8 for bin type I was removed as a plot of π_1 versus π_4

indicated it was not reliable. To prevent the data from being weighted excessively with runs for $\pi_5 \neq 1$, additional data were interpolated for the runs of $\pi_5 = 1$, runs 6 and 20 for bins type I and II respectively. The limited data available for bin type III did not include any for $\pi_5 = 1$. At least one datum for the two-foot diameter bins, actual or interpolated, was pooled with the miniature bin data in the final solution for the P_i for each bin. This was done so that there would be a variation of bin hydraulic radius in the data. The solution for the P_i would converge after six to eight iterations for the successful attempts of running the program.

The most appropriate sets of values for the C_i are listed below and resulted from the method of evaluating C_1 and C_2 from the $(\pi_1)_{max}$ versus π_2 relationship, Figure 6-20, and using the electronic computer program for regression analysis of C_3, C_4, C_5, C_6, and C_7:

	Bin Type		
	I	II	III
C_1	91.314	91.314	91.314
C_2	0.40531	0.40531	0.40531
C_3	0.000087761	0.00010767	0.000060956
C_4	0.34480	0.25258	0.65780
C_5	6.3612	3.1832	9.1730
C_6	23,253.	22,593.	20,443.
C_7	-899,833.	-1,037,483.	-619,520.

Actual observed values of π_1 used in the solution for the P_i, predicted values of π_1, and per cent difference/100 are listed in Tables B-XI, B-XII, and B-XIII for the miniature bins type I, II, and III respectively. Also included in the Tables are the statistical standard

error of estimates for the miniature bin data listed, and observed and predicted values for the two-foot diameter bins. The computed δ increments of π_4 are listed in Table B-XIV for the miniature bin experiments.

Validity of the prediction equation for evaluating conditions in prototype installations was tested by considering the miniature bins as the model system and the two-foot diameter bins as the prototype system. Plots of predicted versus observed values for the two systems are shown in Figures 6-21, 6-22, and 6-23 for bins type I, II, and III respectively. The data were from experimental runs 6 and 20 of the miniature bins type I and II respectively and for all the applicable data available for bin type III. Run 1 of the two-foot diameter bins was used in the figures. The data for the other runs of the two-foot diameter bins were for intermittent operation and after a rewetting process occurred in run 2. For these reasons, the data of the other runs of the two-foot diameter bins were not considered applicable for direct comparison to predicted values and were omitted from Figures 6-21, 6-22, and 6-23 although comparison of observed and predicted for all the runs is included in Tables B-XI, B-XII, and B-XIII. Run 1 of the two-foot diameter bin type I was for $\pi_5 = 0.966$ which was the lowest value of π_5 obtained during the research project.

A moisture balance was made on some of the runs of the miniature bins to determine if the moisture removed from the grain was equal to the moisture gained by the air. Examples of graphical representations of moisture gained by the air are shown in Figures 6-24 and 6-25. These figures are for the same runs as shown in Figures 6-8 and 6-9 respectively. The moisture gained by the air was determined by

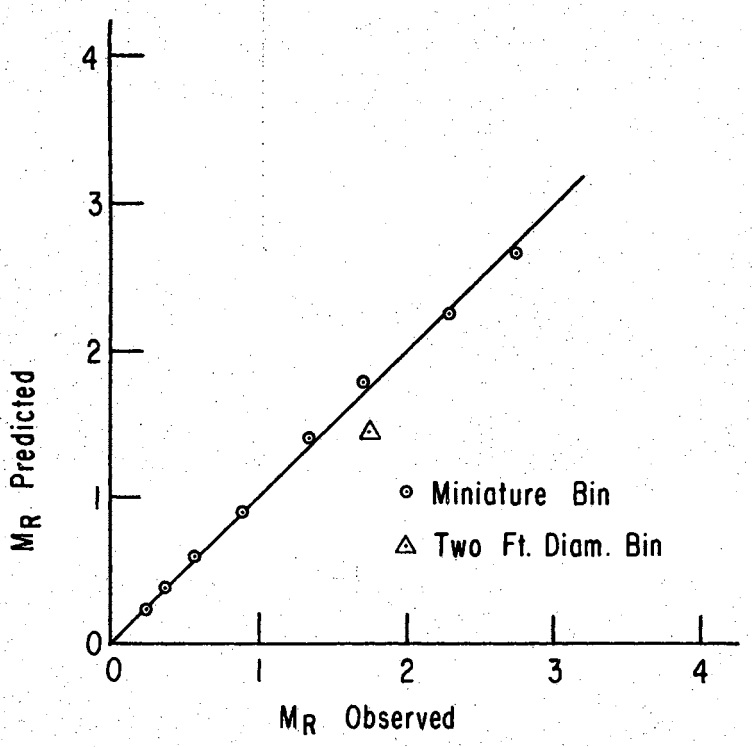

FIGURE 6-21. Predicted versus observed values of π_1 for miniature and two-foot diameter bins type I.

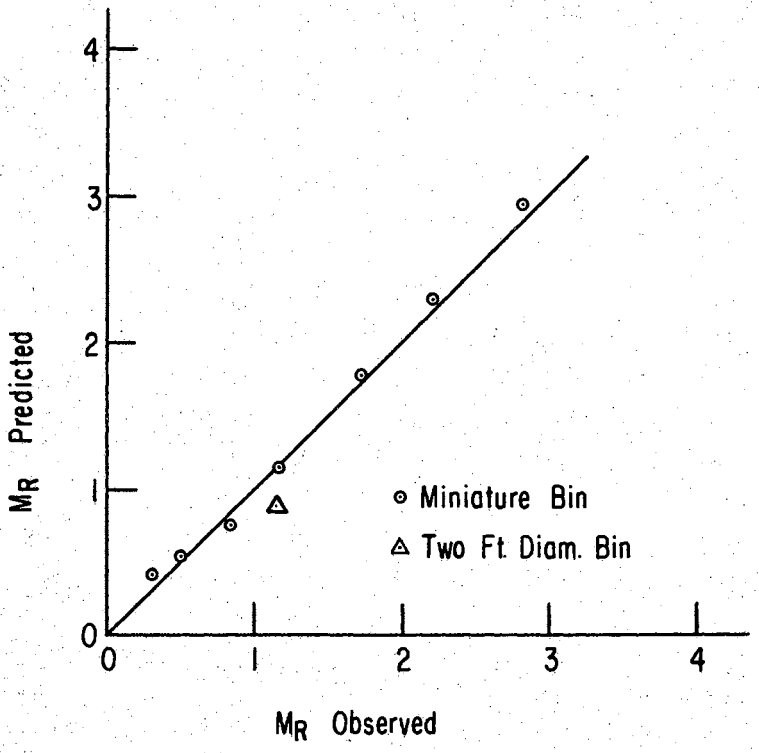

FIGURE 6-22. Predicted versus observed values of π_1 for miniature and two-foot diameter bins type II.

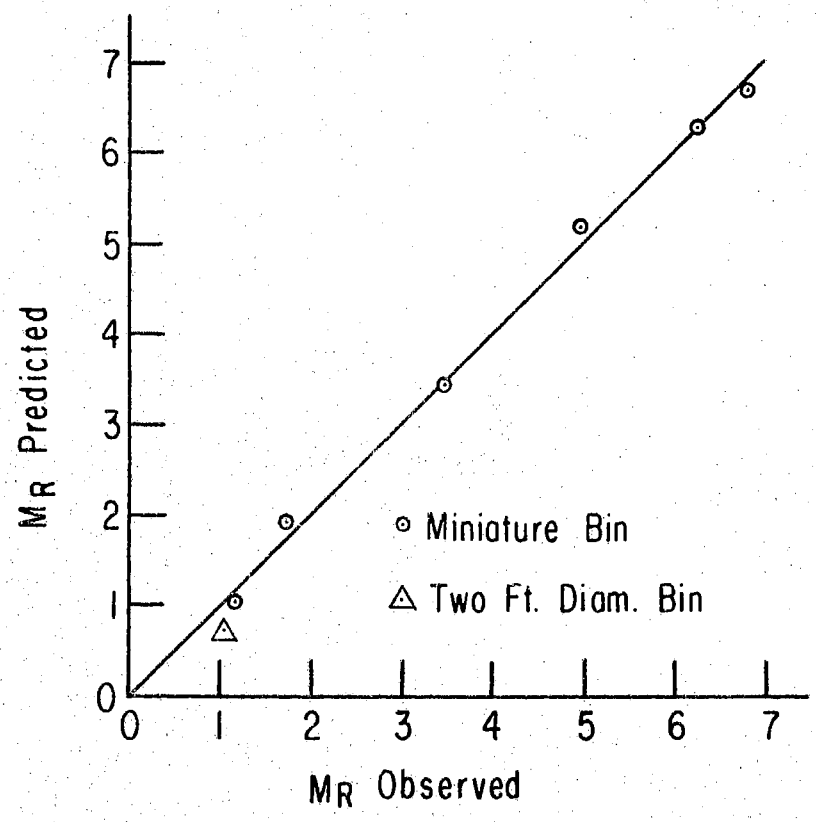

FIGURE 6-23. Predicted versus observed values of π_1 for miniature and two-foot diameter bins type III.

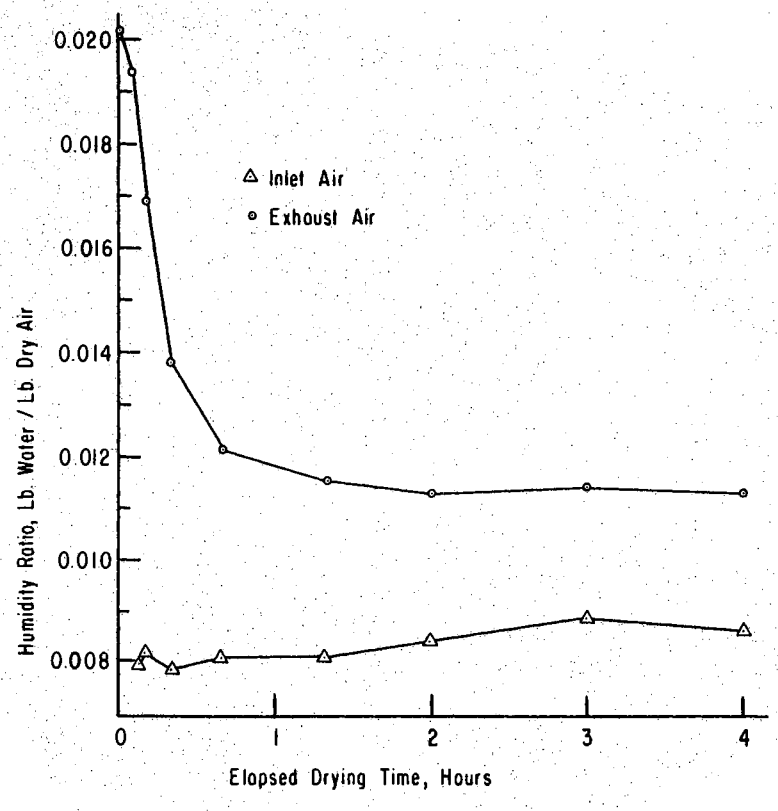

FIGURE 6-24. Moisture content of inlet and exhaust air, bin type I, run 6.

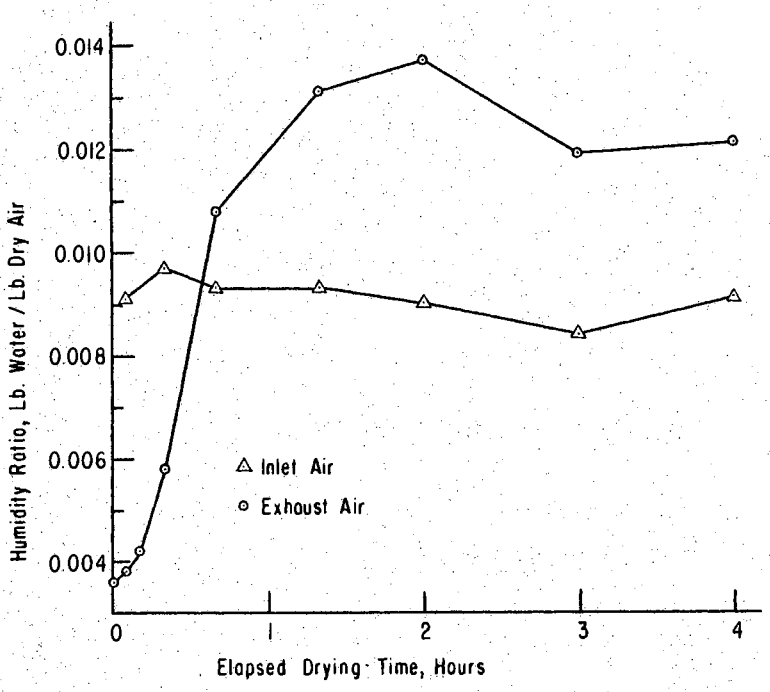

FIGURE 6-25. Moisture content of inlet and exhaust air, bin type I, run 9.

measuring the area between inlet and exhaust air curves by using a Keuffel and Esser Company Planimeter, model 4237. The area was converted into units of pounds of moisture. Comparison of moisture removed from the grain as determined by weighing the bins and moisture gained by air as determined from psychrometric analysis of exhaust air is listed below for seven runs.

	Run	Moisture removed from grain, lbs	Moisture gained by air, lbs
Bin Type I	1	0.1631	0.1240
	5	0.5200	0.5416
	6	0.2090	0.1784
	9	0.1345	0.1211
Bin Type II	15	0.1760	0.0796
	19	0.5300	0.5100
	23	0.1675	0.1018

A standard deviation of differences of 0.0297 lbs water was obtained for the runs analyzed. This was 0.45 per cent moisture content dry basis.

Internal Moisture and Temperature Gradients

The internal moisture and temperature gradients during drying with atmospheric air were analyzed from the results of the drying experiments using the two-foot diameter bins. The moisture content, flow rate, and ambient air data are listed in Tables B-VII and B-VIII for grain sorghum and wheat experiments respectively. The intergranular temperature data, assumed equal to grain temperature, are listed in Tables B-IX and B-X respectively for the grain sorghum and wheat experiments. Values of the dimensionless groups, pi terms, are listed in Table B-VI for the

wheat experiment. The values in Table B-VI are accumulative from the beginning of the experiment.

Grain moisture distributions for successive stages of drying are shown in Figures 6-26, 6-27, and 6-28 for drying of grain sorghum and in Figures 6-29, 6-30, 6-31, and 6-32 for the drying of wheat.

The initial grain moisture contents and temperature were not quite equal for each of the three bins at the beginning of an experiment. Also, the air flow rates were not equal for the three bin types during the experiments although attempts were made to exhaust enough air from the blowers of bin types II and III so that the flow rate to them would not exceed the flow rate to bin type I. The full output from the blower of bin type I was utilized, but the grain offered more resistance to air flow in this bin since the air traveled a greater distance through the grain.

Since the initial and operating conditions were not quite equal in the three bins during an experiment, the successive stages of drying are not applicable for direct comparison between bin types although some trends are indicated. Comparison of the grain moisture distributions revealed the zones in each type bin which dried the slowest, these zones were: Bin type I, the zone next to the bin wall on the exhaust air side; Bin type II, the zone across the bin (through the center) between the exhaust air ducts; and Bin type III, the zone at the center of the bin. In actual prototype installations, more uniform drying might occur if an operational system were developed for switching the blowers to different ducts as drying progressed.

A typical set of internal temperature gradients are shown in Figure 6-33, for each of the three bin types for the wheat drying

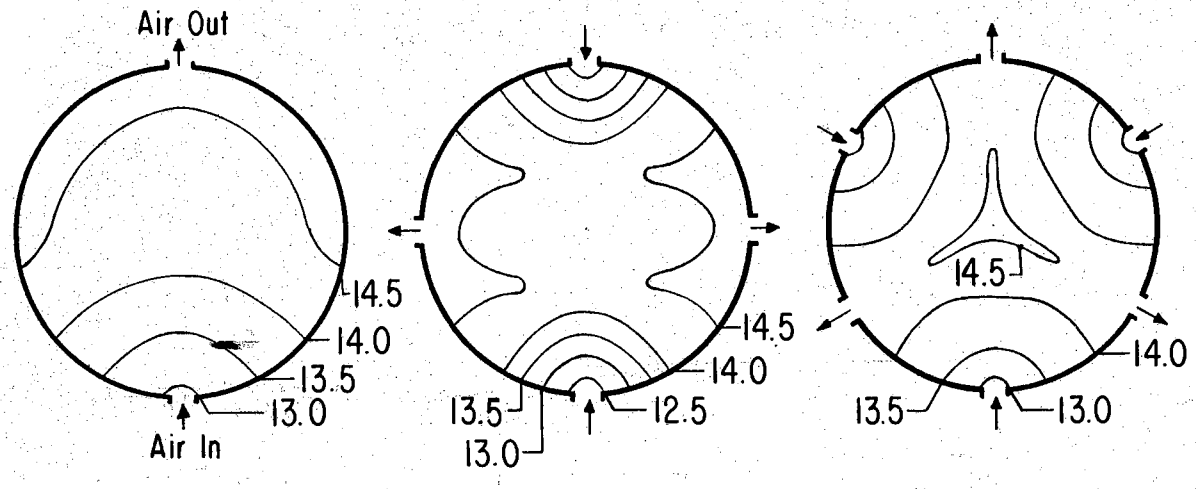

BIN TYPE I BIN TYPE II BIN TYPE III

Average = 14.1 14.1 14.0

FIGURE 6-26. Distribution of moisture content of grain sorghum in the two-foot diameter bins, % wet basis, run 1. (4 hrs drying)

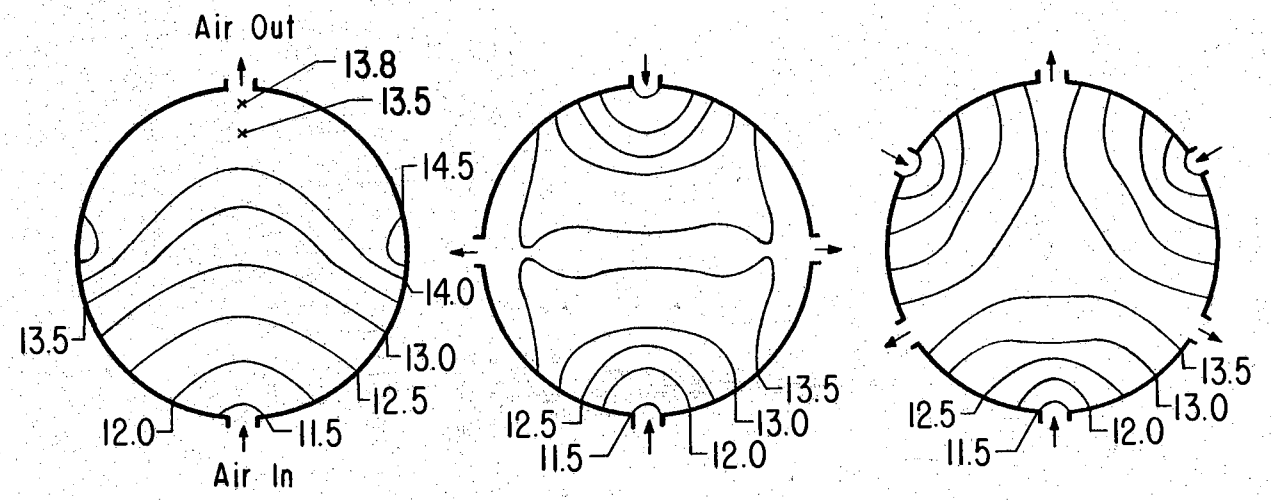

BIN TYPE I BIN TYPE II BIN TYPE III

Average = 13.2 13.1 13.1

FIGURE 6-27. Distribution of moisture content of grain sorghum in the two-foot diameter bins, % wet basis, run 2. (8 hrs additional drying, 12 hrs total)

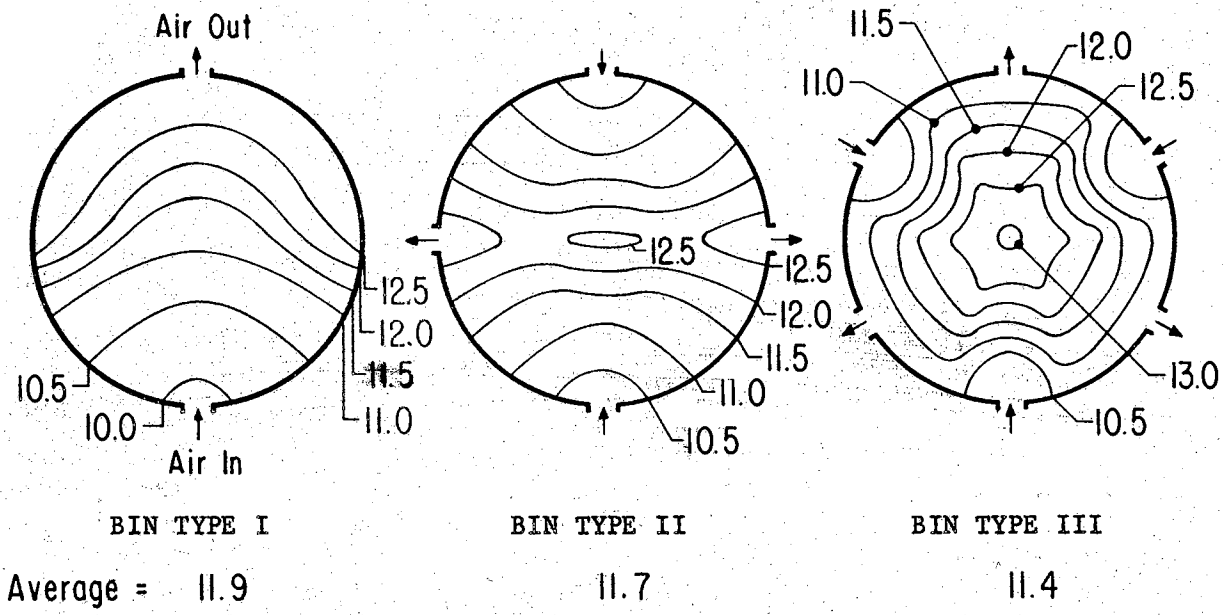

FIGURE 6-28. Distribution of moisture content of grain sorghum in the two-foot diameter bins, % wet basis, run 3. (37 hrs additional drying, 49 hrs total)

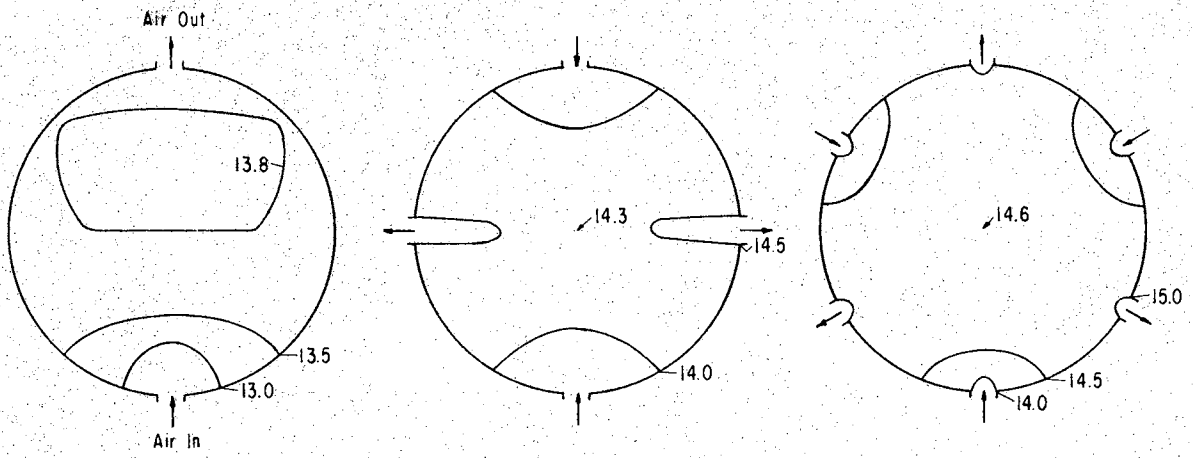

BIN TYPE I BIN TYPE II BIN TYPE III

Average = 13.5 14.3 14.6

FIGURE 6-29. Distribution of moisture content of wheat in the two-foot diameter bins, % wet basis, run 1. (3 hrs of drying)

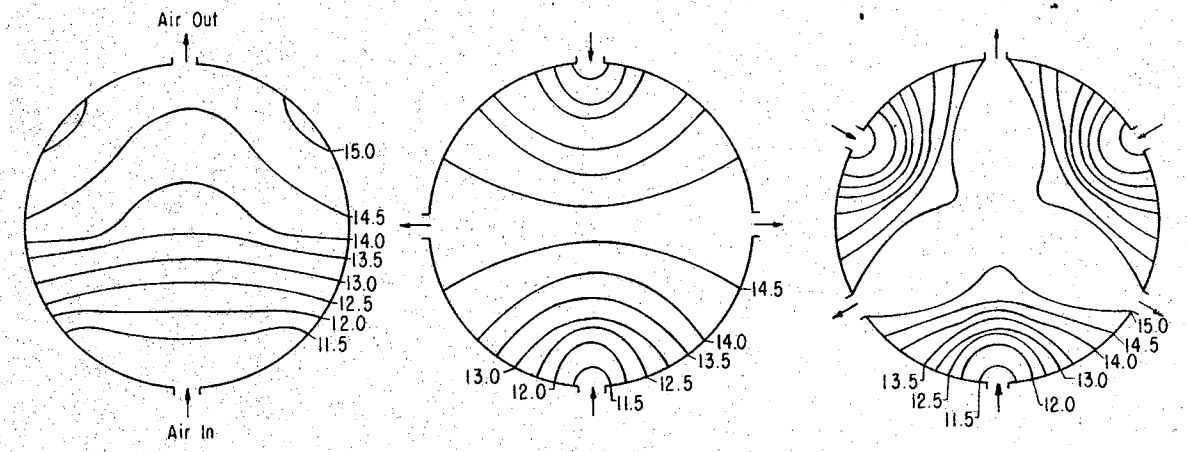

BIN TYPE I BIN TYPE II BIN TYPE III

Average = 13.6 13.9 14.2

FIGURE 6-30. Distribution of moisture content of wheat in the two-foot diameter bins, % wet basis, run 3. (11.8 hrs additional drying past run 2, 20.8 hrs total operation. Run 2 was 6 hrs of rewetting.)

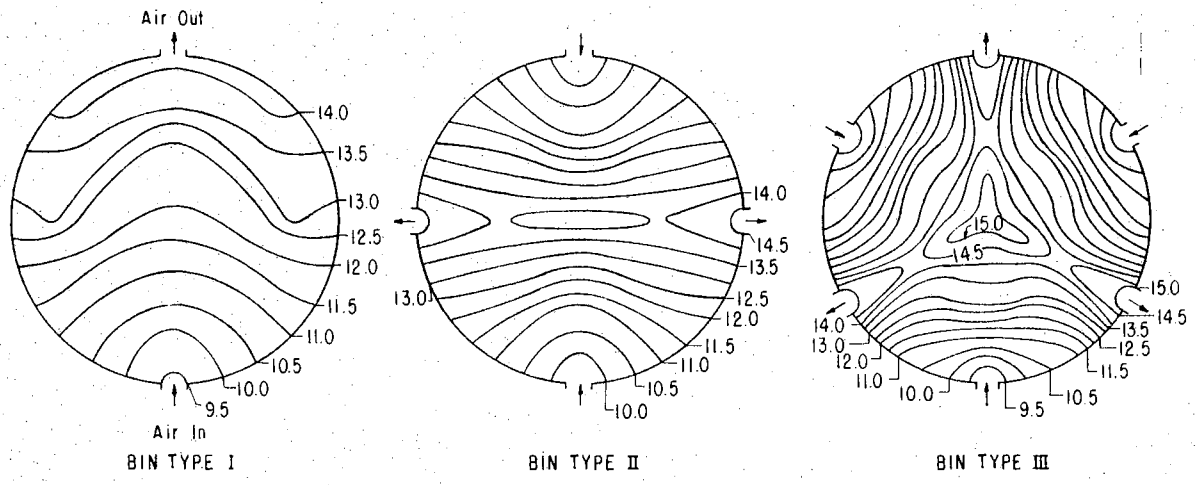

Average = 12.0 12.5 14.2

FIGURE 6-31. Distribution of moisture content of wheat in the two-foot diameter bins, % wet basis, run 4. (24.2 hrs additional drying, 45 hrs. total)

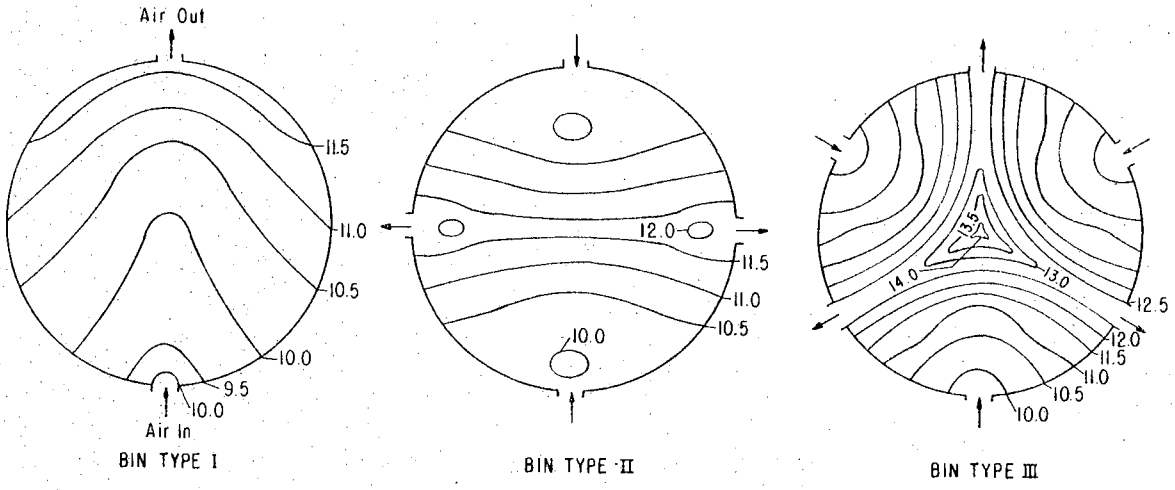

Average = 10.5 10.9 11.7

FIGURE 6-32. Distribution of moisture content of wheat in the two-foot diameter bins, % wet basis, run 5. (54.4 hrs additional drying, 99.4 hrs total)

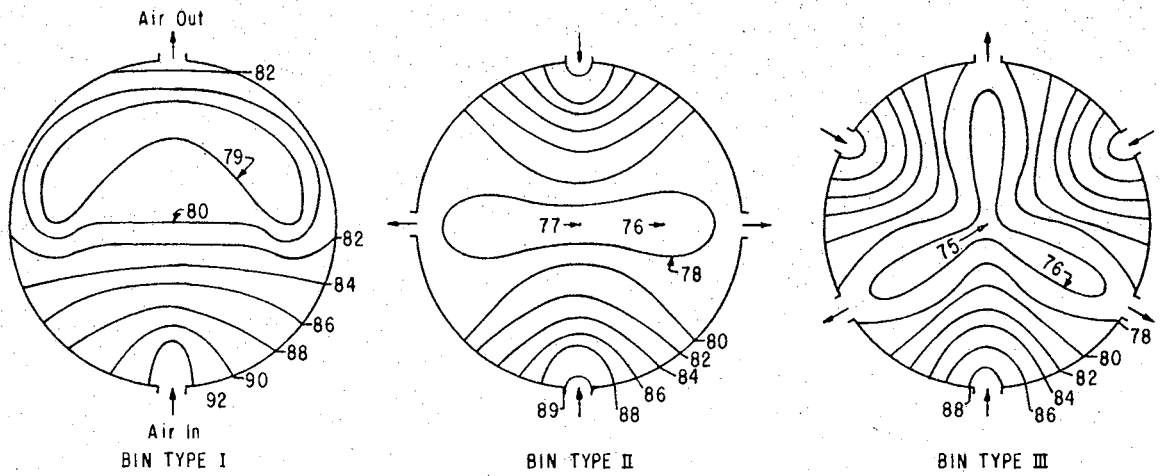

Average = 83.3 80.9 79.9

FIGURE 6-33. Distribution of temperature of wheat in the two-foot diameter bins, F, run 3.

experiment. The temperature gradients correspond to the drying gradients of Figure 6-30.

Redistribution of temperature and moisture content was indicated for intermittent blower operation by comparison of these properties at identical positions at the time the blowers were switched off and at some later time, usually overnight. The data referred to are included as the runs with suffix A in Tables B-VIII and B-X for grain moisture and temperature respectively of wheat in the two-foot diameter bins.

Discussion of Prediction Equation

The prediction equation for the thermal drying system, equation 6-13, gives the average moisture removed from a bin of grain and does not indicate from where the moisture is removed inside the bin. The equation is for a bin completely full so that short circuiting of air is prevented. Effects due to grain variety, amount of foreign material present, cracked kernels, and compaction of grain were not studied in this research.

When the initial grain temperature is equal to the temperature of the air entering the grain, $\pi_5 = 1$, $\delta = 0$, and the equation reduces to:

$$\pi_1 = C_1 \pi_2^{C_2} \left[1 - e^{-C_3 \pi_{10}^{C_4} \pi_4}\right] \qquad 6\text{-}19$$

When initial grain temperature is higher than the temperature of the entering air, $\pi_5 < 1$, an initial increase in the drying effect will result. Conversely, if the initial grain temperature is less than the entering air temperature, $\pi_5 > 1$, an initial decrease in drying effect will occur. These effects are illustrated in Figure 6-34. The prediction equation defines the $\pi_5 = 1$ curve and approximates the effect for $\pi_5 \neq 1$. For $\pi_5 \neq 1$, the equation is limited in application

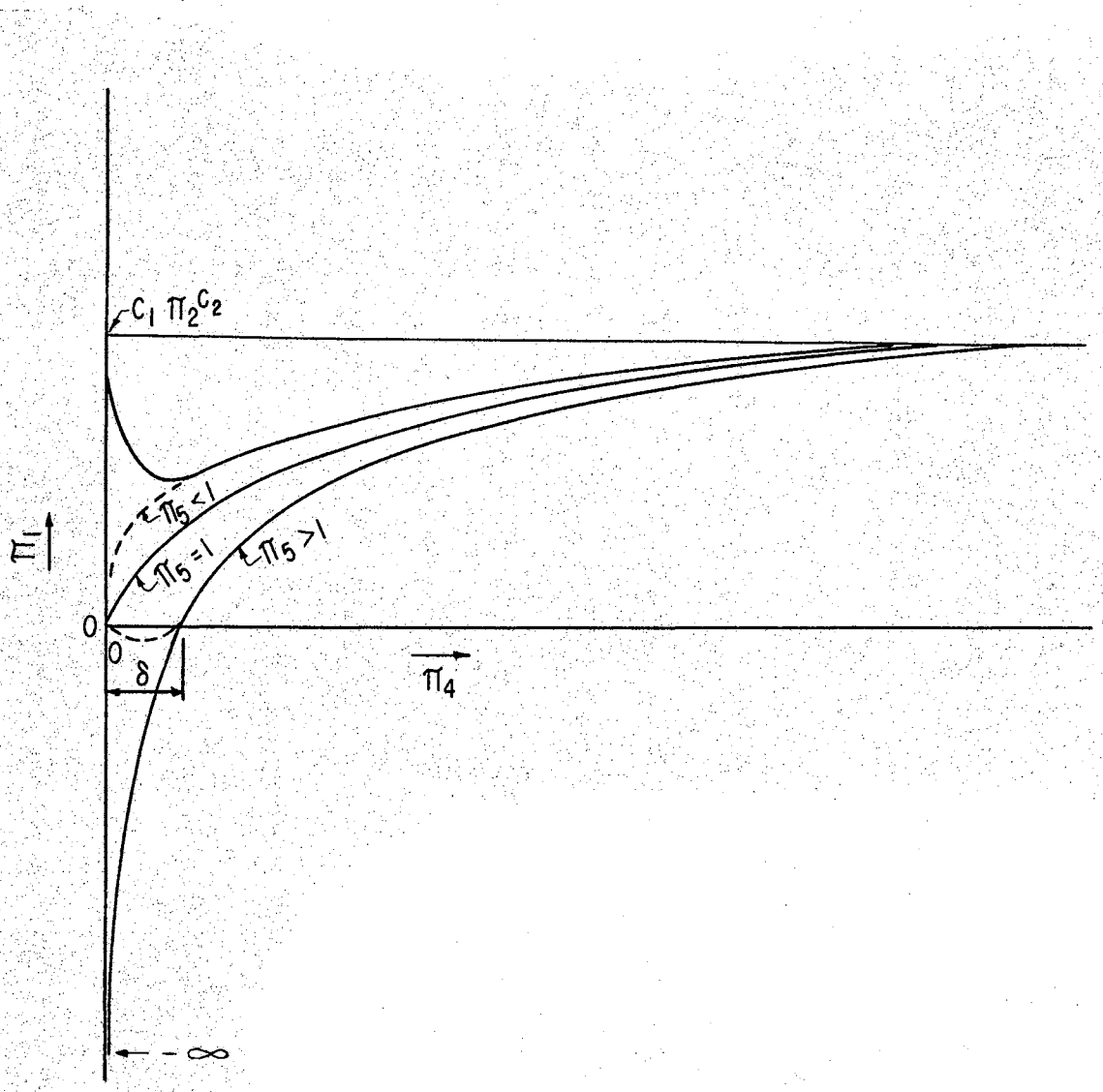

FIGURE 6-34. Drying Effects and Region of Applicability of Prediction Equation.

until an increment of π_4 of magnitude equal to or greater than the absolute value of δ has elapsed. δ is negative for $\pi_5 < 1$ and positive for $\pi_5 > 1$.

When the C_i resulting from the analysis were used for a bin type to compare the predicted drying effects obtained for $\pi_5 < 1$, $\pi_5 = 1$, and $\pi_5 > 1$, for other conditions equal, the plots were not in complete agreement with the relative effects shown in Figure 6-34. After an increment of π_4 somewhat greater than δ had elapsed, the position of the $\pi_5 < 1$ and $\pi_5 > 1$ curves interchanged as compared to their respective positions in Figure 6-34. These comparisons were evaluated by varying the initial grain temperature to obtain a variation in π_5 so that the asymptotes of the curves remained equal. The discrepancies between the hypothesized relationships of Figure 6-34 and predicted values were considered due to evaluating the C_i using observed data which were predominently for $\pi_5 > 1$. It appears that additional experimental observations for $\pi_5 = 1$ and $\pi_5 < 1$ are necessary to be included in the data for empirically evaluating the C_i. Since the C_i were evaluated from data which were predominently for $\pi_5 > 1$, the resulting C_i are considered most appropriate for applications of $\pi_5 > 1$ although the plots of Figures 6-21 and 6-22 verify that very good agreement was also obtained between predicted and observed values for bin type I and II for $\pi_5 = 1$.

Data for $\pi_5 = 1$ for bin type III were extrapolated by a graphical method of displacing the π_1 versus π_4 curves for $\pi_5 > 1$ to the left an increment of π_4 equal to the estimated δ for each run. Pooling these data with the actual observations and using the electronic computer program to evaluate the P_i resulted in the following:

$C_3 = 0.0001272$, $C_4 = 0.1495$, $C_5 = -2.942$, $C_6 = 7{,}912$, and $C_7 = -675{,}594$ which are quite different from the P_i of the analysis using only observed data of $\pi_5 > 1$, page 124. Curves plotted from predicted values using C_1 and C_2 as listed on page 124 and the P_i listed above for comparing the effects of $\pi_5 < 1$, $\pi_5 = 1$ and $\pi_5 > 1$ are shown in Figure 6-35. These curves are in agreement with the behavior of the plots of Figure 6-34. The differences between the above evaluations of the P_i for bin type III and the P_i listed on page 124 illustrate the sensitivity of the computer program for least squares regressions of nonlinear equations.

An example of comparison of predicted drying effects for bins type I and II is shown in Figure 6-36 for $\pi_5 > 1$. Bin type III predictions were omitted from the figure since insufficient observed data were available for evaluating the P_i.

The prediction equation indicates, as did the experimental research, that an increased drying effect occurs for an increase in:

π_2, the drying potential of the air,

bin hydraulic radius, r,

air flow rate, Q_a, and

elapsed drying time, t.

Since drying time t is included in π_{10} as well as in π_4, the drying effect is not the same for equal values of π_4 obtained from the product of different combinations of Q_a and t. For example, doubling the air flow rate and reducing the elapsed time by one-half results in an increased drying effect for the doubled air flow rate as shown by the example in Figure 6-37 which was plotted from evaluations using the prediction equation for a bin type. Also included in π_{10} are grain

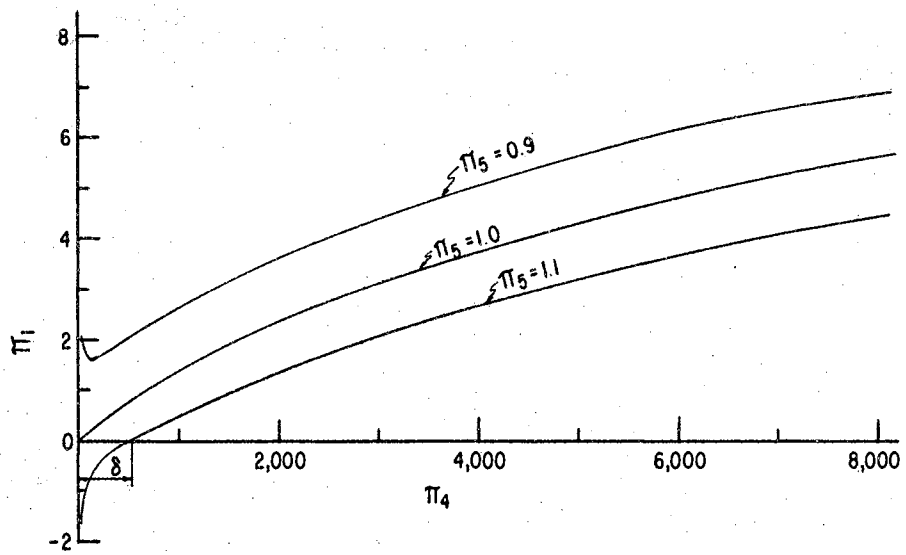

FIGURE 6-35. Set of predicted drying curves for bin type III using C_i from analysis of observed and extrapolated data.

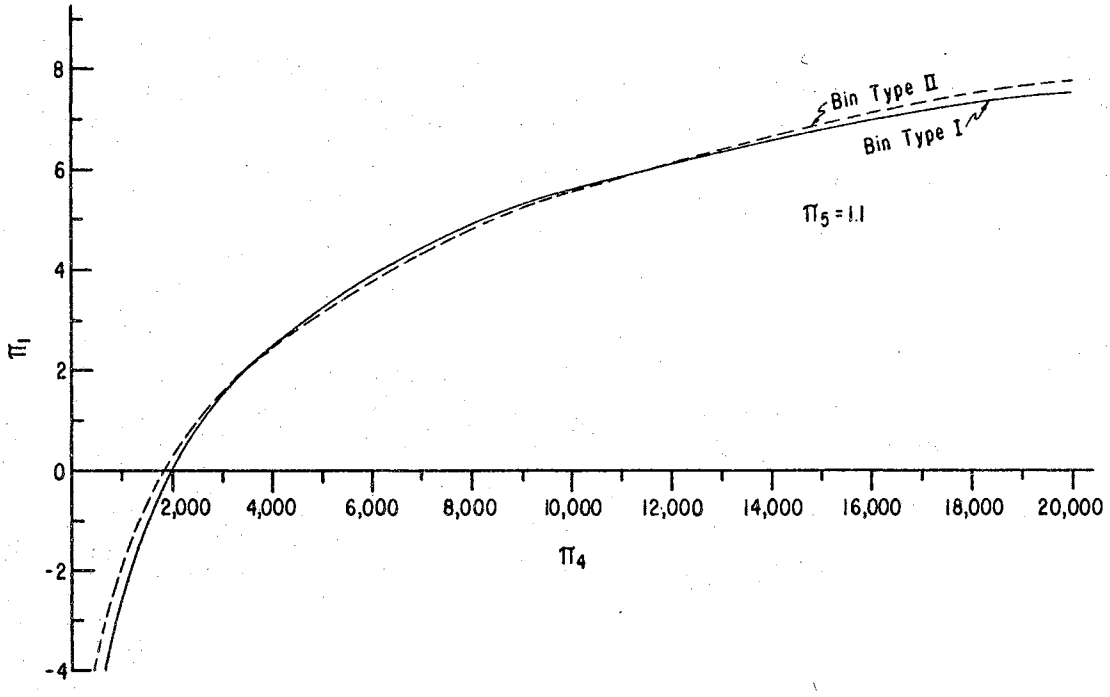

FIGURE 6-36. Comparison of drying effects for bin types I and II using prediction equations for $\pi_5 > 1$.

thermal diffusivity and bin hydraulic radius.

The form of the prediction equation seems general in nature and not limited to cross-flow arrangements. The C_i would require re-evaluation for different bin configurations and for different grains.

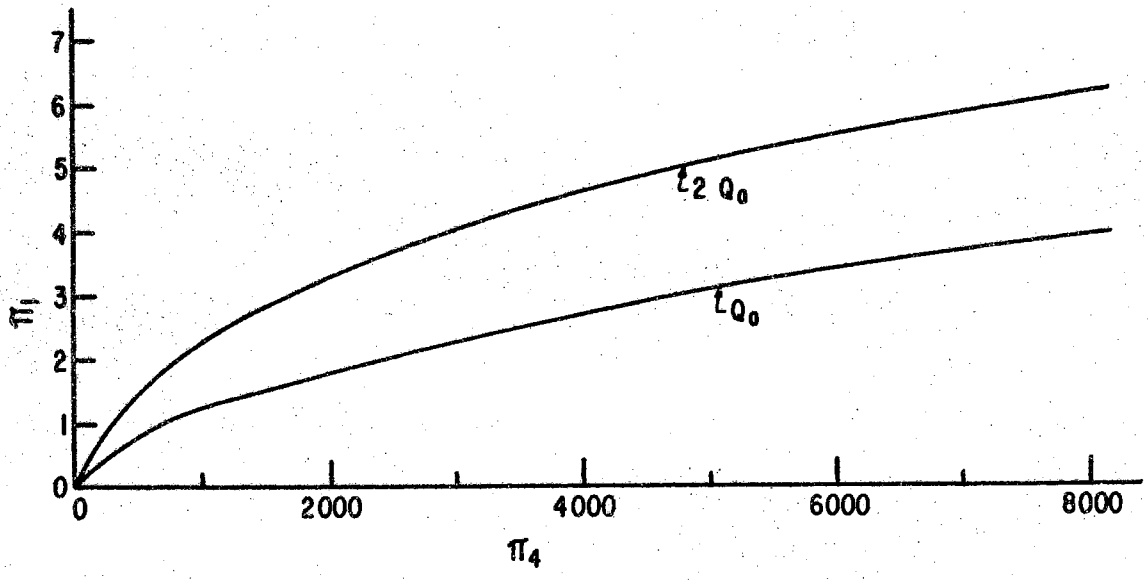

FIGURE 6-37. Effect of a doubled air flow rate on drying obtained.

CHAPTER VII

SUMMARY AND CONCLUSIONS

Summary

The objective of the study was to formulate a prediction equation relating the physical factors involved in drying cereal grain in deep cylindrical bins using cross-flow forced circulation of air. The prediction equation would be useful in design and operation of cross-flow grain drying installations. The study pertained to drying grain in storage as opposed to aeration systems which are primarily for cooling and freshening grain and which are systems of low air flow rates as compared to that required of a drying installation. Grain sorghum and wheat were to be used in the research.

The drying phase of the problem was complicated by lack of adequate information pertaining to the resistance offered to air flow in a non-uniform air circulation system. Also, the moisture sorption properties of grain are not well defined for varying temperatures. The research evolved into somewhat separate studies of the air circulation system, the hygroscopic properties of grain in the desorptive phase, and the thermal drying system. Available wheat desorptive data were used in formulating an equilibrium moisture relationship for wheat in the desorptive phase by analytical methods. Experiments were performed to analyze the air circulation system and the thermal drying system.

Principles of dimensional analysis and similitude were employed to

facilitate the research. By using dimensional analysis and similitude, factors could be formed into dimensionless groups which were fewer in number than the original set; and model drying set ups were more convenient to control than full size installations. Two sizes of models were used so that the larger set were prototypes of the smaller set.

Since a variety of cross-flow air circulation systems would be possible, three systems were selected for study. The three bin configurations consisted of two duct, four duct, and six duct arrangements. The vertical air supply and exhaust ducts were located at equal intervals around the periphery of each bin. Half the ducts were air inlets and the other half were air exhausts. The inlet and exhaust ducts were located alternately around the bin. To reduce the experiments to manageable proportions, it was considered necessary to formulate separate prediction equations for each bin configuration and for each kind of grain studied.

A set of miniature model bins, approximately six inches in diameter, was tested in an indoor laboratory where control was maintained of such factors as: air temperature, moisture content, and flow rate; initial grain and bin temperature; and temperature surrounding the bin. The average drying effect, amount of moisture removed, was measured in these experiments; but the bins were not of adequate size to measure internal moisture and temperature distributions or gradients. However, these experiments served as the basis for forming prediction equations for the air circulation system and the thermal drying system. Only wheat was used in the miniature bin experiments.

A set of two-foot diameter bins served as prototypes for checking the validity of the prediction equations formulated from results of the

miniature bins. Internal grain moisture contents, pressures, and temperatures were measured for plotting of gradients in addition to determining average drying effect. The two-foot diameter bins were tested in an open shed using atmospheric air. Grain sorghum and wheat were used in these bins.

An equilibrium moisture content relationship was developed which adequately accounted for the temperature effect for relative humidities of 70 per cent or lower. The relationship above 70 per cent relative humidity was not defined mathematically but was estimated by using a relationship for obtaining the maximum grain moisture content for an isotherm. In a plot of an isotherm, a smooth curve was drawn from about 70 per cent relative humidity to 100 per cent relative humidity. The form of the equilibrium moisture relationship was:

$$1-rh = e^{-P_1 T^{P_2} M_e^{P_3} T^{P_4}}$$

where rh = air relative humidity as a decimal

e = base of Napierian logarithms

T = temperature, F, (not absolute)

M_e = equilibrium grain moisture content, % dry basis

P_i = constants for a kind of grain.

The form of the equation for maximum grain moisture content was:

$$(M_e)_{max} = P_1 T^{P_2}$$

where $(M_e)_{max}$ = equilibrium grain moisture content at 100% relative humidity, dry basis as a decimal

T = temperature, F, absolute

P_i = constants for a kind of grain.

The prediction equation relating static pressure and air flow rate was of the form:

$$n(P/r) = P_1(\rho_a r^2 Q_a N_e/\mu_a)^{P_2}.$$

(Refer to Table III for definition of symbols)

The term $\rho_a r^2 Q_a N_e/\mu$ was regarded as a form of Reynolds Number. The range of Reynolds Number covered in the miniature and two-foot diameter bins was from 5 to 85. An extrapolation was developed for higher values of the Reynolds Number term based on data from the two-foot diameter bins. The extrapolated relationship can be used for approximating the static pressure drop in large prototype drying installations.

The form of the prediction equation for the thermal drying system was:

$$M_R = C_1(\Delta M\, \Delta\tau/\tau_e)^{C_2}\left[1-e^{-C_3(c_g\rho_g r^2/h_g t)^{C_4}(\tau_e/\tau_g)^{C_5}(Q_a t-\delta)}\right]$$

where $\delta = \left[(\tau_e/\tau_g)-1\right](C_6+C_7\Delta M\, \Delta\tau/\tau_e)$

C_i = constants for a kind of grain.

(Refer to Table II for definition of the other symbols)

The ranges of the dimensionless terms covered in the experiments of the miniature model bins were approximately:

M_R, -0.83 to 7.34

$\Delta M\Delta\tau/\tau_e$, 0.00403 to 0.0195

$c_g\rho_g r^2/h_g t$, 0.88 to 42

τ_e/τ_g, 0.996 to 1.141

$Q_a t$, 0 to 3,500

In the two-foot diameter bin experiments, the lower limit of τ_e/τ_g

was extended to 0.966 and the upper limit of $Q_a t$ was extended to approximately 20,000. The ranges covered are adequate for full size drying installations for practical purposes.

Conclusions

Conclusions drawn from the three major phases of the study are listed as follows:

Grain Hygroscopicity

1. There exists a finite maximum value of equilibrium grain moisture content for an isotherm. The maximum value can be related to temperature by an equation of the form:

$$(M_e)_{max} = P_1 T^{P_2}$$

where $(M_e)_{max}$ = equilibrium grain moisture content at 100% relative humidity, dry basis as a decimal

T = temperature, F, absolute

P_i = constants for a kind of grain. For wheat, $P_1 = 1{,}315$ and $P_2 = -1.33$.

2. A dimensionally nonhomogeneous equation adequate for drying purposes for relating grain equilibrium moisture content, temperature, and air relative humidity of 70 per cent or below is of the form:

$$1\text{-}rh = e^{-P_1 T^{P_2} M_e^{P_3} T^{P_4}}$$

where rh = air relative humidity as a decimal

T = temperature, F, (not absolute)

M_e = equilibrium grain moisture content, % dry basis

P_i = constants for a kind of grain. For wheat, $P_1 = 5.7336 \times 10^{-10}$, $P_2 = 3.3718$, $P_3 = 14.863$, and $P_4 = -0.41733$

Air Circulation System

1. A relationship to predict static pressure required to force air across deep cylindrical bins is an equation of the form:

$$n(P/r) = C_1(\rho_a r^2 Q_a N_e/\mu_a)^{C_2}$$

where n = length scale ratio of prototype to 0.438 ft diam model

P = static pressure head of air entering bin, ft of water

r = hydraulic radius of prototype cylindrical bin, ft

ρ_a = air density, $lb_{(M)}/ft^3$

Q_a = air flow rate, $(ft^3$ air/min)/ft^3 grain

N_e = Newton's Second Law constant, $lb_{(F)}/lb_{(M)}ft/min^2$

μ_a = air absolute viscosity, $lb_{(F)}min/ft^2$

C_i for wheat in the three cross-flow bins studied for the Reynolds Number term from 5 to 40 were:

	two duct bin	four duct bin	six duct bin
C_1	17.03×10^{-4}	7.942×10^{-4}	3.912×10^{-4}
C_2	1.324	1.213	1.239

2. The relative magnitude of the static pressure drop across the three type bins for equal flow rates is approximately as indicated by the relative values of C_1 for the bins in 1 above. An example of relative pressures at a Reynolds number term of 40 is: the pressure in the two duct bin is 5.9 times the pressure in the six duct bin and the pressure in the four duct bin is 1.9 times the pressure in the six duct bin. This effect corresponds to the relative length of path traveled by the air from inlet to exhaust in the bin configurations, the longest path being in the two duct bin for equal diameter bins.

3. Results from the two-foot diameter bins indicated that for practical purposes, the pressure requirements for wheat and grain sorghum can be considered equal.

Thermal Drying System

1. Factors considered most important in drying grain in deep cylindrical bins can be related by a prediction equation of the form:

$$Y = C_1 X_1^{C_2}\left[1-e^{-C_3 X_2^{C_4} X_3^{C_5}(X_4-\delta)}\right]$$

where $\delta = -C_6 - C_7X_1 + C_6X_3 + C_7X_1X_3 = (X_3-1)(C_6+C_7X_1)$, an increment of X_4

$Y = M_R$, avg moisture removed from grain, % dry basis

$X_1 = \Delta M\, \Delta\tau/\tau_e$, drying potential of the air with respect to the initial grain moisture content for an ideal constant wet bulb drying process

$X_2 = c_g\rho_g r^2/k_g t$, a term consisting of thermal properties of the grain c_g and k_g, density of the grain ρ_g, bin hydraulic radius r, and elapsed drying time t

$X_3 = \tau_e/\tau_g$, ratio of absolute temperature of air entering bin to initial grain absolute temperature

$X_4 = Q_a t$, product of air flow rate Q_a, cu ft of air per min/ cu ft of grain; and elapsed drying time t, min

e = base of Napierian logarithm

C_i = coefficients and exponents for kind of grain.

For wheat, the C_i were evaluated as:

	two duct bin	four duct bin	six duct bin
C_1	91.314	91.314	91.314
C_2	0.40531	0.40531	0.40531
C_3	0.000087761	0.00010767	0.000060956
C_4	0.34480	0.25258	0.65780
C_5	6.3612	3.1832	9.1730
C_6	23,258.	22,593.	20,443.
C_7	-899,833.	-1,037,483.	-619,520.

Only a very limited amount of experimental observations were available for evaluating the C_i of bin type III.

2. When the initial grain temperature is equal to the temperature of the entering air, $X_3 = 1$, $\delta = 0$, and the prediction equation reduces to:

$$Y = C_1 X_1^{C_2}\left[1-e^{-C_3 X_2^{C_2} X_4}\right]$$

When $X_3 \neq 1$, the equation is limited in application until an increment of X_4 equal in magnitude to the absolute value of δ has elapsed. An initial grain temperature greater than air temperature results in an increased drying effect in the early drying stages as compared to the drying effect obtained if initial grain temperature were equal to entering air temperature. An initial grain temperature less than air temperature results in a decreased initial drying effect. The range of δ encountered in the study was from -800 to 2,772. The negative values were for $X_3 < 1$.

3. The drying rates in the three cross-flow bins studied were approximately equal. The most pronounced differences between the bins were the internal moisture contents and temperature distributions during drying.

4. The term X_2 which includes thermal diffusivity accounts for a transient increased drying effect in the early stages of drying. If the term were omitted, the predicted drying effect would be only about one-half the actual drying effect until an increment of X_4 of approximately 1000 had elapsed.

5. The dimensionless group $U\,\Delta\tau_w/\rho_a c_a Q_a r\tau_e$, which was indicative of the ratio of heat input to bin to heat loss through the bin walls, resulted in an insignificant effect for the range of values covered in the miniature bin research. The range covered was from 0.000325

to 0.00313 which was an adequate range for prototype installations.

6. Redistribution of grain moisture and temperature towards uniformity occurred after the blowers were inoperative from 12 to 24 hours or more. Examples of spreads of moisture contents and temperatures for the two-foot diameter bins after the blowers had been inoperative for 8 days were:

	two duct bin	four duct bin	six duct bin
Moisture content, % dry basis			
End of run	4.5	4.7	6.2
8 days later	2.1	2.0	4.0
Temperature, F			
End of run	5	9	11
8 days later	2	1	3

Suggestions For Further Research

Formulation of a dimensionally homogeneous equation would be desirable for the equilibrium grain moisture relationship, especially in the desorptive phase for application to grain drying systems.

The results of the experimental work in this study need to be compared with performance of full size prototype installations. Additional studies in which the drying is continued longer than was done in this study may lead to re-evaluation of the coefficients and exponents in the prediction equation for the thermal drying system. The present study would need to be extended to other grains in order to increase the scope of the analysis to drying other grains and possibly other crops such as peanuts.

The effect of intermittant blower operation should be evaluated for its effect upon thermal efficiency. Improved methods of measuring air flow rate and grain moisture content would be desirable in grain drying research. A method of accurately determining grain moisture content at some position in the grain mass without removing a sample would be particularly helpful.

Exploring new concepts of maintaining crops in good condition from harvest to utilization may possibly result in methods considerably different from drying grain with forced circulation of air to prevent invasion by microorganisms.

SELECTED BIBLIOGRAPHY

1. Agricultural Engineers Yearbook. Engineering Data on Grain Storage. St. Joseph, Michigan: American Society of Agricultural Engineers, 1961.

2. American Society of Mechanical Engineers. ASME Power Test Code. Supplement. Flow Measurement. New York: American Society of Mechanical Engineers, PTC 19.5:4, 1959.

3. Anderson, J. A., and A. W. Alcock. Storage of Cereal Grains and Their Products. Monograph Series, Vol. II. St. Paul, Minn: American Association of Cereal Chemists, 1954.

4. Babbit, J. D. "Hysteresis in the Adsorption of Water Vapour by Wheat" Nature, 156:265-266, London, 1945.

5. Babbit, J. D. "Observation on the Adsorption of Water Vapor by Wheat," Canadian Journal of Research, 27.F:55-72, Canada, 1949.

6. Becker, H. A. and H. R. Sallans. "A Study of the Desorption Isotherms of Wheat at 25 C. and 50 C." Cereal Chemistry. 33:79-90, 1956.

7. Brunauer, Stephen. The Adsorption of Gases and Vapor. Vol. I, Princeton: Princeton University Press, 1945.

8. Brunauer, Stephen, P. H. Emmett, and Edward Teller. "Adsorption of Gases in Multimolecular Layers." Journal of the American Chemical Society, 60:309-319, 1938.

9. Day, D. L. and G. L. Nelson. "Effects of Basic Parameters in Drying Grain Sorghums," Technical Bulletin T-85. Oklahoma State University Experiment Station, Stillwater, Oklahoma, 1960.

10. Eshbach, O. W. Handbook of Engineering Fundamentals. Second Edition. New York: John Wiley and Sons, Inc., 1952. p. 6-06

11. Fairbrother, Thomas H. "The Influence of Environment on the Moisture Content of Flour and Wheat." Cereal Chemistry. 6:379-395, 1929.

12. Fenton, F. C. "Storage of Grain Sorghums," Agricultural Engineering, 22:185-188, 1941.

13. Gane, R. "The Water Content of Wheats as a Function of Temperature and Humidity." Journal of the Society of Chemical Industry Transactions and Communications, 60:44-46, London, 1941.

14. Granet, William and Clark Edwards. "IBM-650 Programs for General Linear and Non-Linear Regression Calculations," Stillwater, Oklahoma: Oklahoma State University Computing Center and Department of Agricultural Economics. (Mimeographed)

15. Hall, C. W. Drying Farm Crops. Reynoldsburg, Ohio: Agricultural Consulting Associates, Inc., 1957.

16. Hartley, H. O. "The Modified Gauss-Newton Method for the Fitting of Non-Linear Regression Functions by Least Squares," Ames, Iowa: United States Army Ordance Corps under contract to Iowa State University Statistical Laboratory. (Mimeographed)

17. Haynes, B. C., Jr. "Vapor Pressure Determination of Seed Hygroscopicity." Technical Bulletin No. 1229. Agricultural Research Service, USDA, in cooperation with College Experiment Station, University of Georgia, Washington, D. C.: Goverment Printing Office, Jan., 1961.

18. Henderson, S. M. "A Basic Concept of Equilibrium Moisture." Agricultural Engineering, 33:29-33, 1952.

19. Henderson, S. M. and R. L. Perry. Agricultural Process Engineering. New York: John Wiley and Sons, Inc., 1955.

20. Hubbard, J. E., F. R. Earle, and F. R. Senti. "Moisture Relations in Wheat and Corn." Cereal Chemistry. 34:422-433, 1957.

21. Hukill, William V. "Basic Principles in Drying Corn and Grain Sorghum." Agricultural Engineering, 28:335-338, 340. 1947.

22. Karplus, Walter J. Analog Simulation: Solution of Field Problems. New York: McGraw-Hill Book Co., 1958.

23. Langhaar, Henry L. Dimensional Analysis and Theory of Models. New York: Wiley, 1957.

24. Mott, R. A. "The Laws of Motion of Particles in Fluids and their Application to the Resistance of Beds of Solids to the Passage of Fluid." Some Aspects of Fluid Flow. pp. 242-256. London: Edward Arnold and Company, 1951.

25. Murphy, Glenn. Similitude in Engineering. New York: The Ronald Press, 1950.

26. Nelson, G. L., W. A. Mahoney, J. I. Fryear. "Grain Drying and Conditioning Investigations," Bulletin B-520. Oklahoma State University Experiment Station, Stillwater, Oklahoma, 1959.

27. Newton, Isaac. Newton's Principia. Trans. Andrew Motte. Revised, Florian Cajori. Berkeley: University of California Press, 1947.

28. Pichler, H. J. "Sorption Isotherms for Grain and Rape," Trans. W. E. Klinner. Journal of Agricultural Engineering Research, 2:159-165, England, 1957.

29. Rose, H. E. "Fluid Flow Through Beds of Granular Material." Some Aspects of Fluid Flow. pp. 136-163. London: Edward Arnold and Co., 1951.

30. Shedd, C. K. "Resistance of Grains and Seeds to Air Flow." Agricultural Engineering, 34:616-619, 1953.

31. Simmonds, W. H. C., G. T. Ward, and Ewen McEwen. "The Drying of Wheat Grain. Part I, The Mechanism of Drying." Transactions, Institution of Chemical Engineers, 31:265-278, London, 1953.

32. Smith, Sherman E. "The Sorption of Water Vapor by High Polmers." Journal of the American Chemical Society, 69.1:646-651, 1947.

33. Soroka, Walter W. Analog Methods in Computation and Simulation. New York: McGraw-Hill Book Company, Inc., 1954.

34. Tuite, John F. and Clyde M. Christensen. "Moisture Content of Wheat Seed in Relation to Invasion of the Seed by Species of the Aspergillus Glacus Group and Effect of Invasion upon Germination of the Seed." Phytopathology. 47.6:323-327, 1957.

35. Wadell, Hakon. "The Coefficient of Resistance as a Function of Reynolds Number for Solids of Various Shapes." Journal of the Franklin Institute, 217:459-490, 1934.

APPENDIX A

CALIBRATION CURVES FOR RELATIVE HUMIDITY RECORDER

AIR VISCOSITY CURVE USED IN EVALUATING DIMENSIONLESS GROUPS

ELECTRONIC COMPUTER PROGRAMS LISTED IN FORTRAN STATEMENTS

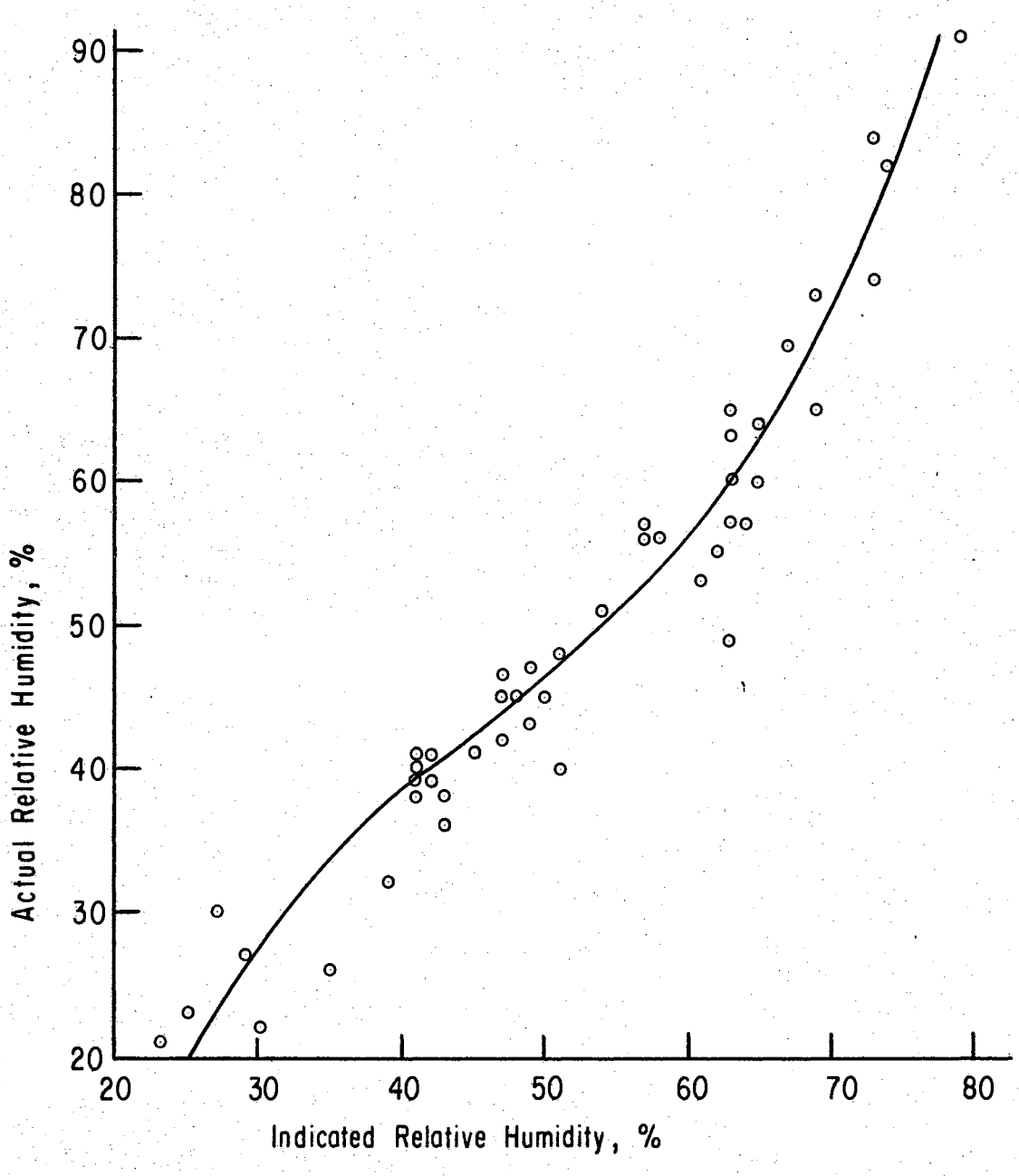

FIGURE A-1. Calibration curve for relative humidity recorder - grain sorghum experiment, fall of 1960.

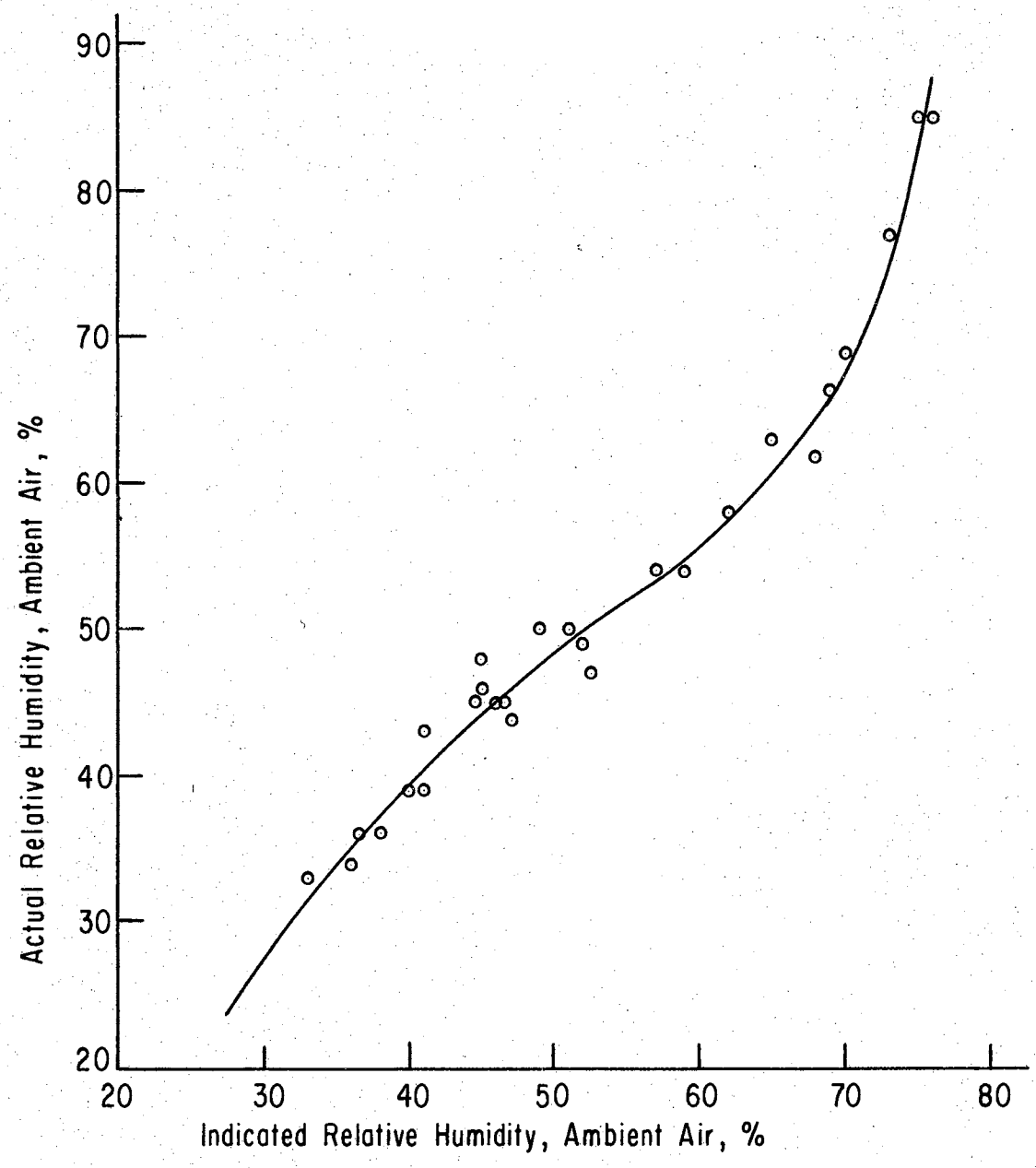

FIGURE A-2. Calibration curve for relative humidity recorder - wheat experiment, summer of 1961.

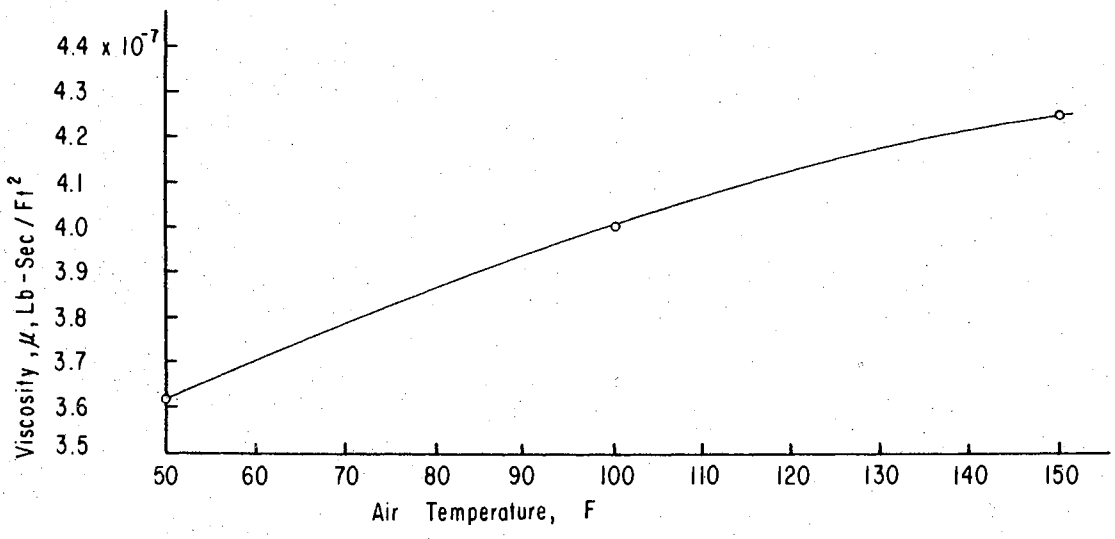

FIGURE A-3. Graph for determining air absolute viscosity for use in evaluating some of the dimensionless groups or pi terms.

TABLE A-I

ELECTRONIC COMPUTER FORTRAN PROGRAM FOR SUCCESSIVE REGRESSIONS OF HYGROSCOPICITY DATA IN LINEAR TRANSFORMATION

```
      DIMENSION S(8),P1(8),P2(8)
      READ, E
      READ,S
      DO3J=1,8
      SUMXY=0.
      SUMX2=0.
      SUMY=0.
      SUMX=0.
1 0   READ,N,CAPN
      DO2I=1,N
      READ,X,Y
      Y=LOGEF(1.0/(1.0-Y))
      Y=LOGF(Y)
      X=LOGF(X)
      SUMX=SUMX+X
      SUMY=SUMY+Y
      SUMX2=SUMX2+X*X
2 0   SUMXY=SUMXY+X*Y
      D=CAPN*SUMX2-SUMX*SUMX
      P2(J)=(CAPN*SUMXY-SUMX*SUMY)/D
      R1=(SUMY*SUMX2-SUMXY*SUMX)/D
3 0   P1(J)=EXPF(R1)
      SUMXY=0.
      SUMX=0.
      SUMY=0.
      SUMX2=0.
      DO4J=1,8
      Y=LOGF(P1(J))
      X=LOGF(S(J))
      SUMX=SUMX+X
      SUMY=SUMY+Y
      SUMX2=SUMX2+X*X
4 0   SUMXY=SUMXY+X*Y
      D=8.*SUMX2-SUMX*SUMX
      P4=(8.*SUMXY-SUMX*SUMY)/D
      P3=(SUMY*SUMX2-SUMXY*SUMX)/D
      P3=EXPF(P3)
      SUMXY=0.
      SUMY=0.
      SUMX2=0.
      SUMX=0.
      DO5J=1,8
      X=LOGF(S(J))
      Y=LOGF(P2(J))
      SUMX=SUMX+X
      SUMY=SUMY+Y
      SUMX2=SUMX2+X*X
5 0   SUMXY=SUMXY+X*Y
      D=8.*SUMX2-SUMX*SUMX
      P6=(8.*SUMXY-SUMX*SUMY)/D
      P5=(SUMY*SUMX2-SUMXY*SUMX)/D
      P5=EXPF(P5)
      PUNCH,P1
      PUNCH,P2
      PUNCH, P3,P4,P5,P6
      DO8I=30,180,5
      X2=I
      DO8J=2,30,2
      X1=J
      Z=P5*X2**P6
      Z=X1**Z
      V=(P3*X2**P4)
      Z=-(V*Z)
      Y=1.-(E**Z)
      PUNCH, Y,X1,X2,
8 0   CONTINUE
      END
```

TABLE A-II

ELECTRONIC COMPUTER FORTRAN PROGRAM FOR REGRESSION OF FIVE CONSTANTS IN NONLINEAR PREDICTION EQUATION

```
      DIMENSION A(8,8),D(8),P(7),
     1 Y(100),X1(100),X2(100),X4(100)
     2 ,X5(100)
      READ,NP,NO
      READ,C1,C2,P(1),P(2),P(3),P(4)
     1 ,P(5)
      DO13I=1,NO
      READ,Y(I),X1(I),X2(I),X3,X4(I)
     1 ,X5(I)
   13 0 CONTINUE
      M=NP+1
      ITER=0
      E=2.7182818
    7 0 CONTINUE
      DO1I=1,M
   21 0 DO1J=I,M
    1 0 A(I,J)=0.0
      DO 2 K=1,NO
      Z=X1(K)**C2
      Z1=X5(K)**P(2)
      Z2=X2(K)**P(3)
      Z3=X4(K)+P(4)+P(5)*X1(K)-P(4)*
     1 X2(K)-P(5)*X1(K)*X2(K)
      Z4=E**(-P(1)*Z1*Z2*Z3)
      Z5=LOGEF(X5(K))
      Z6=LOGEF(X2(K))
      Z7=C1*Z*Z1*Z2*Z4
      D(1)=Z3*Z7
      D(2)=P(1)*D(1)*Z5
      D(3)=P(1)*D(1)*Z6
      D(4)=P(1)*Z7-P(1)*Z7*X2(K)
      D(5)=X1(K)*D(4)
      D(6)=Y(K)-C1*Z+C1*Z*Z4
      DO2I=1,M
   23 0 DO2J=I,M
    2 0 A(I,J)=D(I)*D(J)+A(I,J)
      M1=NP
      DO3I=1,M1
   24 0 MA=I+1
      DO3J=MA,M1
    3 0 A(J,I)=A(I,J)
      M2=M-2
      DO5I=1,M2
   25 0 M3=I+1
      DO4J=M3,M
    4 0 A(I,J)=A(I,J)/A(I,I)
      DO5L=I,M2
   26 0 DO5K=M3,M
    5 0 A(L+1,K)=A(L+1,K)
    5 1 -A(L+1,I)*A(I,K)
      A(M-1,M)=A(M-1,M)/A(M-1,M-1)
      L=M2
      K=M1
      DO6J=1,M2
      32 0 DO31I=1,L
      31 0 A(I,M)=A(I,M)-A(I,K)*A(K,M)
           L=L-1
       6 0 K=K-1
           ITER=ITER+1
           DO10I=1,M1
      10 0 P(I)=A(I,M)+P(I)
      99 0 PUNCH,P
           GO TO 7
      12 0 BIPCT=0.0
           DO 17 K=1,NO
           Z=X1(K)**C2
           Z1=X5(K)**P(2)
           Z2=X2(K)**P(3)
           Z3=X4(K)+P(4)+P(5)*X1(K)-P(4)*
          1 X2(K)-P(5)*X1(K)*X2(K)
           Z4=E**(-P(1)*Z1*Z2*Z3)
           YCAL=C1*Z-C1*Z*Z4
           YNOW=Y(K)
           PCTPD=(Y(K)-YCAL)/YCAL
      14 0 PUNCH,YNOW,YCAL,PCTPD
           IF(BIPCT-ABSF(PCTPD))16,17,17
      16 0 BIPCT=ABSF(PCTPD)
           DYNOW=YNOW
      17 0 CONTINUE
      15 0 PUNCH,P,ITER
      19 0 PUNCH,BIPCT,DYNOW
      11 0 CONTINUE
      20 0 DO 34 I=1,M
      33 0 PUNCH,A(I,M)
      34 0 CONTINUE
           END
```

APPENDIX B

TABLES OF VALUES OF FACTORS AND DIMENSIONLESS GROUPS FOR THE EXPERIMENTAL OBSERVATIONS AND ANALYSES OF THE MINIATURE AND TWO-FOOT DIAMETER BINS

Explanation of Tables

The pi terms listed in the Tables are defined in the text in Tables II and III except for an additional π_{10} which is defined on page 111. The treatment schedule, Table VIII in the text, outlines the conditions of the experimental runs in these tables for the miniature bin experiments.

The values in Tables B-III, B-IV, B-V, B-VI, B-XI, B-XII, and B-XIII are listed in the floating point system. Floating point numbers have a mantissa of eight significant digits followed by a two digit characteristic. The numbers are of the form .XXXXXXXXPP where PP is the power of 10 with 50 added. Examples are:

1234567851 = 1.2345678

1234567850 = 0.12345678

1234567849 = 0.012345678

The number is positive if a + or blank space follows it and negative if a - follows it.

The observed values of π_1 in Tables B-III, B-IV, B-V, and B-VI are to be interpreted to only two decimal places.

TABLE B-I

VALUES OF PRESSURE AND FLOW RATE DIMENSIONLESS GROUPS AND FACTORS FOR WHEAT IN THE MINIATURE MODEL BINS

BIN TYPE	π_{11}	π_{12}	P	Q_a
I	0.01369	4.804	0.00167	3.397
	0.02737	8.500	0.00333	6.010
	0.04105	10.446	0.00500	7.386
	0.05474	14.093	0.00667	9.965
	0.06842	16.049	0.00833	11.348
	0.08210	18.970	0.01000	13.413
	0.09578	21.388	0.01167	15.123
	0.10947	23.342	0.01333	16.505
	0.12315	24.716	0.01500	17.476
II	0.006842	5.642	0.000833	3.984
	0.013680	11.421	0.00167	8.064
	0.020525	14.385	0.00250	10.157
	0.027365	18.340	0.00333	12.950
	0.034212	22.225	0.00417	15.693
	0.041051	25.325	0.00500	17.882
	0.047890	28.546	0.00583	20.156
III	0.0068415	9.982	0.000833	7.048
	0.013686	17.932	0.00167	12.662
	0.027365	31.023	0.00333	21.905
	0.034212	36.834	0.00417	26.008
	0.041051	42.579	0.00500	30.065

TABLE B-II

VALUES OF PRESSURE AND FLOW RATE DIMENSIONLESS GROUPS AND FACTORS FOR WHEAT AND GRAIN SORGHUM IN THE TWO-FOOT DIAMETER BINS

BIN TYPE	π_{11}	π_{12}	P	Q_a
WHEAT				
I	0.0995	68.32	0.0498	3.01
II	0.0495	72.63	0.0248	3.19
III	0.0263	74.27	0.0132	3.26
GRAIN SORGHUM				
I	0.10667	70.33	0.0533	2.98
II	0.06500	94.87	0.0325	4.02
III	0.0350	96.76	0.0175	4.10

TABLE B-III

VALUES OF DIMENSIONLESS GROUPS, MINIATURE BIN TYPE I

Run No	π_1	π_2	π_5	π_6	π_4	π_{10}
1	1200000050	4032000048	1109000051	1165000048	8180000052	4208000052
	1200000050	4032000048	1109000051	1165000048	1635000053	2104000052
	9000000049	4032000048	1109000051	1165000048	3270000053	1052000052
	1200000050	4032000048	1109000051	1165000048	6540000053	5263000051
	4700000050	4032000048	1109000051	1165000048	1308000054	2628000051
	9100000050	4032000048	1109000051	1165000048	1962000054	1757000051
	1580000051	4032000048	1109000051	1165000048	2943000054	1166000051
	2160000051	4032000048	1109000051	1165000048	3924000054	8784000050
9	3400000049-	3570000048	1138300051	1092000048	8175000052	4208000052
	9200000049-	3570000048	1138300051	1092000048	1635000053	2104000052
	1790000050-	3570000048	1138300051	1092000048	3270000053	1052000052
	2080000050-	3570000048	1138300051	1092000048	6540000053	5263000051
	2500000049	3570000048	1138300051	1092000048	1308000054	2628000051
	4610000050	3570000048	1138300051	1092000048	1962000054	1757000051
	1160000051	3570000048	1138300051	1092000048	2943000054	1166000051
	1771000051	3570000048	1138300051	1092000048	3924000054	8784000050
10	00 51	3397000048	1120100051	3257000047	8175000052	4208000052
	8730000049-	3397000048	1120100051	3257000047	1635000053	2104000052
	1750000050-	3397000048	1120100051	3257000047	3270000053	1052000052
	3330000050-	3397000048	1120100051	3257000047	6540000053	5263000051
	8730000049	3397000048	1120100051	3257000047	1308000054	2628000051
	4660000050	3397000048	1120100051	3257000047	1962000054	1757000051
	1190000051	3397000048	1120100051	3257000047	2943000054	1166000051
	1800000051	3397000048	1120100051	3257000047	3924000054	8784000050
11	29100000049	4100000048	1120100051	5566000047	8175000052	4208000052
	00 51	4100000048	1120100051	5566000047	1640000053	2104000052
	00 51	4100000048	1120100051	5566000047	3270000053	1052000052
	1460000050	4100000048	1120100051	5566000047	6540000053	5263000051
	4070000050	4100000048	1120100051	5566000047	1308000054	2628000051
	8440000050	4100000048	1120100051	5566000047	1962000054	1757000051
	1480000051	4100000048	1120100051	5566000047	2943000054	1166000051
	2100000051	4100000048	1120100051	5566000047	3924000054	8784000050
12	00 51	4203000048	1120100051	1400000048	8175000052	4208000052
	29100000049	4203000048	1120100051	1400000048	1645000053	2104000052
	29100000049-	4203000048	1120100051	1400000048	3270000053	1052000052
	00 51	4203000048	1120100051	1400000048	6540000053	5263000051
	3490000050	4203000048	1120100051	1400000048	1308000054	2628000051
	7560000050	4203000048	1120100051	1400000048	1962000054	1757000051
	1340000051	4203000048	1120100051	1400000048	2943000054	1166000051
	2060000051	4203000048	1120100051	1400000048	3924000054	8784000050

TABLE B-III (continued)

Run No	π_1	π_2	π_5	π_6	π_4	π_{10}
6	2290000050	3731000048	1000000051	1133000048	8175000052	4208000052
	3720000050	3731000048	1000000051	1133000048	1635000053	2104000052
	5720000050	3731000048	1000000051	1133000048	3270000053	1052000052
	8860000050	3731000048	1000000051	1133000048	6540000053	5263000051
	1342000051	3731000048	1000000051	1133000048	1308000054	2628000051
	1713000051	3731000048	1000000051	1133000048	1962000054	1757000051
	2284000051	3731000048	1000000051	1133000048	2943000054	1166000051
	2740000051	3731000048	1000000051	1133000048	3924000054	8784000050
13	00 51	4091000048	1120100051	2108000048	8175000052	4208000052
	00 51	4091000048	1120100051	2108000048	1630000053	2104000052
	2900000049-	4091000048	1120100051	2108000048	3270000053	1052000052
	00 51	4091000048	1120100051	2108000048	6540000053	5263000051
	2340000050	4091000048	1120100051	2108000048	1308000054	2628000051
	6720000050	4091000048	1120100051	2108000048	1962000054	1757000051
	1290000051	4091000048	1120100051	2108000048	2943000054	1166000051
	1900000051	4091000048	1120100051	2108000048	3924000054	8784000050
7	1460000050	3522000048	1044800051	1144000048	8175000052	4208000052
	1750000050	3522000048	1044800051	1144000048	1635000053	2104000052
	2630000050	3522000048	1044800051	1144000048	3270000053	1052000052
	4950000050	3522000048	1044800051	1144000048	6540000053	5263000051
	8440000050	3522000048	1044800051	1144000048	1308000054	2628000051
	1251000051	3522000048	1044800051	1144000048	1962000054	1757000051
	1832000051	3522000048	1044800051	1144000048	2943000054	1166000051
	2123000051	3522000048	1044800051	1144000048	3433500054	8784000050
14	5820000049	3483000048	1124600051	3126800048	8175000052	4208000052
	5820000049	3483000048	1124600051	3126800048	1640000053	2104000052
	5820000049	3483000048	1124600051	3126800048	3270000053	1052000052
	8730000049	3483000048	1124600051	3126800048	6540000053	5263000051
	4360000050	3483000048	1124600051	3126800048	1308000054	2628000051
	9900000050	3483000048	1124600051	3126800048	1962000054	1757000051
	1690000051	3483000048	1124600051	3126800048	2943000054	1166000051
	2270000051	3483000048	1124600051	3126800048	3924000054	8784000050
8	00 51	3756000048	1077000051	1133000048	8175000052	4208000052
	2900000049	3756000048	1077000051	1133000048	1635000053	2104000052
	8700000049	3756000048	1077000051	1133000048	3270000053	1052000052
	2670000050	3756000048	1077000051	1133000048	6540000053	5263000051
	6990000050	3756000048	1077000051	1133000048	1308000054	2628000051
	1195000051	3756000048	1077000051	1133000048	1962000054	1757000051
	1952000051	3756000048	1077000051	1133000048	2943000054	1166000051
	2564000051	3756000048	1077000051	1133000048	3924000054	8784000050

TABLE B-III (continued)

Run No	x_1	x_2	x_5	x_6	x_4	x_{10}
2	9200000049	6667000048	1117900051	1142000048	8180000052	4208000052
	1220000050	6667000048	1117900051	1142000048	1635000053	2104000052
	1530000050	6667000048	1117900051	1142000048	3270000053	1052000052
	3060000050	6667000048	1117900051	1142000048	6540000053	5263000051
	8250000050	6667000048	1117900051	1142000048	1308000054	2628000051
	1530000051	6667000048	1117900051	1142000048	1962000054	1757000051
	2540000051	6667000048	1117900051	1142000048	2943000054	1166000051
	3450000051	6667000048	1117900051	1142000048	3924000054	8784000050
3	2160000050	1101000049	1122000051	9405000047	9830000052	2805000052
	2780000050	1101000049	1122000051	9405000047	1970000053	1403000052
	3090000050	1101000049	1122000051	9405000047	3930000053	7013000051
	7410000050	1101000049	1122000051	9405000047	7870000053	3506000051
	1850000051	1101000049	1122000051	9405000047	1573000054	1757000051
	3120000051	1101000049	1122000051	9405000047	2360000054	1166000051
	4230000051	1101000049	1122000051	9405000047	3146000054	8784000050
	4760000051	1101000049	1122000051	9405000047	3540000054	7776000050
4	1540000050	1591000049	1123700051	1067000048	1030000053	2805000052
	3070000050	1591000049	1123700051	1067000048	2050000053	1403000052
	5230000050	1591000049	1123700051	1067000048	4100000053	7013000051
	1110000051	1591000049	1123700051	1067000048	8200000053	3506000051
	2610000051	1591000049	1123700051	1067000048	1640000054	1757000051
	4150000051	1591000049	1123700051	1067000048	2461000054	1166000051
	5530000051	1591000049	1123700051	1067000048	3281000054	8784000050
	6180000051	1591000049	1123700051	1067000048	3691000054	7776000050
5	3070000050	1948000049	1121200051	1023000048	1050000053	2805000052
	6140000050	1948000049	1121200051	1023000048	2090000053	1403000052
	9210000050	1948000049	1121200051	1023000048	4190000053	7013000051
	1840000051	1948000049	1121200051	1023000048	8370000053	3506000051
	3410000051	1948000049	1121200051	1023000048	1674000054	1757000051
	5070000051	1948000049	1121200051	1023000048	2511000054	1166000051
	6600000051	1948000049	1121200051	1023000048	3348000054	8784000050
	7340000051	1948000049	1121200051	1023000048	3767000054	7776000050

TABLE B-IV

VALUES OF DIMENSIONLESS GOUPS, MINIATURE BIN TYPE II

Run No	π_1	π_2	π_5	π_6	π_4	π_{10}
20	3060000050	4454000048	9964000050	1060000048	8375000052	4208000052
	4990000050	4454000048	9964000050	1060000048	1675000053	2104000052
	7760000050	4454000048	9964000050	1060000048	3350000053	1052000052
	1163000051	4454000048	9964000050	1060000048	6700000053	5263000051
	1716000051	4454000048	9964000050	1060000048	1340000054	2628000051
	2213000051	4454000048	9964000050	1060000048	2010000054	1757000051
	2822000051	4454000048	9964000050	1060000048	3015000054	1166000051
21	1140000050	4609000048	1040000051	1051000048	8375000052	4208000052
	2250000050	4609000048	1040000051	1051000048	1675000053	2104000052
	3910000050	4609000048	1040000051	1051000048	3350000053	1052000052
	6680000050	4609000048	1040000051	1051000048	6700000053	5263000051
	1195000051	4609000048	1040000051	1051000048	1340000054	2628000051
	1693000051	4609000048	1040000051	1051000048	2010000054	1757000051
	2413000051	4609000048	1040000051	1051000048	3015000054	1166000051
22	3000000049	4338000048	1079100051	1030000048	8375000052	4208000052
	8500000049	4338000048	1079100051	1030000048	1675000053	2104000052
	1680000050	4338000048	1079100051	1030000048	3350000053	1052000052
	3340000050	4338000048	1079100051	1030000048	6700000053	5263000051
	8040000050	4338000048	1079100051	1030000048	1340000054	2628000051
	1357000051	4338000048	1079100051	1030000048	2010000054	1757000051
	2104000051	4338000048	1079100051	1030000048	3015000054	1166000051
24	5720000049-	3803000048	1117900051	3480000047	8510000052	4208000052
	8580000049-	3803000048	1117900051	3480000047	1700000053	2104000052
	1430000050-	3803000048	1117900051	3480000047	3400000053	1052000052
	1430000050-	3803000048	1117900051	3480000047	6810000053	5263000051
	2000000050	3803000048	1117900051	3480000047	1362000054	2628000051
	6870000050	3803000048	1117900051	3480000047	2042000054	1757000051
	1370000051	3803000048	1117900051	3480000047	3064000054	1166000051
	1970000051	3803000048	1117900051	3480000047	4085000054	8784000050
25	2770000049-	4597000048	1117900051	5987000047	8380000052	4208000052
	5540000050-	4597000048	1117900051	5987000047	1680000053	2104000052
	8300000050-	4597000048	1117900051	5987000047	3350000053	1052000052
	8300000050-	4597000048	1117900051	5987000047	6700000053	5263000051
	2770000050	4597000048	1117900051	5987000047	1340000054	2628000051
	8300000050	4597000048	1117900051	5987000047	2010000054	1757000051
	1490000051	4597000048	1117900051	5987000047	3015000054	1166000051
	2160000051	4597000048	1117900051	5987000047	4020000054	8784000050

TABLE B-IV (continued)

Run No	π_1	π_2	π_5	π_6	π_4	π_{10}
15	3000000049-	4326000048	1120100051	1090000048	8500000052	4208000052
	6000000049-	4326000048	1120100051	1090000048	1700000053	2104000052
	8000000049-	4326000048	1120100051	1090000048	3400000053	1052000052
	6000000049-	4326000048	1120100051	1090000048	6800000053	5263000051
	4600000050	4326000048	1120100051	1090000048	1360000054	2628000051
	9100000050	4326000048	1120100051	1090000048	2040000054	1757000051
	1660000051	4326000048	1120100051	1090000048	3015000054	1166000051
	2310000051	4326000048	1120100051	1090000048	4080000054	8784000050
26	00 51	4091000048	1117900051	1547000048	8580000052	4208000052
	2820000049-	4091000048	1117900051	1547000048	1720000053	2104000052
	1130000050-	4091000048	1117900051	1547000048	3430000053	1052000052
	8500000049-	4091000048	1117900051	1547000048	6860000053	5263000051
	3110000050	4091000048	1117900051	1547000048	1372000054	2628000051
	7900000050	4091000048	1117900051	1547000048	2058000054	1757000051
	1440000051	4091000048	1117900051	1547000048	3087000054	1166000051
	2060000051	4091000048	1117900051	1547000048	4116000054	8784000050
27	00 51	4151000048	1119000051	1996000048	8480000052	4208000052
	2850000049-	4151000048	1119000051	1996000048	1700000053	2104000052
	5700000049-	4151000048	1119000051	1996000048	3390000053	1052000052
	5700000049-	4151000048	1119000051	1996000048	6780000053	5263000051
	2850000050	4151000048	1119000051	1996000048	1356000054	2628000051
	7700000050	4151000048	1119000051	1996000048	2034000054	1757000051
	1460000051	4151000048	1119000051	1996000048	3051000054	1166000051
	2080000051	4151000048	1119000051	1996000048	4068000054	8784000050
28	2800000049-	4350000048	1117900051	3058000048	8480000052	4208000052
	5700000049-	4350000048	1117900051	3058000048	1700000053	2104000052
	1130000050-	4350000048	1117900051	3058000048	3390000053	1052000052
	8500000049-	4350000048	1117900051	3058000048	6780000053	5263000051
	3110000050	4350000048	1117900051	3058000048	1356000054	2628000051
	7060000050	4350000048	1117900051	3058000048	2034000054	1757000051
	1380000051	4350000048	1117900051	3058000048	3051000054	1166000051
	1980000051	4350000048	1117900051	3058000048	4068000054	8784000050
23	00 51	4491000048	1140600051	1047000048	8365000052	4208000052
	2900000049-	4491000048	1140600051	1047000048	1673000053	2104000052
	1130000050-	4491000048	1140600051	1047000048	3346000053	1052000052
	1410000050-	4491000048	1140600051	1047000048	6692000053	5263000051
	1670000050	4491000048	1140600051	1047000048	1338400054	2628000051
	6980000050	4491000048	1140600051	1047000048	2007600054	1757000051
	1424000051	4491000048	1140600051	1047000048	3011400054	1166000051
	2123000051	4491000048	1140600051	1047000048	4015200054	8784000050

TABLE B-IV (continued)

Run No	π_1	π_2	π_3	π_6	π_4	π_{10}
16	00 51	7981000048	1113400051	1067000048	8430000052	4208000052
	00 51	7981000048	1113400051	1067000048	1690000053	2104000052
	3000000049	7981000048	1113400051	1067000048	3370000053	1052000052
	2710000050	7981000048	1113400051	1067000048	6740000053	5263000051
	1150000051	7981000048	1113400051	1067000048	1348000054	2628000051
	1990000051	7981000048	1113400051	1067000048	2022000054	1757000051
	3100000051	7981000048	1113400051	1067000048	3033000054	1166000051
	4130000051	7981000048	1113400051	1067000048	4044000054	8784000050
17	6020000049	1195000049	1122000051	1199000048	9080000052	2805000052
	1200000050	1195000049	1122000051	1199000048	1820000053	1403000052
	2710000050	1195000049	1122000051	1199000048	3630000053	7013000051
	6620000050	1195000049	1122000051	1199000047	2770000053	3506000051
	1780000051	1195000049	1122000051	1199000048	1453000054	1757000051
	2860000051	1195000049	1122000051	1199000048	2180000054	1166000051
	3940000051	1195000049	1122000051	1199000048	2906000054	8784000050
	4430000051	1195000049	1122000051	1199000048	3270000054	7776000050
18	1790000050	1617000049	1121600051	9437000047	9790000052	2805000052
	3870000050	1617000049	1121600051	9437000047	1960000053	1403000052
	6550000050	1617000049	1121600051	9437000047	3920000053	7013000051
	1310000051	1617000049	1121600051	9437000047	7830000053	3506000051
	2800000051	1617000049	1121600051	9437000047	1566000054	1757000051
	4260000051	1617000049	1121600051	9437000047	2349000054	1166000051
	5630000051	1617000049	1121600051	9437000047	3132000054	8784000050
	6250000051	1617000049	1121600051	9437000047	3524000054	7776000050
19	2980000050	1946000049	1126300051	1036000048	1030000053	2805000052
	5650000050	1946000049	1126300051	1036000048	2070000053	1403000052
	9520000050	1946000049	1126300051	1036000048	4140000053	7013000051
	1820000051	1946000049	1126300051	1036000048	8270000053	3506000051
	3510000051	1946000049	1126300051	1036000048	1655000054	1757000051
	5090000051	1946000049	1126300051	1036000048	2482000054	1166000051
	6550000051	1946000049	1126300051	1036000048	3310000054	8784000050
	7200000051	1946000049	1126300051	1036000048	3723000054	7776000050

TABLE B-V

VALUES OF DIMENSIONLESS GROUPS, MINIATURE BIN TYPE III

Run No	π_1	π_2	π_5	π_6	π_4	π_{10}
30	8300000049	4320000048	1077000051	1009200048	8280000052	4208000052
	1110000050	4320000048	1077000051	1009200048	1660000053	2104000052
	1660000050	4320000048	1077000051	1009200048	3310000053	1052000052
	3320000050	4320000048	1077000051	1009200048	6620000053	5263000051
	7200000050	4320000048	1077000051	1009200048	1324000054	2628000051
	1160000051	4320000048	1077000051	1009200048	1986000054	1757000051
	1740000051	4320000048	1077000051	1009200048	2979000054	1166000051
29	2110000050	2184000049	1125300051	1134000048	1010000053	2805000052
	4220000050	2184000049	1125300051	1134000048	2020000053	1403000052
	8730000050	2184000049	1125300051	1134000048	4040000053	7013000051
	1720000051	2184000049	1125300051	1134000048	8080000053	3506000051
	3490000051	2184000049	1125300051	1134000048	1616000054	1757000051
	5000000051	2184000049	1125300051	1134000048	2425000054	1166000051
	6270000051	2184000049	1125300051	1134000048	3233000054	8784000050
	6840000051	2184000049	1125300051	1134000048	3637000054	7776000050

TABLE B-VI

VALUES OF DIMENSIONLESS GROUPS, TWO-FOOT DIAMETER BINS

Bin Type	Run No	π_1	π_2	π_5	π_4	π_{10}
I	1	1740000051	1305000048	9660000050	6080000053	1959800052
	2	9300000050	1345000048	9350000050	1796000054	6530000051
	3	1700000051	1380000048	9520000050	4020000054	2830000051
	4	3740000051	1464000048	9570000050	8462000054	1066000051
	5	5700000051	1432000048	9780000050	1819000055	5900000050
II	1	1160000051	1443000048	1000000051	6370000053	1959800052
	2	1090000051	1485000048	9680000050	1939000054	6530000051
	3	1710000051	1528000048	9860000050	4598000054	2830000051
	4	3540000051	1613000048	9940000050	9126000054	1066000051
	5	5500000051	1585000048	1017000051	2069500055	5900000050
III	1	1030000051	1564000048	1041000051	6370000053	1959800052
	2	9000000049	1590000048	1007000051	1912000054	6530000051
	3	1590000051	1631000048	1026000051	4418000054	2830000051
	4	3370000051	1732000048	1035000051	9207000054	1066000051
	5	4920000051	1700000048	1058000051	2025500055	5900000050

TABLE B-VII

MOISTURE CONTENT OF GRAIN SORGHUM IN TWO-FOOT DIAMETER BINS, % WET BASIS

	Run No.	Time of Run Hours	Position in bin 1	2	3	4	5	6	7	8	9	10	Bin Avg	Air Flow Rate cfm/ft^3	Temp F	Relative Humidity %
Bin	0	0.0	14.3	14.5	14.6	14.3	14.3	14.7	15.1	14.3	14.5	14.5	14.51			
Type	1	4.0	13.0	12.9	13.9	14.7	14.5	14.3	14.9	14.4	14.3	14.2	14.11	3.38	84.	28.
I	2	8.1	11.5	11.4	12.3	13.8	13.5	14.1	14.6	14.1	13.6	13.1	13.20	2.98	80.	27.
	3	36.6	10.2	9.8	10.2	12.8	15.7	12.1	12.5	12.4	11.7	11.1	11.85	2.98	77.	38.
	4	76.2	11.9	11.2	11.4	12.6	12.2	12.1	12.5	12.5	12.2	12.1	12.07	3.30	65.	39.
	Total	124.9											Avg through Run 3		78.2	35.0
													Total avg	3.16	70.1	37.5
Bin	0	0.0	14.7	14.2	14.3	14.7	13.9	14.3	14.5	14.0	14.1	14.2	14.29			
Type	1	4.0	13.0	13.3	14.0	14.8	14.4	14.3	14.4	14.2	14.5	14.4	14.13	3.78	84.	28.
II	2	8.1	11.6	11.8	12.9	13.8	13.6	13.7	13.5	13.0	13.2	13.6	13.07	3.94	80.	27.
	3	36.6	10.6	10.5	11.1	12.9	12.9	12.4	11.3	11.3	11.4	12.6	11.70	4.02	77.	38.
	4	76.2	12.1	11.8	11.8	12.8	12.8	12.6	12.6	12.0	11.9	12.7	12.31	4.02	65.	39.
	Total	124.9											Avg through Run 3		78.2	35.0
													Total avg	3.94	70.1	37.5
Bin	0	0.0	14.4	14.0	14.1	14.5	14.1	14.0	14.6	14.0	14.3	14.3	14.23			
Type	1	4.0	13.0	13.5	14.0	14.4	14.4	14.5	13.9	13.9	14.1	14.6	14.03	3.94	84.	28.
III	2	8.1	11.7	12.2	13.4	13.9	13.4	13.9	12.7	12.8	13.3	13.6	13.09	4.02	80.	27.
	3	36.6	10.4	10.4	11.5	10.6	11.4	12.1	10.8	11.3	12.2	13.2	11.39	4.10	77.	38.
	4	76.2	12.3	11.8	12.3	13.1	13.2	13.1	11.6	11.5	12.0	13.6	12.45	4.18	65.	39.
	Total	124.9											Avg through Run 3		78.2	35.0
													Total avg	4.06	70.1	37.5

TABLE B-VIII

MOISTURE CONTENT OF WHEAT IN TWO-FOOT DIAMETER BINS, % WET BASIS

	Run No	Time of Run Hours	Position in bin 1	2	3	4	5	6	7	8	9	10	11	12	Bin Avg	Air Flow Rate cfm/ft^3	Ambient Air Temp F	Ambient Air Relative Humidity %
Bin	0	0.0								14.7	14.8	14.9			14.80			
Type	1	3.0	12.7	12.8	13.5	13.7	13.8	13.9	13.6	13.6	13.8	13.8	13.8	13.6	13.52	3.38	84.	39.
I	1A		13.1			14.2						14.3						
	2	6.0	12.6	13.7	14.4	14.5	13.8	15.4	15.4	14.7	13.9	12.9	15.4	14.6	14.12	3.30	80.	37.
	2A		12.1			14.6						14.3						
	3	11.8	12.4	11.3	12.0	14.6	14.5	14.3	14.4	14.4	14.1	13.7	11.4	15.1	13.55	3.14	84.	37.
	4	24.2	9.5	9.7	10.5	14.0	13.8	12.6	12.8	13.1	12.3	11.8	14.1	11.0	12.00	3.06	84.	37.
	4A		10.7			12.9						10.5						
	5	54.4	10.0	9.5	9.8	11.5	11.1	10.5	10.9	10.9	10.5	9.9	10.2	11.7	10.45	2.98	87.	39.
	5A		11.3			11.6						9.9						
	Total	99.4													Total avg	3.17	85.4	38.2
Bin	0	0.0								15.2	15.0	15.1			15.10			
Type	1	3.0	14.3	13.7	14.3	14.5	14.5	14.5	14.2	14.2	14.1	14.3			14.26	3.54	84.	39.
II	1A		13.3			14.6						14.7						
	2	6.0	13.5	13.8	14.6	14.2	13.0	16.0	15.7	15.0	14.1	13.2			14.31	3.62	80.	37.
	2A		12.4			15.0						15.0						
	3	11.8	11.3	11.9	13.3	15.0	15.0	14.9	14.0	14.0	14.3	14.8			13.85	3.38	84.	37.
	4	24.2	9.8	10.2	11.0	14.5	14.4	13.9	11.8	12.0	12.6	14.5			12.47	3.30	84.	37.
	4A		11.0			13.2						13.0						
	5	54.4	10.1	10.0	10.3	11.9	12.1	11.7	10.4	10.5	10.6	11.8			10.94	3.54	87.	39.
	5A		10.1			12.2						11.8						
	Total	99.4													Total avg	3.47	85.4	38.2
Bin	0	0.0								15.2	15.4	15.4			15.33			
Type	1	3.0	14.0	14.5	14.6	14.9	14.8	14.6	14.7	14.6	14.6	14.6			14.59	3.54	84.	39.
III	1A		13.8			14.9						15.0						
	2	6.0	13.4	15.5	15.8	15.5	14.5	16.1	15.9	16.0	15.4	14.6			15.27	3.54	80.	37.
	2A		12.8			15.3						15.2						
	3	11.8	11.3	12.0	14.3	15.3	15.2	15.3	13.6	14.1	15.2	15.5			14.18	3.54	84.	37.
	4	24.2	9.2	10.9	13.1	15.0	14.9	14.3	10.8	11.7	13.2	15.4			12.85	3.30	84.	37.
	4A		10.5			13.2						14.5						
	5	54.4	9.9	10.1	10.7	12.7	12.7	12.8	10.8	11.1	11.4	14.3			11.65	3.38	87.	39.
	5A		10.1			12.0						13.0						
	Total	99.4													Total avg	3.46	85.4	38.2

TABLE B-IX

TEMPERATURE OF GRAIN SORGHUM IN TWO-FOOT DIAMETER BINS, F

	Run No	Position in bin 1	2	3	4	5	6	7	8	9	10	Bin Avg
Bin Type I	0	75.	77.	81.	78.	80.	82.	77.	78.	82.	85.	79.5
	1	83.	83.	79.	73.	71.	71.	75.	71.	71.	70.	74.7
	2	81.	82.	80.	72.	70.	69.	72.	70.	71.	72.	73.9
	3	71.	74.	76.	71.	73.	75.	70.	77.	75.	78.	74.0
	4	77.	78.	77.	76.	76.	76.	75.	74.	75.	76.	76.0
Bin Type II	0	79.	80.	82.	76.	78.	81.	82.	82.	83.	85.	80.8
	1	82.	82.	77.	75.	72.	71.	75.	74.	73.	72.	75.3
	2	80.	80.	76.	70.	69.	69.	74.	74.	72.	69.	73.3
	3	72.	73.	75.	71.	73.	75.	70.	72.	73.	76.	73.0
	4	77.	75.	75.	76.	75.	75.	75.	74.	75.	77.	75.4
Bin Type III	0	77.	80.	82.	77.	78.	81.	83.	82.	83.	84.	80.7
	1	81.	78.	72.	73.	72.	74.	75.	73.	71.	78.	74.7
	2	81.	80.	75.	71.	69.	68.	76.	74.	70.	69.	73.3
	3	70.	71.	73.	68.	71.	73.	70.	73.	74.	75.	71.8
	4	75.	73.	74.	75.	76.	76.	75.	74.	75.	76.	74.9

TABLE B-X

TEMPERATURE OF WHEAT IN TWO-FOOT DIAMETER BINS, F

	Run No	Position in bin 1	2	3	4	5	6	7	8	9	10	11	12	Bin Avg
Bin	0								87.	87.	88.			87.3
Type	1	81.	82.	80.	78.	77.	77.	78.	77.	77.	77.	79.	79.	78.5
I	1A	72.			73.						75.			
	2	79.	80.	77.	72.	71.	71.	73.	72.	71.	72.	73.	75.	73.8
	2A	71.			68.						71.			
	3	92.	92.	88.	82.	79.	79.	81.	79.	80.	80.	87.	80.	83.3
	4	82.	82.	82.	77.	75.	75.	76.	77.	77.	79.	77.	78.	78.1
	4A	86.			84.						84.			
	5	85.	86.	85.	83.	83.	84.	84.	83.	83.	83.	84.	83.	83.8
	5A	85.			86.						83.			
Bin	0								84.	84.	84.			84.0
Type	1	80.	79.	76.	77.	78.	78.	77.	76.	75.	77.			77.3
II	1A	73.			73.						75.			
	2	77.	77.	74.	72.	71.	71.	73.	72.	71.	70.			72.8
	2A	70.			68.						70.			
	3	89.	88.	83.	79.	77.	76.	80.	80.	80.	77.			80.9
	4	81.	81.	79.	73.	73.	71.	76.	78.	77.	72.			76.1
	4A	84.			85.						85.			
	5	84.	83.	83.	82.	81.	81.	82.	83.	83.	81.			82.3
	5A	84.			85.						84.			
Bin	0								81.	81.	80.			80.7
Type	1	80.	78.	75.	76.	77.	78.	77.	76.	77.	79.			77.3
III	1A	72.			73.						75.			
	2	77.	75.	72.	72.	71.	71.	72.	73.	70.	72.			72.5
	2A	67.			68.						70.			
	3	89.	86.	82.	77.	75.	75.	81.	81.	78.	75.			79.9
	4	82.	81.	76.	73.	72.	72.	79.	79.	75.	71.			76.0
	4A	86.			84.						83.			
	5	84.	84.	83.	81.	80.	80.	82.	82.	81.	80.			81.7
	5A	86.			84.						83.			

TABLE B-XI

OBSERVED AND PREDICTED VALUES, BIN TYPE I

RUN NO.	OBSERVED	PREDICTED	DIFF/PRED	
	Miniature bin			
6	2290000050+	2434970050+	5953666849-	
	3720000050+	3806237050+	2265676049-	
	5720000050+	5924565050+	3452827349-	
	8860000050+	9162653050+	3303115449-	
	1342000051+	1401681051+	4257816249-	
	1713000051+	1787105651+	4146682849-	
	2284000051+	2257708251+	1164534949+	
	2740000051+	2657284551+	3112783049+	
1	2160000051+	2454873451+	1201175650-	
9	1771000051+	1840510151+	3776675849-	STANDARD
10	1800000051+	2078421151+	1339579850-	ERROR
11	2100000051+	2342068751+	1033567950-	OF
12	2060000051+	2380282051+	1345563350-	ESTIMATE
13	1900000051+	2338724751+	1875914350-	FOR
7	1251000051+	1285666051+	2696345749-	MINIATURE
	1832000051+	2045438451+	1043484950-	BIN
	2123000051+	2266476951+	6330393249-	DATA
14	2270000051+	2044567851+	1102591050+	= 0.29
2	3450000051+	3300967051+	4514828549+	
3	4230000051+	3417428051+	2377729750+	
	4760000051+	4020759051+	1838560850+	
4	4150000051+	3947325051+	5134489849+	
	5530000051+	5428694051+	1866121049+	
	6180000051+	6033973051+	2420080449+	
5	3410000051+	3599230051+	5257513449-	
	5070000051+	5440285051+	6806353049-	
	6600000051+	6836707051+	3462295549-	
	7340000051+	7414937051+	1010622249-	
	Two-foot diameter bins			
1	1740000051+	1449427251+	2004742350+	
2	9300000050+	1862305351+	5006189450-	
3	1700000051+	2358877351+	2793181750-	
4	3740000051+	3057194751+	2233437450+	
5	5700000051+	4461761251+	2775224350+	

TABLE B-X II

OBSERVED AND PREDICTED VALUES, BIN TYPE II

RUN NO.	OBSERVED	PREDICTED	DIFF/PRED	
	Miniature bin			
20	3060000050+	4051980050+	2448136550-	
	4990000050+	5286590050+	5610232749-	
	7760000050+	7549450050+	2788944949+	
	1163000051+	1141239051+	1906787349+	
	1716000051+	1767919051+	2936729649-	
	2213000051+	2287362051+	3250993949-	
	2822000051+	2938520051+	3965261449-	
21	1693000051+	1721148051+	1635420149-	
	2413000051+	2612700051+	7643434049-	
22	2104000051+	2035604051+	3359985549+	
24	1970000051+	2332917251+	1555636950-	STANDARD
25	2160000051+	2556353051+	1550462750-	ERROR
15	2310000051+	2493027051+	7341557149-	OF
26	2060000051+	2475705151+	1679138250-	ESTIMATE
27	2080000051+	2429822751+	1439704650-	FOR
28	1380000051+	1375409051+	3337916248+	MINIATURE
	1980000051+	2519770051+	2142140050-	BIN
23	2123000051+	2151084051+	1305574349-	DATA
16	3100000051+	2567526051+	2073879750+	= 0.328
	4130000051+	3852560051+	7201445349+	
17	3940000051+	3356191051+	1739498750+	
	4430000051+	3881933051+	1411840450+	
18	2800000051+	2443254051+	1460126550+	
	4260000051+	3991700051+	6721447049+	
	5630000051+	5236319051+	7518277649+	
19	6250000051+	5772796051+	8266427649+	
	1820000051+	1975981051+	7893851249-	
	3510000051+	4019181051+	1266877550-	
	5090000051+	5541171051+	8142159849-	
	6550000051+	6790625051+	3543488349-	
	7200000051+	7328882051+	1758549349-	
	Two-foot diameter bin			
1	1160000051+	8721587050+	3300331750+	
2	1090000051+	2181703851+	5003904750-	
3	1710000051+	3169331551+	4604540450-	
4	3540000051+	4244431851+	1659661050-	
5	5500000051+	5808042151+	5303716749-	

TABLE B-XIII

OBSERVED AND PREDICTED VALUES, BIN TYPE III

RUN NO.				
	Miniature bin			
29	3490000051	3442916051	1367561749	STANDARD
	5000000051	5172816051	3340849549-	ERROR OF
	6270000051	6275677051	9046036047-	ESTIMATE FOR
	6840000051	668199605l	2364622849	MINIATURE
30	1160000051	1026821051	1297003150	BIN DATA
	1740000051	1940522051	1033340550-	0.17
	Two-foot diameter bin			
1	1030000051	7055163050-	2459923751-	
2	9000000049	2193938851	9589778950-	
3	1590000051	3049221151	4785553650-	
4	3370000051	3639508951	7405089749-	
5	6270000051	6275677051	9046036047-	

TABLE B-XIV

δ INCREMENTS FOR EACH RUN OF THE MINIATURE BINS

BIN TYPE I

RUN NO.	
1	2,139
2	2,034
3	1,628
4	1,106
5	694
6	0
7	900
8	1,530
9	2,772
10	2,426
11	2,350
12	2,339
13	2,351
14	2,507

BIN TYPE II

RUN NO.	
15	2,174
16	1,623
17	1,244
18	707
19	304
20	-64
21	712
22	1,431
23	2,522
24	2,200
25	2,101
26	2,163
27	2,176
28	2,132

BIN TYPE III

29	866
30	1,368

VITA

DONALD LEE DAY

Candidate for the Degree of

Doctor of Philosophy

Thesis: EXPERIMENTAL ANALYSIS OF CROSS-FLOW GRAIN DRYING SYSTEMS IN DEEP CYLINDRICAL BINS

Major Field: Agricultural Engineering

Biographical:

Personal Data: Born in Dewey County, Oklahoma, August 14, 1931, the son of George D. and Mildred Twyman Day.

Education: Graduated from Leedey High School in 1949; received the Bachelor of Science degree from Oklahoma State University in 1954 with a major in Agricultural Engineering; received the Master of Science degree from University of Missouri in 1959 with a major in Agricultural Engineering; completed the requirements for the Doctor of Philosophy degree from Oklahoma State University in August, 1962.

Professional Experience: During college: worked one summer for Soil Conservation Service, and one summer for the Farm Tractor Division of International Harvester Co. After graduation: employed as Assistant Engineer in the Farm Tractor Division of Allis-Chalmers Mfg. Co., 4 months; Pilot in the United States Air Force, 1954-1957; Instructor in Agricultural Engineering Department at Texas Technological College, 1957-1958; Graduate Teaching Assistant at University of Missouri, 1958-1959; Graduate Research Assistant at Oklahoma State University, 1959-1962.

Professional and Honorary Organizations: Associate member of the American Society of Agricultural Engineers; member of Sigma Tau, honorary engineering fraternity; member of Gamma Sigma Delta, honorary agricultural society; associate member of Sigma Xi, honorary science society.